UNIVERSITÀ DEGLI STUDI DI TRIESTE

DIPARTIMENTO DI INGEGNERIA E ARCHITETTURA

XXIX CICLO DEL DOTTORATO DI RICERCA IN INGEGNERIA E ARCHITETTURA INDIRIZZO INGEGNERIA MECCANICA, NAVALE, DELL'ENERGIA E DELLA PRODUZIONE

THEORETICAL AND EXPERIMENTAL ANALYSES OF MICRO ORC SYSTEMS FOR LOW GRADE HEAT SOURCES

DR. SERGIO BOBBO	REFEREE
PROF. STEFANO SAVINO	REFEREE
PROF. LUCA CASARSA	EXAMINER
PROF.SSA ERMINA BEGOVIC	EXAMINER
PROF. ALBERTO FRANCESCUTTO	CHAIRMAN
PROF. RODOLFO TACCANI	SUPERVISOR
PROF DIEGO MICHELI	COORDINATOR

JOHN BESONG OBI — CANDIDATE

A.A. 2015-2016

UNIVERSITÀ DEGLI STUDI DI TRIESTE

DIPARTIMENTO DI INGEGNERIA E ARCHITETTURA

XXIX CICLO DEL DOTTORATO DI RICERCA IN INGEGNERIA E ARCHITETTURA INDIRIZZO INGEGNERIA MECCANICA, NAVALE, DELL'ENERGIA E DELLA PRODUZIONE

THEORETICAL AND EXPERIMENTAL ANALYSES OF MICRO ORC SYSTEMS FOR LOW GRADE HEAT SOURCES

dr. Sergio BOBBO	referee
prof. Stefano SAVINO	referee
prof. Luca CASARSA	examiner
prof.ssa Ermina BEGOVIC	examiner
prof. Alberto FRANCESCUTTO	chairman
prof. Rodolfo TACCANI	supervisor
prof Diego MICHELI	coordinator

John Besong OBI — Candidate

A.A. 2015-2016

Contents

List of Tables

List of Figures

Dedication

I would like to dedicate this thesis to *Beatrice*, without whose support I would not have been able to complete this work and *Victor Besong*, your presence in our life is a form of regeneration.

Acknowledgements

First of all, I would like to thank my professors at the University of Trieste, the PhD coordinator Professor Diego Micheli and my supervisor Professor Rodolfo Taccani for the collaboration and support they have given me over these years of the PhD; my thanks goes as well to Professor Reini Mauro, Professor Roberto Petrella (UNIUD) and Engineer Giuseppe Toniato of KAYMACOR who pioneered the project and collaborated in this great adventure.
I owe personal gratitude to Professor Taccani, not only for giving me the opportunity to participate in the development of this project, but also for his infinite patience, moral support professionallity and friendship without whom this work would not have gone to completion.I will keep a good memory of the long afternoons spent in the laboratory for the experimental activities, and I will keep in mind his advice and suggestions.
Remaining in the University context, I can't forget the psychological and moral support provided by my colleagues at the ENESYSLAB as well as graduate students I personally coached within these years of the PhD program.
I also want to sincerely thank the reviewers of this thesis: Dr. Sergio Bobbo and Professor Stefano Savino whose observations and remarks have been constructive for the drafting of this manuscript.
With great affection and gratitude, I thank my large and numerous family without which I would not be what I have become today: thanks to my parents Pah sam and Mah Nchung who, despite the difficulties and the little they afforded, they have always encouraged my brothers, sisters and I, to study and follow our ambitions. Thanks in particular to my brothers: Mr. Peter Enowobi, Dr. Gabriel Egbe, Engineer Louis Ketchen, Valentine Tanyi, Cletus Atabe, and my sisters: Esther Ngware, Joana Nkongho, Lydia Ngwai, Jessica Bakume and their respective families, I also thank all the other relatives who, despite the distance, have always made me feel closer.
Thanks to my adopted family who have accepted me like a brother and son, especially maman Blandine and her daughters Léo, Betty and their respective boyfriends, for all their support and team spirit.
Last but not the least, thanks to my small family founded with Beatrice

who has been my backbone throughout these years and whose presence has been felt at every single moment, finally the new entry, Victor Besong, our 19 months old son who arrived midway this adventure, injecting a breath of indescribable love and great fortune in my life.
Lastly, I would like to thank all the friends and well-wishers who have given me support in one way or the other unconditionally and who never lost the opportunity to show me their love and affection. While I type these lines I also think of President Bisaro who personally believe strongly in my personality and offered me a good job with good prospects for professional and career growth as well as my new colleagues of Gruppo Bisaro.

Abstract

The growing cost for energy production and distribution as well as problems related to environmental pollution have motivated the increasing interest in the research of alternative solutions and, in particular, innovative technologies capable of compromising efficient use of energy, production cost, optimization and guaranteeing environmental sustainability. One of the promising technologies suitable for waste heat recovery and low grade heat is the Organic Rankine Cycle (ORC). ORC's offer some advantages such as: reliability, safety, noise, emissions and flexibility. The work presented in this thesis is aimed at studying and developing systems capable converting thermal energy that can be low grade heat sources like solar systems or waste heat recovery from industrial wastes or wastes from Internal Combustion Engine (ICE) into electrical and/or mechanical energy, based on the ORC technology in the power range of 1-10 kWe. The work consists essentially of two parts. The first part includes literature overview, state of the arts on ORC systems in general and the implementation of a process simulation model of micro ORC system and its integration in a solar thermal plant. The second part includes laboratory work on both ORC test bench and prototype, and the field tests on a combined solar ORC facility. As for the first part, the literature work overviews the major fluids commonly employed in ORC applications in general and the micro systems up to a 100 kWe in particular, the overview extends to the main components installed in a simple ORC like the expander types, feed pump types and finally the heat exchangers suitable for heat recovery and low grade heat systems. The overview ends with a general description of the various potential uses of this technology, with particular focus on the kWe size applications. The thermodynamic cycle of the ORC has been studied by creating a simulation model for the considered working fluid, R245fa, but capable of running with different working fluids using the Engineering Equation Solver (EES) software. Considering system integration, a co-simulator has been created using the Trnsys-EES platforms to study the possibility of coupling an ORC to a solar collector system. Trnsys is suitable for the modeling of the solar system and is largely used by professionals in assessing the performance of thermal and electrical energy systems. In the second part the experimental activity is

presented. The laboratory is equipped with an ORC test bench used to investigate the performance of the expander and a separate test bench used to characterize the feed pump both available at the ENESYSLAB of the University of Trieste-Italy. During the laboratory experiments, the expander isentropic efficiency measured is above 60%.
Considering integration of the ORC system analyses have been performed on the ORC prototype coupled to a solar field at the University of Florence Italy. The developed models have been used to study and predict some cycle performance parameters, in particular, the model developed for the combined solar ORC offers a fast comprehensive analysis of the system and allows to easily predict and assess the performance of a solar powered ORC and its system behavior at different operating conditions, in particular, the model show efficiencies above 4% for the combined solar ORC system. An economic analysis concludes the work where the cost of realizing a solar-ORC is presented, in the analyses, it has been shown that the payback time of the considered plant is 10 years with reference to the Italian plan of incentives as a plan of investment. This analyses confirms the numerous advantages obtainable from this type of technology and highlights improvements that could be made to achieve better performance hence the feasibility of the system if the installation cost is reduced.

Sommario

L'aumento dei costi della produzione e distribuzione dell'energia, nonché il problema dell'inquinamento ambientale hanno portato all'aumento dell'interesse per quanto riguarda la ricerca di soluzioni alternative e, in particolare, di tecnologie innovative capaci di dimostrare un compromesso tra uso efficiente dell'energia, costi di produzione della stessa, e ottimizzazione dei sistemi in modo tale da garantire una sostenibilità ambientale. Una tecnologia molto promettente da questi punti di vista, capace di sfruttare il calore di scarto a basse temperature, è rappresentata dai cicli ORC, ossia cicli a vapore utilizzanti fluidi organici diversi dal comune vapore acqueo. I sistemi ORC offrono molti vantaggi, tra cui: affidabilità, sicurezza di impiego, basse emissioni di agenti inquinanti e in termini di rumore, nonché flessibilità di utilizzo. Il lavoro presentato in questa tesi riguarda lo studio e lo sviluppo di sistemi ORC in grado di convertire energia termica a basse temperature, tipicamente disponibile in sistemi di tipo solare o di recupero di calore da processi industriali e motori a combustione interna, in potenza elettrica o meccanica, con taglie tra gli 1 e i 10 kWe. Il lavoro presentato si costituisce principalmente di due parti. La prima parte riguarda una ricerca bibliografica inerente lo stato dell'arte della tecnologia ORC e l'implementazione di un modello di simulazione di processo di un sistema micro ORC e la sua integrazione in un impianto di tipo solare termico. La seconda parte include la descrizione del lavoro svolto in laboratorio sul prototipo ORC e i test operati sul campo su un sistema combinato ORC solare. Per quanto riguarda la prima parte, una ricerca è stata svolta sui fluidi operativi più utilizzati in applicazioni ORC con taglie elettriche fino a 100 kWe. I componenti più importanti del sistema sono stati investigati, con particolare attenzione per quanto riguarda i tipi di espansore, di pompe e scambiatori di calore, impiegati per sistemi a bassa temperatura. Le principali applicazioni dei sistemi nella taglia considerata sono state considerate nel lavoro di ricerca svolto. Il ciclo termodinamico del sistema ORC è stato studiato tramite lo sviluppo di un modello di simulazione per il fluido scelto, R245fa, ma in grado di essere utilizzato anche per lo studio di diverse tipologie di fluido. Il modello è stato sviluppato in EES. Per quanto riguarda l'integrazione del modello nel sistema a col-

lettori solari, un modello di co-simulazione è stato sviluppato considerando una sinergia tra EES e il software Trnsys. Nella seconda parte di questo lavoro, l'attività sperimentale svolta è presentata in dettaglio. Il laboratorio è attrezzato con un banco di prova per un sistema ORC usato per lo studio delle performance in particolare del componente espansore, nonché un banco di prova è anche disponibile, sempre presso l'ENESYSLAB dell'Università di Trieste, per lo studio del componente pompa. Durante le prove sperimentali è stata misurata un'efficienza isentropica superiore al 60% per quanto riguarda l'espansore.
Per quanto riguarda la parte di integrazione con il sistema a collettori solari, una campagna sperimentale è stata condotta, utilizzando un prototipo ORC collegato ad un campo a pannelli solari termici disponibile presso l'Università di Firenze. I modelli sviluppati sono stati utilizzati per studiare e predire alcuni parametri operativi del sistema e, in particolare, con l'intendo di stimare il comportamento del sistema stesso quando funzionante in diverse condizioni operative. Dalle prove sperimentali condotte, sono state ottenute efficienze superiori a 4% per il sistema solare-ORC. Una analisi di tipo economico è stata riportata a conclusione del lavoro, per quanto riguarda lo sviluppo di un sistema solare-ORC, ottenendo un periodo di ritorno dell'investimento di circa 10 anni, facendo riferimento al piano di incentivi energetici presenti in Italia. L'analisi conferma i numerosi vantaggi che possono essere ottenuti mediante l'uso di tale tecnologia e permette di evidenziare i possibili miglioramenti che potrebbero essere implementati in modo tale da ottenere un sistema più efficiente ed economicamente più conveniente.

Chapter 1

Introduction

1.1 Background

Waste heat losses arise both from conversion device inefficiencies and from thermodynamic limitations on equipment and processes [1]. This concept is not limited to industrial heat but also to conversion processes that involve heat production. Heat recovery can be achieved through numerous methods amongst which with the reuse of the heat within the same process and heat transfer to other processes. In the second case, the most common method is by means of a HE to transfer the unused heat to a secondary fluid, thus replacing the fossil fuels that would have been used as primary energy source. Similarly to low temperature waste heat, low grade heat often obtained from renewable sources like solar energy are generally ignored for power generation processes and can represent a reliable option for the generation of additional power or alternative for power generation. Amongst the recovery options is the power generation using the Rankine cycle. The Steam Rankine Cycle remains the widest used technology for power generation and covers approximately 85% of the world's electricity production [2]. When water steam is not appropriate for an optimal heat recovery other working fluids, such as organic fluids, can be used in a so called Organic Rankine Cycle ORC.

1.2 Global energy scenario

The world today is faced with different challenges amongst which energy requirements with two major impacts: the intensive consumption of fossil fuels resulting to the depletion of fuel reserves and emissions resulting from energy conversion processes. In terms of the global demand for energy, the expectations is a drastic increase over the next 30 years, mostly due to an

increase in the quality of life in developing countries including China and India. According to reports from the U.S. Energy Information Administration EIA2016 in International Energy Outlook 2016 [3], the global energy demand is expected to increase by about 56% between 2010 and 2050 Figure 1.1. Much of the growth of energy consumption occurs in the so-called Non-OECD countries, where demand is driven by strong economic growth and expanding population in the long term. In Figure 1.1, it is possible to see the energy consumption by region.

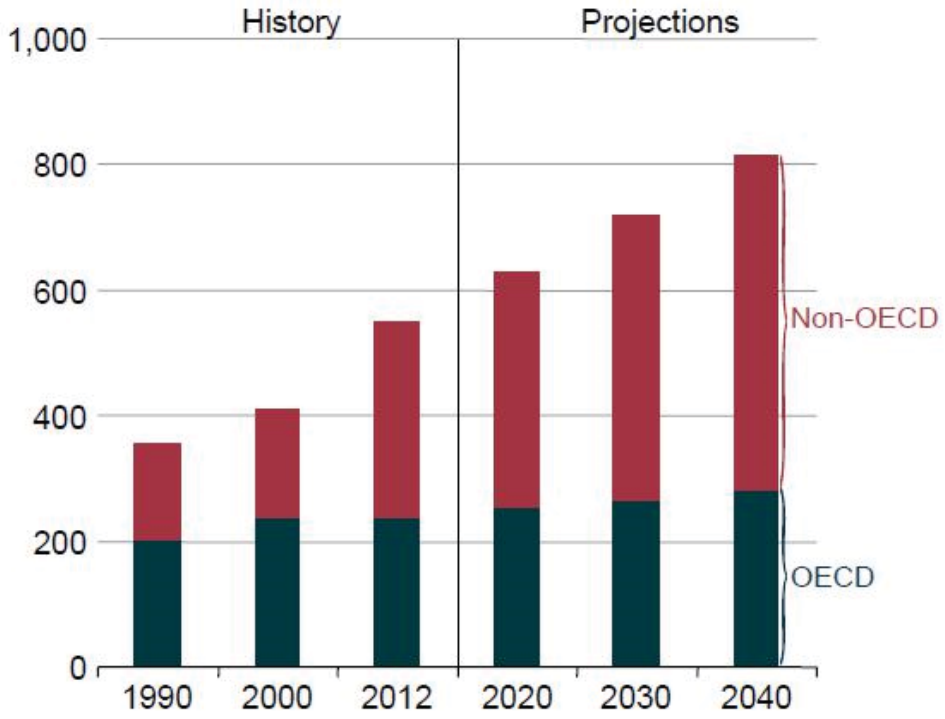

Figure 1.1: world energy consumption.

Based on the 2016 projection, between 2012-2040, the increase in energy demand from Non-OECD countries is expected to rise by 71% while the slower-growing OECD economies are considered to have gained a more mature energy consumption, are estimated with about 18% increase for the considered period. To every increase in the consumption of energy is associated a corresponding increase of Green House Gas (GHG) emissions resulting from the process of energy production, and in particular CO_2.

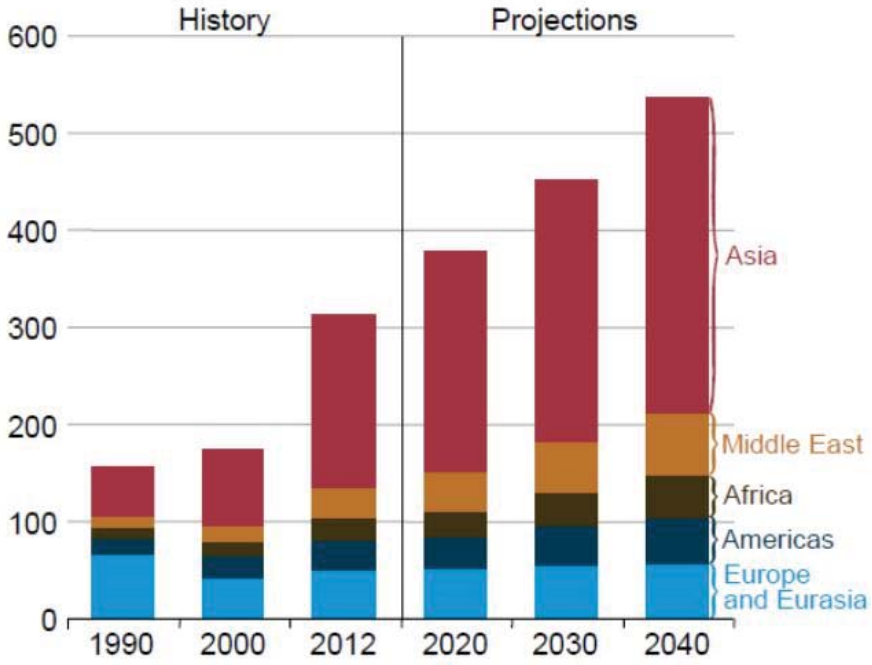

Figure 1.2: non-OECD energy consumption by region.

The projections also predict that in 2040, the value of the CO_2 emissions will correspond to an increase of about 46% respect to 2012. As can be seen in Figure 1.2 and Figure 1.3 there is a great contribution to the increase of such emissions from coal, this increase is very pronounced in developing countries, in particular the production of carbon dioxide as regards Non-OECD Nations in the year 2040, according to the forecast models, should not exceed 127% of the OECD Nations. A projection of the global energy related to CO_2 emissions is shown in Figure 1.4.

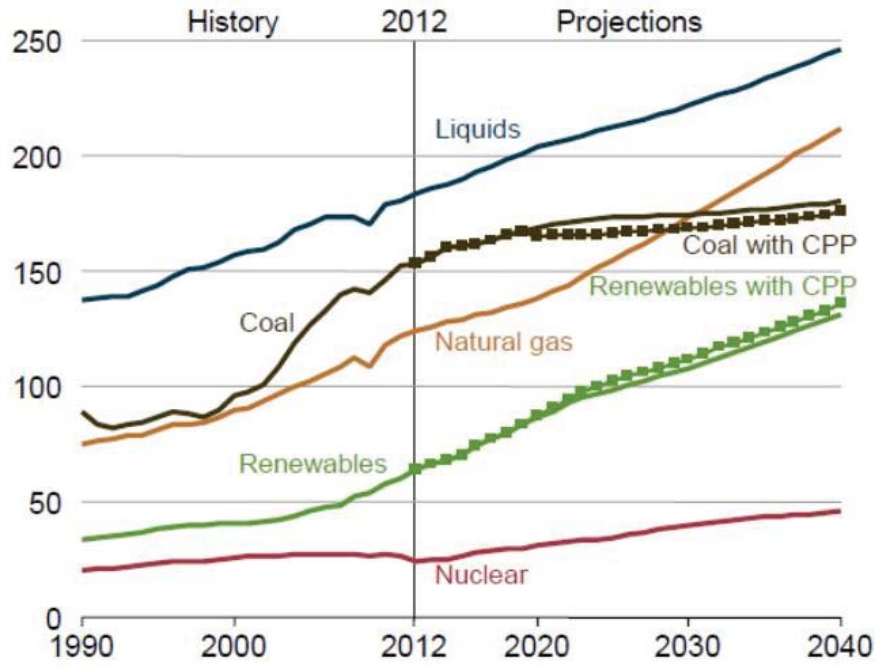

Figure 1.3: energy consumption projections 1990-2040 by fuel type.

The world energy consumption relative to 2010 by fuel type assumes the following distribution: petroleum and other liquid fuels amounts with a share of about 30%, followed by coal 29%, natural gas grows with a share of 28%, about 5.7% from the nuclear and the remaining 14.2% renewables (mainly biomass and hydro). In recent years, the global energy consumption increased at an average of about 2% per year, but the classification between the various primary sources has not undergone major changes, so also the contribution of renewable energy sources (including biomass, waste, wind, hydroelectric, solar and geothermal) increased in absolute terms but continues to contribute to the total with a share of approximately 14%.

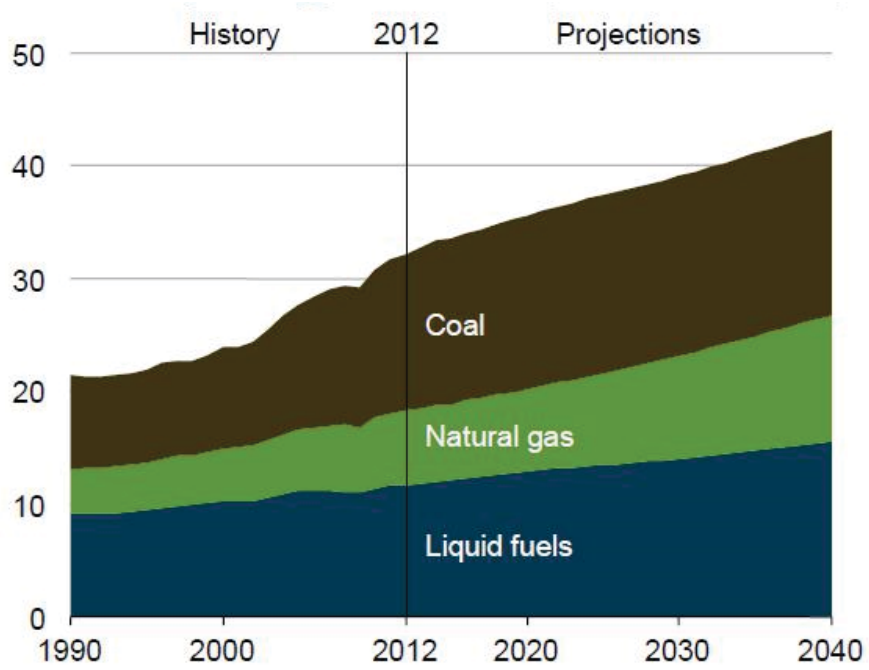

Figure 1.4: world energy-related CO_2 emissions by fuel type 1990-2040.

In the current world energy landscape, electricity plays a major role with about 40% of the total consumption of primary energy, about 67% of this electricity production comes from thermal power plants largely fuelled by coal and natural gas. Nuclear and hydroelectric plants provide a share of about 16.3% and 12.8% respectively of the gross electricity production, while the remaining 3.6% comes with other renewable sources (geothermal, wind, solar and biomass, etc) Figure 1.5. Renewable energy, especially the so-called non-traditional renewable sources: wind, solar, biofuels, waste and biogas, offer a contribution still marginal, although still growing, especially in the european countries. Globally speaking, fossil fuels (oil, natural gas and coal) currently contribute to the coverage of the world's energy demand for a share of 80%.

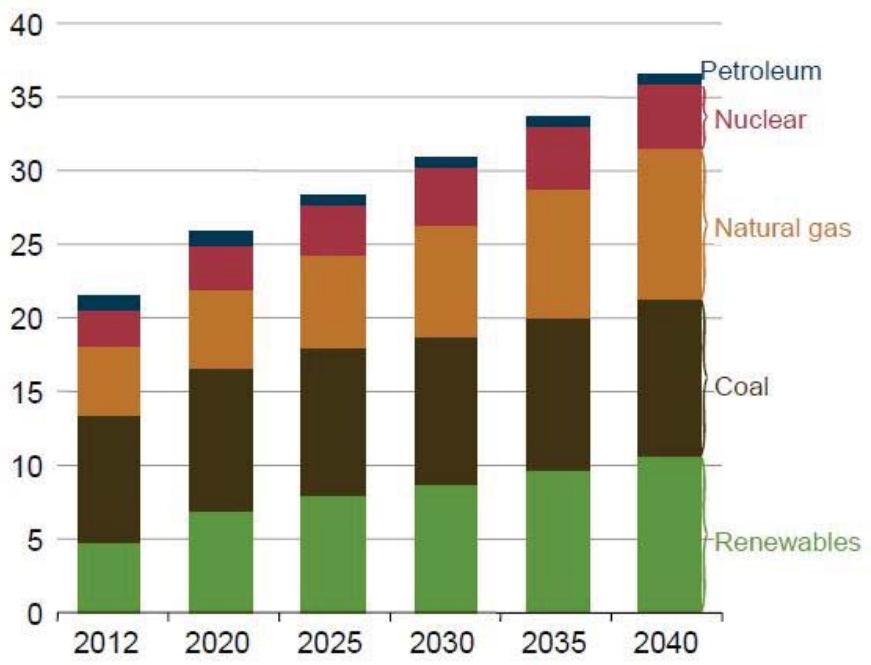

Figure 1.5: world net electricity generation by energy source 2012-2040.

1.3 Renewable energy sources

According to the IEA2016 [3], renewables account for an increasing share of the world's total electricity supply Figure 1.6, and they are the fastest growing source of electricity generation expected to grow from 22% in 2012 to 29% in 2040. Solar is the world's fastest growing form of renewable energy, with net solar generation estimated to increase by an average of 8.3%/year with an increase of 15% while hydroelectric and wind both accounts for 33%, other renewables (mostly biomass and waste) account for the remaining 14%. The increase in energy generation using solar sources is partially due to the drop in prices of the photovoltaic technology. As already discussed above power generation nowadays is based on fossil fuels with the consequent emissions of GHG and other pollutants compromising the environment. In order to make the development of our civilization sustainable and causing less harm to our environment, institutions and organizations are involved in research of new energy sources for the production of clean energy.

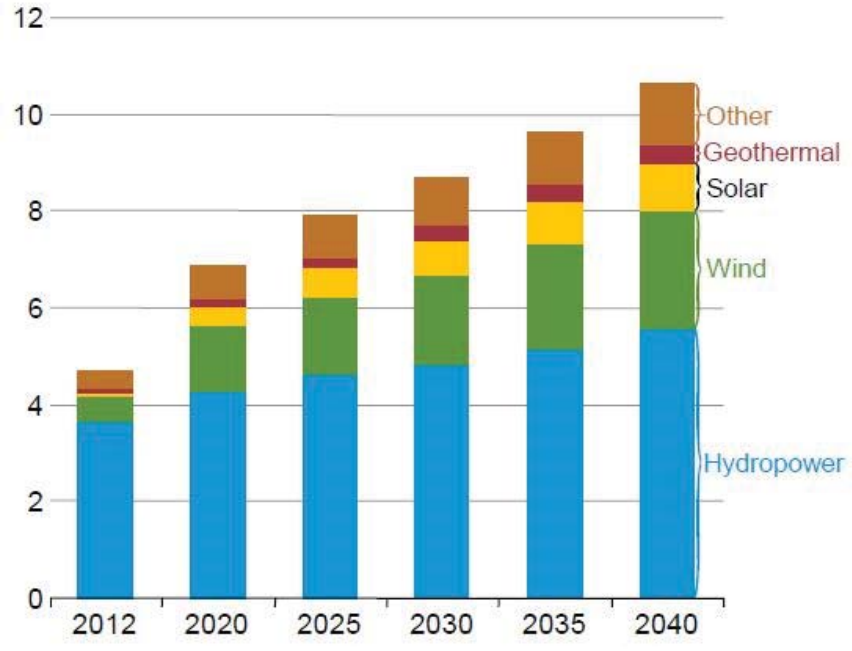

Figure 1.6: world net electricity generation from renewable power by fuel type 2012-40. [3]

1.4 Waste heat recovery

An energy recovery from waste heat, even partial, would allow energy savings of absolute interest and can be applied to all processes that involve conversion associated with production of heat energy. For example, an ICE for the automotive sector has a conversion efficiency that ranges from 20-35% depending on the application and the size (considered as the ratio between the available useful mechanical energy and the energy introduced by the fuel). It follows that the remaining share of energy between 80-65% is released to the environment in the form of heat. Similarly, if we consider electricity generation plants, the conversion efficiency varies between 40 to 55%. Even in this case, almost half of the introduced energy is released and dispersed to the environment as heat. Very often the temperatures at which this energy is released is too low to justify energy recovery and transformation into electrical energy. However, in most cases as in internal combustion engines, the temperature of the exhaust gas is enough to justify, at least from a thermodynamic point of view, heat recovery and the subsequent conversion into mechanical/electrical energy. Apart from ICE, high temperature waste heat from industrial processes could constitute a source that if carefully recovered could contribute to respond to the energy demand. This process could be

for example cement manufacturing, where clinker, an intermediate product should be cooled from about 1000 to say 100 °C using ambient air. In a similar manner, the exhaust gases from a micro gas turbine contains a considerable amount of heat that can be recovered providing additional electric power, thus increasing the system's overall efficiency. In all of the above mentioned cases, the heat could be recovered by direct heating, making it pass directly through the evaporator of an ORC or by means of an intermediate fluid (diathermic oil) to serve as he heat source. In case of intermediate fluid as heat carrier, the evaporator is preferred to the boiler implemented in other ORC machines available on the market [4]. The choice of an evaporator for a boiler makes it possible to use the same design with standardized components for all possible ORC applications: waste heat recovery from small industrial processes or from ICE.

1.5 Aim of this research

Energy transformation processes are associated with the production of heat that is often discharged as wastes, this, due to the inefficiency in the conversion technology usually employed. Low grade heat is generally less exploited as primary energy source due to its poor quality compared to conventional energy sources, even when exploited, there is a general use of medium-large plant sizes with relatively high costs. The benefits attainable by recovering energy from waste heat or exploiting low grade heat could be non negligible if efficient and cost effective conversion technologies are employed both on environmental basis as well as economic savings. Among the different technologies employed for the conversion of thermal energy into mechanical/electrical energy, the use of technologies involving thermodynamic cycles like the ORC of the micro size range, continue to be a challenge for the scientific community. A contribution in the diffusion of this technology, will be a first step towards its maturity thus feasibility. In this framework, this research aims to assess the potentials of Organic Rankine Cycles ORC for the recovery of low grade waste heat through theoretical and experimental analysis considering system of 1-10 kWe power range, contributing to the development of small ORC's. In particular, solar energy has been considered as the heat source. An ORC prototype has been developed, coupled to a solar collector system and the combined solar-ORC system characterized.

1.6 Methodology

To meet the objectives of this research, both the theorical and experimental approaches have been considered: The first is based on literature review of ORC in general and its applications that will be covered in chapter two, followed by system modeling (simulation of both solar and ORC plants separately and the combined system) by using process modeling tools that will be presented in chapter three. The literature review discusses the evolution of this technology as seen by the number of publications available on the subject, the criticisms of the working fluids and the selection criteria. The approach concludes with a revision of the components that make up a simple ORC underlying some of their design aspects and adapted application. To better understand the behavior of the proposed system; models have been developed for the solar collector system as well as the ORC thermodynamic cycle, the later has also been used for fluid screening considering the fluid selection criteria discussed in chapter two. After observing the two models separately, a model of the combined system was developed to investigate the dynamic behavior of the combined system described in chapters three and six. The second approach is experimental and based on data collection and elaboration as will be detailed in chapters four and five. The laboratory at the University of Trieste is equipped with an ORC test bench that uses electric heaters to simulate the heat source and has been used to test the performance of the scroll expander and the selected working fluid (R245fa), also available is a specific pump test bench that has been used to characterize the pump flow rate as well as the critical pressure and the relationship that exist between both parameters. Once the components have been characterized the ORC prototype was designed, constructed and tested in the laboratory using the electric resistances as the heat source. The prototype was later coupled to a solar field and tested. Data collected from the experimental activities is available for the study of ORC systems of larger plant sizes as well as studying different applications.

1.7 Outline of this thesis

The contents of each chapter is briefly presented in this section.

1.7.1 Chapter one

This chapter presents the motivation, the aim of the research and the methodology.

1.7.2 Chapter two

This chapter contains a literature review on the ORC systems and the working fluids employed especially in mirco ORC systems.

1.7.3 Chapter three

The chapter presents a process simulation model of the proposed solar ORC system. The main objective of the simulation analysis is to assess the influence of different parameters settings like: the recoverable heat temperature, fluids flow rate, auxiliary components consumption, evaporation and condensation temperature profiles, in order to achieve the best result in terms of the electric power developed by the ORC expander. The model is developed using two different platforms: Trnsys used to handle the solar collector system and EES used to solve analysis thermodynamic cycle of the ORC, EES contains libraries rich with thermodynamic properties of fluids. The EES model was then coupled to Trnsys as an external application, obtaining in this manner a co-simulator.

1.7.4 Chapter four

The chapter presents the experimental activities carried out in this research. The components of the ORC facilities used for the experimental activities are described in details. These activities include both the laboratory work as well as field work on an ORC prototype. The laboratory work includes tests on an ORC test bench, test on the ORC prototype and tests on a pump test bench. The field tests includes the tests carried out on the combined solar-ORC obtained by coupling the constructed ORC prototype to a solar collector system.

1.7.5 Chapter five

The chapter discusses the results obtained with the simulation model as well as the results obtained for both the laboratory and field tests. Some qual-

itative considerations about the results are discussed, the analyses though points out the feasibility of the technology also presents the limits of the technology at present.

1.7.6 Chapter six

This chapter presents a simplified economic analysis of the ORC solar powered system. A sensitivity analysis has been carried out to highlight the influence of the design choice of certain parameters.

Chapter 2

The Organic Rankine Cycle (ORC)

2.1 Overview on ORC

The ORC has been widely studied in the recent years as it is a very promising technology for the conversion of thermal energy at low and medium temperatures into electrical energy. The field of applications include: biomass and geothermal, extending to solar energy and heat recovery systems. Environmental issues such as climate change and rising oil prices are strong reasons to support the growth of this efficient, clean and reliable technology. ORC's also offer advantages such as: low maintenance, favorable operating pressures and autonomous operation. In Figure 2.1 a scheme of a simple RORC can be seen with the major components that make up the system.

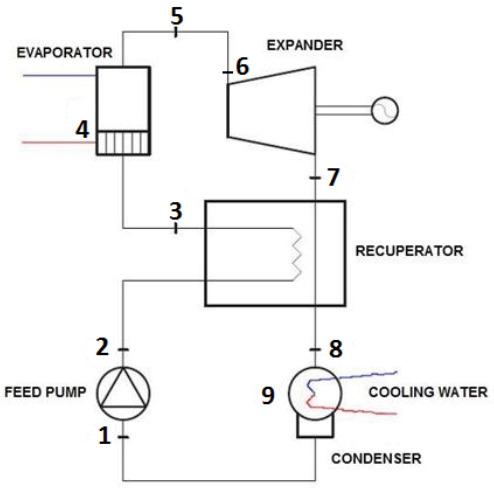

Figure 2.1: simplified schematic of a regenerative ORC.

With reference to the schematic view of the cycle in Figure 2.2, the different phases of the cycle are briefly described.

- **Phase 1→2:** Fluid compression by feed pump increasing the pressure;
- **Phase 2→3:** The fluid in the cold side of the regenerator is preheated by that in the hot side returning from the expander;
- **Phase 3→4:** The fluid is heater by the Heat Transfered Fluid (HTF) in the evaporator;
- **Phase 4→5:** Fluid is heated to evaporation by the HTF;
- **Phase 5→6:** Fluid is superheated to avoid premature condensation in the expander;
- **Phase 6→7:** Fluid expands and mechanical work is produced;
- **Phase 7→8:** Fluid in the hot side of the regenerator is cooled down as heat is transfered to the fluid in the cold side;
- **Phase 8→9:** Fluid is condensed to liquid state by means of a heat rejection system that could be air or water cooled;
- **Phase 9→1:** Subcooling of the fluid in order to avoid cavitation at pump suction side.

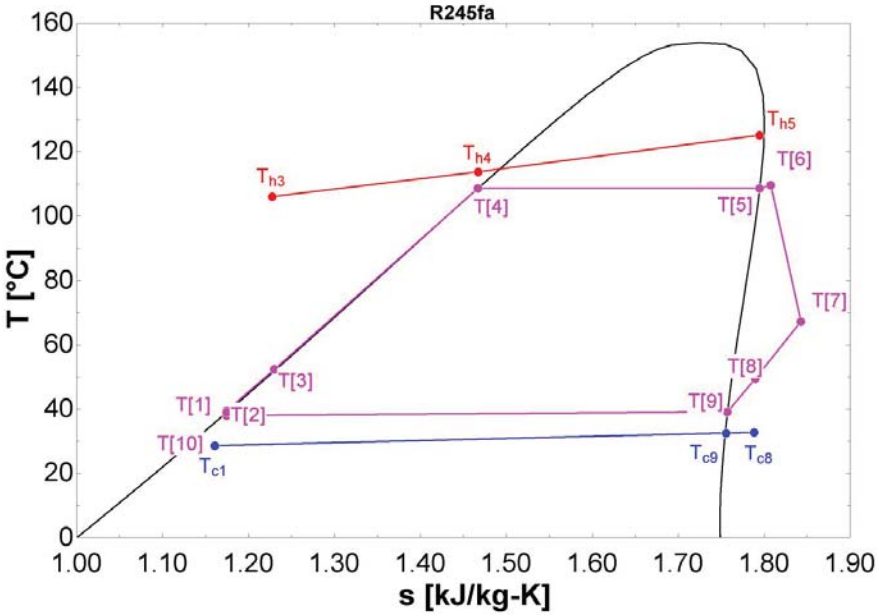

Figure 2.2: thermodynamic diagram of an ORC on the T-s plane.

The thermodynamic cycle is shown on the T-s plane for the WF (R245fa) in Figure 2.2. An example of an ORC generator produced by Turboden in Brescia is presented in Figure 2.3 with its major components [5].

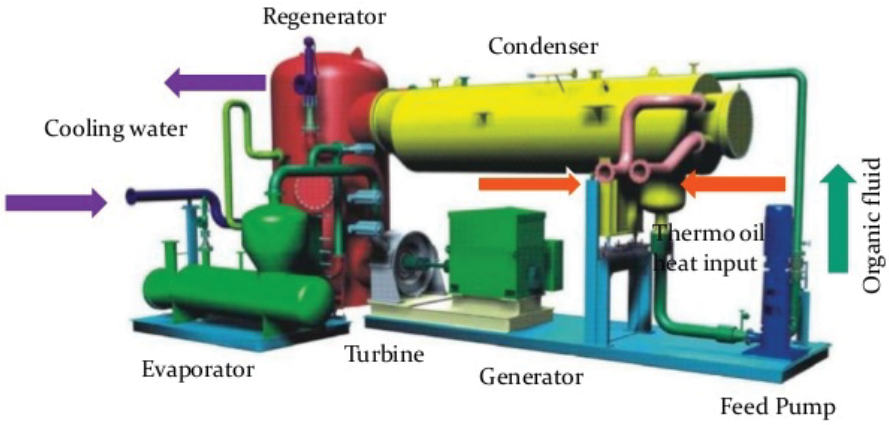

Figure 2.3: ORC module produced by Turboden.

2.2 Literature review

2.2.1 Overview

William J. M Rankine a Scottish Engineer, developed a complete theory of heat engines and thermodynamic cycles. The Rankine cycle is traditionally based on water as WF. Early applications of Rankine cycle with fluids (organic) different from water, like the engine boat developed by Frank W. Ofeldt in 1883 used Naphtha as the WF. Naphta was used both as fuel as well as a lubricant for the moving parts such as the piston. The evolution of ORC systems and applications have widely been discussed in literature; early system architecture and component layout have been discussed in [6, 7, 8], recent and extensive publication on system architecture can be found in [9, 10, 11]. WF screening methods in [12, 13, 14, 15], potential WFs for ORC applications have been reported with their thermo-physical properties discussed. In [14] a comparison of different WFs has been presented and suggestions on the choice of the WF based on the target application. In recent years developments have been made to improve ORC systems addressing the choice of the WFs [16, 17, 18]. Cayer [19, 20] in their papers on WF selection also give indications on plant design specifications and the financial aspect. Regarding the components of an ORC, a historic paper on expanders was presented by Badr [21]. In studying the system architecture it is very fundamental taking into consideration the expander isentropic efficiency, pinch point temperature differences as well as the heat source temperatures as underlined by Lecompte [9] where he suggests some common architectures like the use of a recuperator, a RORC, an Organic Flash Cycle (OFC), a Transcritical Cycle (TCC), or a Trilateral Cycle (TLC). Studies on expanders for energy conversion systems from low grade heat sources have been covered by the authors [22, 23, 24, 25]; where different expander types have been investigated including traditional expanders as well the use of other devices like compressors modified to function as expanders; this aspect is very important as the economic feasibility of an ORC system largely depends on the availability and the costs of the system components. ORC performance and cycle parameter optimization has been covered in [26, 27, 28, 29], like the expander volumetric efficiency, the isentropic efficiency, system heat balance, system overall efficiency. Although most of the studies found in literature are focused on static models of ORC, Quoilin proposes a dynamic model in [30] with reference to typical system control strategy and the main control parameters. Other recent studies on dynamic modeling and control strategy of ORC are presented by [31, 32, 33]. Bernardo et *al* [34] put in evidence the performance of an ORC module for power generation, where, they showed the correlation between heat source temperatures and consequently the fluid

temperature, pressure, mass flow rate and the gross as well as net electrical power increase. In the case study, the thermal power obtained ranged from 95.14 to 146.41kWt with a gross and net electrical power of 18.03 and 15.93 kWe respectively and the respective efficiencies of 12.32% and 10.88%. Several researches on energy sustainability have been carried out in the recent years on ORC plants as can be found by the number of articles available in literature.

2.2.2 Working Fluids (WF) in ORC

For every power cycle, the WF is fundamental for the definition of the thermodynamic properties, economic and technical flexibility of the plant. A large number of articles have been published on the WF in the ORC and their criteria of choice [35]. Several authors [15, 36, 37] converged on the fact that the characteristics of a good ORC WF should include: high thermodynamic performances in terms of power output, these may highly depend on some interdependent thermodynamics properties like density, specific heat capacity, acentric factor, critical point whose optimal is difficult to determine individually. A recent study on ORC WF is provided by Guo [18] in which pure fluids and fluid mixtures and their matches with the heat source are considered. In an earlier study, Chen [38] presented the selection criteria of an appropriate WF for different heat sources, optimal cycle design and design of cycle components. Publications can also be found on pure and mixed fluids with focus on their thermo-physical properties [17, 39, 40]. Other authors [41, 42, 43] showed that fluid mixtures have phase change profiles that well matches the heat source and suggests that this aspect can improve the cycle performance. Tchanche [44] reviews the ORC applications according to the WFs used. He added that, the choice between these types of fluids, depending on different criteria leads to different conclusions, depending on the specific application and working condition. However, only a few amongst the potential fluids are currently employed in the ORC as WFs as reported in Table 2.2.

Application	T_c[°C]	T_{evap}[°C]	Considered WF	Recommended fluid
WHR	30-50	120	R11,R113,R114	R113
WHR	n/a	120	R290,R600a,R134a,RR227ea,R245fa,R600a/R601, R290/R600a, R134a/R245fa	R600a, R601
WHR	25	145	H2O,NH4,Butane,Isobutane,R11,RC123,R141B	R236a
WHR	20-35	150	R245fa, R245fa/R152a,R245fa/R600a R113/R245fa, R601a/R600a,R236ea	n/a
WHR	30	150-200	RC123,HFE7100,Benzene,Toluene,P-xylene	benzene,Toluene,RC123
WHR	25	100-210	R113,R123,R245fa,Isobutane	R113
WHR	50	80-220	R600a,R245fa,RC123,R113	R113,Rc123
WHR	n/a	277	R12,RC123,R134a,R717	RC123
WHR	27-87	327	R245fa,R245ca,R235ea,R141b,R114,R11,R141b,RC123, R113,R11,Butane	RC123,R245fa
WHR-ICE	76	n/a	R124,R134a,R245fa,R600,R600a,R1234yf	R134a
WHR-ICE	95	n/a	R125,R143a, R218	R134a
WHR-ICE	35	96-221	R134,R11,Benzene	Benzene
ICE	55-100	60-150	H2O,RC123,Isopentane,R245ca,R245fa, Butane,Isobutane, R152a	H2O,R245ca,Isobutane
Geothermal	30	100	Alkanes,Fluoro-alkanes,Ethers,Fluoro-ethers	RE133, R600, R601, R245fa, R245ca
Geothermal	25	80-115	Propylene,R227ea,RC318,R236fa,Isobutane,R245fa	Propylene,R227ea,R245fa
Geothermal	30	150	R1225yeZ,R1234yf,R1234zeE,R245zeZ, R1234zf, R1234yf, R1225yeE, R1225zc, R1234yeE	R1234yf,R1225yeE
Geothermal	30	150	R1225yeZ,R1234yf,R1234zeE,R245zeZ, R1234zf, R1234yf, R1225yeE, R1225zc, R1234yeE	R1234yf,R1225yeE
Solar	35	60-100	Refrigerant	R152a,R600,R290
Solar	30	150	n-pentane,SES36,R245fa,R134a	R245fa,R134a
Solar	45	120-230	H2O, n-pentane	n-dodecane
CHP	50	170	R365mfc,Heptane,Pentane,R12,R141b,Ethanol	Ethanol
CHP	90	250-350	Butyl-Benzene,Propyl-Benzene,Ethyl-Benzene, Toluene, OMTS, Ammonium, R123, PF5050	Butyl-Benzene
n/a	35-60	80-110	non conventional WF	RC123,R124
n/a	40-60	220-350	HMDSO,OMTS,HMDSO/OMTS	HMDSO/OMTS

Table 2.2: potential WFs for ORC applications elaborated from [45].

Table 2.2 has been elaborated from [45] and presents a comparison of the choice of WFs in ORC applications for three different characteristics; the target destination, the temperature ranges of evaporation and condensation. Further analyses on fluid selection was performed by Jinliang et *al* [46] by screening 53 different potential WFs for heat recovery application solutions. Bensi Dong et *al* [47] used a numerical model to predict the first law thermal efficiency of the cycle, they further investigated on the effects of mixture concentration, temperature gradient of the heat transfer fluid, pinch temperature difference, pressure ratio and condensation pressure on the first law efficiency. They concluded in their analyses that zeotropic mixtures lead to high efficiencies compared to pure fluids. In [48, 49, 50] are analyses carried out on screening of different WFs for ORC applications. The WFs can be classified under three major categories: dry, wet or isentropic, the differences of the saturation curves of the three different categories of fluids can be seen in Figure 2.4. Fluids classified in the first category such as n-pentane,

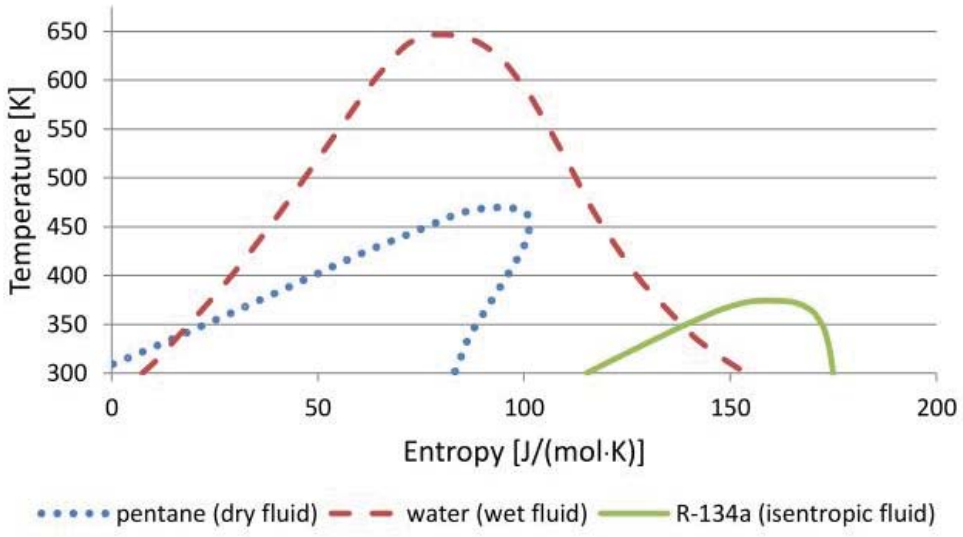

Figure 2.4: classification of WFs in categories.

benzene and toluene have a positive slope of the saturation curve. Those classified in the second category such as water and ammonia have a negative slope of the saturation curve. Fluids considered as isentropic such as dichlorofluoromethane and the trichlorofluoromethane, have a vertical saturation curve. When using dry fluids, there is no need for superheating to avoid droplet formations at the end of expansion as is the case for wet fluids. The absence of these droplets also reduces the risk of corrosion of the blades and increase the lifetime of the expander. Another consequence is linked to the lower boiling point of the organic fluid. This enhances heat recovery at

low temperature making the ORC technology a suitable and reliable option. This allows the use of low temperature heat sources such as geothermal and solar irradiation. An additional difference between a traditional steam cycle and ORC is the different amount of enthalpy drop in the expander. Steam cycles have higher enthalpy drops and the employment of turbines provided with several expansion stages, a situation overcome with the ORC where the enthalpy drops are quite lower, and a single stage expander could generally be sufficient. This aspect represents a consistent reduction in terms of plant cost. In some cases an additional effects of the low enthalpy drop include a lower rotation speed and a lower tip speed of the expander. The lower rotating speed allows direct drive of the electric generator without any reduction mechanism, while the low tip speed reduces the stresses on the blades and makes the design easier.

Selection criteria for the WFs

The choice of the organic fluid most suited for a particular application is made through an optimization process where numerous factors, both technical and economic, are contending their peculiar importance.

Physical properties

- **Fluid density:** High fluid density is of key importance for the determination of cycle performance be it in liquid or vapor state as such, fluids of this nature should be preferably chosen especially for systems characterized by very low condensing pressures like the ORCs. In fact, a low density leads to a higher volumetric flow rate with related increase of pressure drops in theHEs and expander hence the cost of the system.

- **Vaporization latent heat:** High vaporization latent heat enables most of the available heat to be added during the phase change, hence avoiding the need to regulate the superheating and expansion of the vapor through regenerative feed heating in order to enable higher efficiency.

- **Fluid pressure:** Working pressures play an important role in ORCs as they highly influence the complexity, technical feasibility and the installation cost of the plant. For pure substances, the phase change is a one degree of freedom system where both temperatures and pressures are directly related, as such, the condensing pressure is largely

dependent on the HE temperature.

- **Vapor saturation curve:** A positive slope of vapor saturation curve on the T-S diagram is required to reduce liquid formation at the end of the expansion.

- **Viscosity:** A low viscosity in both the liquid and vapor phases is required to maintain high heat transfer coefficients and low friction losses in the HEs.

- **Thermal stability:** Organic fluids generally suffer from chemical damage and decomposition at high temperatures contrary to water vapor. Some substances are suitable for the ORC application only if their temperature of chemical equilibrium is greater than the maximum operating temperatures of the cycle, besides the WF should be compatible with all the parts of the cold side of the system.

- **Conductivity:** High conductivity is required to obtain a high heat transfer coefficient in HEs.

- **Critical temperature:** Depending on the type of cycle, the critical temperature should be above the maximum operating temperature of the cycle.

Safety and environmental aspect

- **High safety level:** An ideal fluid for ORC application is expected to be non-corrosive, non-toxic and non-flammable. The ASHRAE standard 34 classifies refrigerants safety groups and can be used for the evaluation of the fluids even though some substances with good performance for ORC applications can present slight flammability and risk of toxicity.

- **Low Ozone Depleting Potential (ODP):** The ODP is a comparison between the fluid impact on ozone layer and the impact of refrigerant R11 [51] which is considered as the reference for all chemicals with assigned value of 1. The ODP of chlorine based refrigerants like Chlorofluorocarbons (CFC)'s and the Hydrochlorofluorocarbons (HCFC)'s have a non-null ODP values between zero and 1 and are

progressively being phased out by the Montreal Protocol [52] because of the negative environmental impact of chlorine. Current refrigerants like Hydrofluorocarbons (HFC)'s and Hydrofluoroethers (HFE)'s do not contain chlorine and are assumed to have zero ODP values.

- **Low Global Warming Potential (GWP):** The GWP is a relative measurement of how much heat a GHG traps in the atmosphere [53], by comparing the amount of heat trapped by a certain amount of the considered gas with that of CO_2 which is the reference substance whose assigned value is 1. The GWP is always calculated for a specified interval of time like 20 or 100 years.

- **The Atmospheric Life Time (ALT):** The ALT index estimates the amount of time an atmospheric pollutant (released from a source) will remain in the atmosphere before being removed from it either by forming another chemical substance or via a sink [54]. This time also depends on pollutants' reactivity as well as its source and sinks.

Economic aspect

Good availability and low cost of WFs is very essential for the feasibility of ORC's in economical terms. Several candidate fluids are already extensively used in various applications such as in Heating Ventilation and Air Conditioning (HVAC) systems and could be easier to find at a lower price and with better reliability.

2.2.3 Main components of the ORC system

The basic components used in an ORC system are described with special features that characterize and differentiate them from the systems based on a traditional Rankine cycle with steam as the WF. The scheme of a simplified ORC configuration with the internal recuperator integrated and can be seen in Figure 2.5 while Figure 2.3 shows the components layout of such a system.

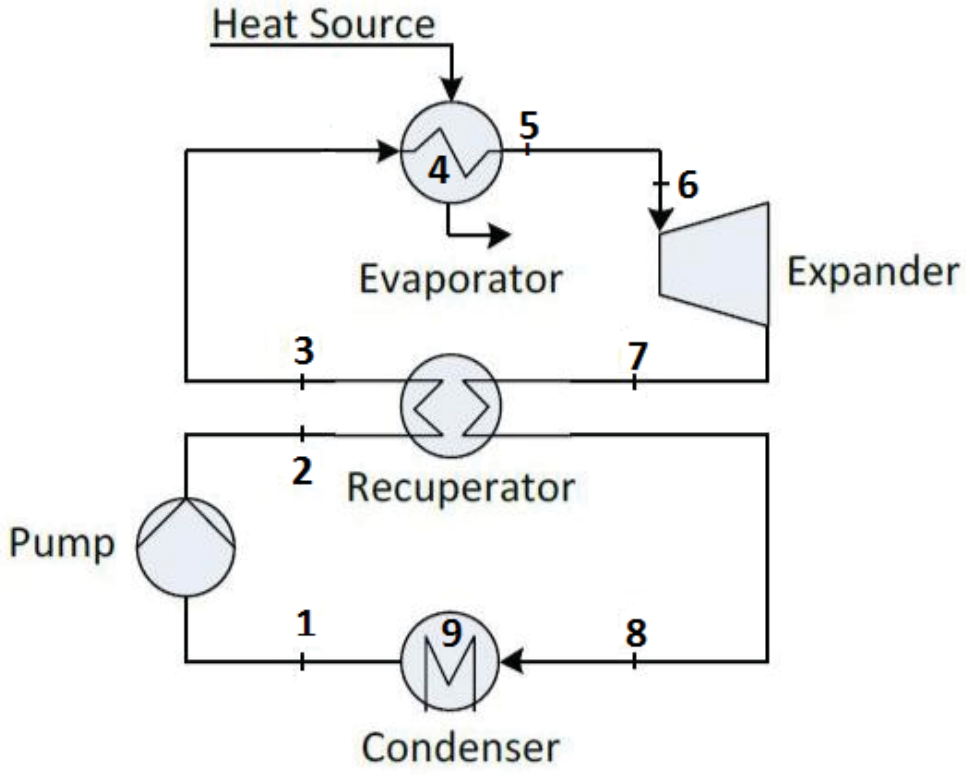

Figure 2.5: main components of the cycle.

Expander

Generally, when we use a low grade heat source (low temperatures) like in typical applications of ORC, the thermal efficiency of the Rankine cycle is inherently low, this could be due to: the limit of the temperature of the heat carrier, the limit of the cycle maximum temperaure linked to type of the fluid employed or both. For this reason, the performance of all the components involved in the system must be as high as possible in order to obtain a generator with an acceptable overall efficiency [56]. However, these small systems should not be too expensive in order to achieve economic competitiveness,

so the cost is another important selection parameter for all components of the circuit. The expander, whose function is to convert the enthalpic energy of the fluid into mechanical work, is one of the elements that most influence the overall performance of the system, so its choice is a fundamental step in the design and optimization of an electric generation system based on the ORC technology. The choice of the most appropriate expander depends on the working conditions and the size of the plant. According to Quoilin et *al* [45] expansion machines can be classified into two main categories: the turbo-machines and the volumetric machines. Similarly, for refrigeration applications, the volumetric machines are more appropriate for small size plants, as they are characterized by low flow rates, high pressure and low rotational speed compared to turbo-machines. For this reason, a large number of articles relating to the expanders can be found in the literature concerning their possible application on small scale ORC systems. An early study aimed at finding a first expander suitable for solar power generators to be installed in developing countries was published in 1984 by Badr [21] where the low cost and mechanical simplicity was the main characteristics required for the system. The investigation was based on the technical data, available for over 2000 ORC plants in the power range from 0.1 kW to 1120kW, and revealed that both volumetric expanders and radial flow turbines have been installed other small-scale applications. The shaft speed in the first case (volumetric expanders) ranged from 1000 rpm to 4000 rpm, while in the second (radial turbine), they were in the range of small turbo-machines ranging from 35000 to 60000 rpm. In a successful article Badr et *al* [57], conducted a research program on volumetric expanders that work with steam and various organic fluids finding many promising performance for these machines, in particular an isentropic efficiency achievable exceeding 73% at rotation speed of up to 3000 rpm. Volumetric expanders are of various types; piston, scroll, screw, and vane expanders; the last three are also called rotatory expanders where both the suction, expansion and the discharge chambers coexist. In piston typt expanders, the same volume is used for aspiration, expansion and discharge commanded by the intake and exhaust valves which are absent in the rotatory expanders. In the rotatory expanders on the other hand, the suction chamber evolves into two expansion chambers which later becomes the discharge chamber once they come in contact with the exhaust pipe, the time of the phases of intake and exhaust are defined by the machine geometry. A major difference between these subclasses of expanders as reported in [45] is that; the piston type presents less leakage losses compared to the rotatory type even though both types for small scale applications are mere prototypes derived from the corresponding existing compressors [22, 58, 59, 60]. Volumetric expanders are generally preferred to turbomachine for small scale power units as; they have a low rotational speed ranging between 1500 to

3000 rpm for the direct coupling to the electrical grid at 50Hz, they are reliable (largely used as compressors) can tolerate the presence of fluid during expansion and have a good isentropic efficiency [61]. Turbo-machines can be classified into two subclasses; axial and radial flow turbines. Axial turbines are generally suitable for rankine cycles with steam as WF as they present a higher enthalpy change respect to cases of organic fluids, nevertheless in the case of an organic fluid it will be sufficient to employ an axial mono stage turbine with evident benefits from an economical point of view for the total cost of the system. On the other hand, radial flow turbines are suitable for high pressure ratios and low volumetric flow rates even though they are not an optimum choice for small scale installations as they have extremely high rotational speed especially at low power output this is related to the fact that, the peripheral speed is directly proportional to the product between the rotational speed and the diameter of the turbine [21] thus the geometry of the turbine. There is abundant literature on expanders for ORC applications in general and in particular small scale units [62, 63, 64, 65, 66]. Farrokhi [67] presented in a recent paper with a case study of natural gas fired ORC based micro-Combined Heat and Power (CHP) systems for residential buildings. The maximum cycle temperature was 85°C, with a corresponding yield of about 77.4 W with a rotatory vane expander as the power generation device [68, 69]. In the study, Isopentane was used as the WF, the net cycle electrical efficiency was quite low 0.0166 and is accounted by the fact that the heat source temperature was quite low. Miao et *al* [70] analyzed an ORC with R134 as WF driven by a scroll expander. The maximum cycle yield of 2.35kW at 160°C was reached. Table 2.3 presents a summary of the different expansion machines available in the market for small scale ORC applications. The table is arranged into expander type and size, carefully looking at the table, it can be observed that scroll and piston types expander are suitable for very small ORC systems, similarly the screw and gear type are preferable for small-medium scale applications, while the turbine tecnology dominates the large scale applications.

Expander type	Expander size [kW]	Manufacturer	Website
gear	40-60	ENER-G-ROTORS (USA)	www.ener-g-rotors.com
scroll	2-4	Kaymacor (Italy)	www.kaymacor.com
scroll	5-30	Eneftech (Switzerland)	www.eneftech.com
piston	1-3	COGEN Microsystems	www.cogenmicro.com
screw	50	Electratherm (USA)	www.electratherm.com
screw	10-100	Infinity turbinellc (USA)	www.inifinityturbine.com
screw	50-100	BEP Europe (Belgium)	www.e-rational.net
screw	50-100	Kholer undZiegler (Germany)	www.koehler-ziegler.de
turbine	70	Durr Cyplan (Germany)	www.durr-cyplan.com
turbine	5-100	Enogia (France)	www.enogia.com
turbine	15-100	Barber-Nichols Inc (USA)	www.barber-nichols.com
turbine	20-100	Verdicorp Inc (USA)	www.verdicorp.com
turbine	25-100	gTET (Australia)	www.g-tet.com
turbine	50-100	GMK (Germany)	www.gmk.info
turbine	50-100	Termocycle (Netherlands)	www.termocycle.com
turbine	60-100	Freepower (UK)	www.freepower.co.uk
turbine	100	TransPacific Energy (USA)	www.transpacenergy.com
turbine	100	Aqylon (Francia)	www.aqylon.com
n/a	20-100	ENERBasque	www.enerbasques.com
n/a	50-100	ENTRANS (Sweden)	www.entrans.se

Table 2.3: main characteristic of some commercial micro ORC systems.

Feed pump

The choice of the feed pump appears to be of crucial importance in the design process of a cogeneration plant with the ORC technology. Although the most important criteria for selection of the pump are recognized in the fluid flow rate and the pressure difference between suction and discharge, the choice of technology best suited for applications such as ORC also depends on other factors such as the operating temperatures and pressures, compatibility of the fluid with materials and viscosity of the WF. In particular, the latter parameter is one of the most critical, since organic fluids have in most cases a very low viscosity, causing major losses through the seals of the machine and by pumping mechanisms, thus, limiting the lubricating properties of the fluid itself. While current technology for large and medium sizes installation of ORC plants is represented by centrifugal type feed pumps, this solution is not suitable for smaller systems; in fact, the competing requirements of low flow rates and high differential pressures may be met by a centrifugal machine if they are considered of multistage architectures, but this option entails excessive costs and occupies considerable space [71]. Volumetric pumps therefore appear as a more suitable alternative for small ORC plants, but present some drawbacks including amongst which: relatively low efficiency. Aoun [60] elaborated extensively in his doctorate thesis, analyses on different pumps potentially suitable for small scale ORC system, considering the main characteristics of many volumetric units commercially available. He tested the diaphragm, vane, gear and piston pumps and came out with the following considerations; diaphragm pumps were suitable for small ORC systems even though they presented overall efficiencies generally lower than 0.20, especially when the process fluid presents low viscosity, he added that a gear pump could be a reliable alternative in which case the WF should be mixed with a lubricant. Other studies of interest related to feed pumps for ORC are available in [30, 72, 73].

Heat exchangers

HEs constitute a great amount of the total cost of a system, for such reasons they must be carefully designed and chosen. In an ORC system HE include; evaporator, condenser and possibly a recovery HE generally called regenerator or recuperator. Different types of HE can be used in this technology, the most common are the bundle tube HE (mainly employed in large installations), and the PHE (mainly for small installations, thanks to their compactness) [60]. A critical HE is the one installed in correspondence to the heat source, depending on the nature of the heat source; the HE must be designed to withstand high temperatures and to resist destructive phenomena such as erosion and corrosion that can occur within it. In the case of

waste heat recovery from internal combustion engines with Sulphur content, dew point temperature must be avoided in order to prevent the condensation of gases with acidic condensate formation which can provoke possible corrosion phenomenon. In fact, as is the case in most commercial installations, it never falls below temperatures of the order of $120 - 180°C$ depending on the content of sulphur in the exhaust gas. Currently, researches are been carried out on designing HE that condense and expel acid gases in an automatic manner. Several studies have been carried out on HEs; some focused on the importance and effect of HEs on an ORC system [74], some authors made a comparison between the shell type and the PHEs, investigating which HE type could be suitable for the ORC systems [75]. Other publications on HEs for use in ORC applications are found in [76, 77].

2.2.4 Applications of ORC

Overview

The ORC technology reveals to be promising to a wide range of different applications, some already commercial installations today, others simply as prototypes for experimental purposes. A general description of the various potential uses of this technology is presented, with particular focus on small and medium sized applications, without ignoring some larger installations.

Solar energy

Renewable energy based technologies on solar energy and their applications are extensively studied nowadays by the scientific community [78]. Often the availability of low-cost electricity from a power grid is a technical barrier to the adoption of solar ORC or other renewable sources of electric power production [79]. On the other hand, several factors are increasing the market potential for small scale power plants like the need for distributed power systems in remote and isolated areas [44] alongside the need for sustainable power for economic growth. A solar thermal power plant can be defined as a system capable of converting heat energy (by means of solar collectors) into electricity using a thermodynamic cycle. Some of the technologies used for converting solar energy into solar power include solar heating, photovoltaics, solar thermal energy, solar architecture and artificial photosynthesis.

It thus follows that the differences in the typologies of plants are linked to the particular cycle of energy conversion and hence the maximum temperatures reached by the heat transfer fluid resulting in the following classification of solar thermal plants as in [80].

- Low temperature: below 100°C
- Medium temperature: up to 400°C
- High temperature: above 400 up to 1500-2000°C

Generally, solar plants classified as low and medium are potential thermal inputs for ORC for the power generation using hot water as heat carrier and are usually of low scale, such as below 1 MW of electrical production. The WF type could be any refrigerant or hydrocarbon; in this case, the heat carrier (water or water-glycol mixture) offers an efficient heat exchange with acceptable conversion efficiency from heat to mechanical. On the other hand, high temperature solar thermal power plants (generally obtained using complex and highly expensive technologies, such as a heliostat field with a central receiver or a dish concentrator), use a Rankine cycle similar to that used in conventional power plants or a Stirling cycle. Low temperature solar thermal power plants use flat-plate collectors, or solar ponds for collection of solar energy. Solar power plants with generation capacities within the above mentioned were installed in many parts of the world, particularly in Africa in the early 1970s. The reported system reached an overall efficiency of about 2%, with the thermal efficiency of about 25% and Rankine cycle efficiency of 7–8%. The main advantages of a solar system have been summarized in [44], benefits offered by a solar-ORC are found in [22]. Both flat and concentrated solar panels can be coupled with an ORC system, depending on the applications and the installations site: while flat plate collectors require a lower capital investment, concentrating systems, such as parabolic trough, ensure a higher total amount of produced energy throughout the panel operating life [81], especially if equipped with sun tracking systems. The latter solution is analyzed in Delgado Torres and Garcia-Rodriguez [82] where they made a comparison between solar ORC systems equipped with different collectors (flat panels, evacuated tube collectors and parabolic concentrators) and running with different WFs, defining the configurations that lead to minimization of the solar panel area. Wang et *al.* [65] made a comparison between a flat plate and the evacuated tube type collectors in a solar-ORC with R245fa as WF, they obtained a higher conversion efficiency in the case of the evacuated tube collectors. The ORC prototype was equipped with a rolling piston type expander with an average power output of 1.73kW with a maximum cycle efficiency of 0.042 for the evacuated solar collectors and 0.032 in the case of flat plate solar collectors. In another article, Wang

[83] developed a small ORC system equipped with flat plate collectors with the aim of comparing different WFs, both pure substances and mixtures. The experimental tests confirmed the potentiality of zeotropic mixtures of achieving good performance in ORC applications due to their typical non isothermal phase changes and revealed the importance of the optimization of the WF flow rate. Jing et *al.* [84] developed a detailed simulation of a solar ORC system with dedicated sub-models for solar radiation, collectors behavior, and thermodynamic cycle performance. The model used for a global optimization of the system revealed that the best configuration varies according to the geographical location since the intensity and the distribution of the solar radiations are the most influencing factors on the facility performance. Kane et *al.* [85] designed, built and optimized a mini-hybrid solar power system suitable for installation in remote areas of developing countries, the field test confirmed the possibility of achieving acceptable performances with the prototype, even at partial loads, a fundamental feature for a system designed to operate in stand-alone mode. As highlighted in [86], the solar thermal power technology has reached the stage of a certain industrial maturity and starts facing the commercial field, as evidenced by the significant number of achievements in different countries and the wide availability of products and companies engaged in the field. However, compared to its potential, the diffusion of this technology is still quite limited for several reasons: due to the big size of the plants, needed if only electrical production is considered, appear an important penalization considering the need of huge financing and large availability of low cost land. This is a limit compared to other technologies, such as the photovoltaic conversion, particularly favored in the realization of medium to small size. Presently, one of the main advantages of solar thermal systems, the low cost storage technology, is not yet adequately enhanced in the electrical market. This technology could be strategic in the energy field if considered an adequate utilization of the combination of electricity and heat production.

Geothermal energy

The hot fluids can be extracted by drilling geothermal well occasionally at high pressures and temperature up to 300°C and exploited for small and medium scale electric power generation [87]. However, the number of sites in the world with high-enthalpy geothermal resources are limited, and their operations are today limited by strict regulations for the reduction of gaseous pollutant emissions (generally geothermal steam contains large amounts of incondensable gases such as CO_2, Hydrogen Sulphide (H_2S), Ammonia (NH_3), methane (CH_4), Nitrogen (N_2) and Hydrogen (H_2)) [88, 55]. On the contrary, the wet steam geothermal systems either require integration of a flash plant or employed in a binary cycle due to the low tempera-

tures of the heat source [82]. Tchanche [44] made a comparison of different types of the installed geothermal plants and the total energy capacity obtained from these installations, a classification of geothermal plants is also presented including binary cycle plants which are suitable for low temperature liquid dominated resources, topic also treated by Villani et *al.* [88]. Geothermal systems coupled with an ORC unit have been developed and commercialized since the 1980s: large scale installations with power ranges up to about 1MW are economically feasible and equipped with conventional turbines, while small scale installations for power range up to about 10 kW can be cost effective if components with large production and market diffusion, such as devices derived from the HVAC field, are used [44]. Also available in literature are publications on the potentialities of geothermal based ORC systems: Borsukiewicz-Gozdur [89], Bruggemann [90], Astolfi [91], Salah [92].

Desalination systems

Water desalination consists of the removal of some amount of salt and other minerals from saline water making it suitable for human consumption. The desalination of water represents one of the most promising solutions to face the increasing world demand of fresh water for drinking, agricultural and industrial uses [93]. According to the separation mechanism, the technology can be classified as thermal or membrane based. Thermal based desalination separates salt from water by evaporation and condensation, in serial processes such as multi effect distillation (MED) or multi stage flash (MSF) desalination. The membrane desalination is based on the Reversed Osmosis (RO) phenomenon, water diffuses through a membrane and the salts are almost completely retained, thanks to a property of certain polymers called semi-permeability [94]. Although the pressure required to overcome the osmotic pressure are high (say between 60-80 bars for sea water and between 15-25 bars for brackish water [44]) and even if the filtration is not perfect RO desalination has great potential market, since it's specific energy consumption close to 6 times lower than thermal based desalination. To reduce the environmental impact of a RO desalination system, the power needed for pumping should be provided from renewable sources. In particular, since mechanical energy is directly required instead of electric, the direct coupling of expander of an ORC with the seawater pump represents a very interesting opportunity, making it possible to exploit low-temperature heat sources, such as the solar energy from non-concentrating collectors for desalination purposes. The solar RO-ORC desalination technology is widely studied today, aiming to reach the economic competitiveness and to design low cost systems suitable for applications in particular, in developing countries with dry climate [95]. Early researches on solar thermal driven pumping systems

involving the rankine power cycle targeted small scale water pumping systems for irrigation of farms with configurations similar to that proposed by Delgado- Torres [96] and Wong et *al.* [97].

Biomass power plants

Biomass represents locally the most adaptable application for micro scale distributed CHP generation as reported in [47] because it is widely available also as a waste product in a number of agricultural or industrial processes. Some common energy conversion technologies of biomass-fueled CHP systems are ORC, steam engines, Stirling engines, micro-turbines, gas turbines, fuel cells and internal combustion engines. For the small size biomass CHP systems, coupling with combustion engines or ORC technologies are rapidly gaining considerable interests. In the second case, a typical system is made of a biomass feed boiler capable of burning solid fuels and an ORC module coupled through a thermal oil loop. The need for an intermediate heat transfer medium, like thermal oil instead of water, provides a number of advantages such as; low pressure in the boiler, larger thermal inertia and lower sensitivity to load changes, simpler and safer control and operations [44]. Regarding the working parameters, they are different from other ORC applications: in particular, the maximum cycle temperature could be close to flame temperature, compatibly with the chemical stability of the ORC WF, allowing also higher condensation temperature and a higher quality of the cogenerated heat, without excessive penalizations in the power cycle efficiency [98]. From an economic point of view Dong [47] underlined that small scale Biomass ORC systems for domestic installation are still under development and not convenient due to high investment cost and long payback periods compared to medium size plants. The diffusion of the small scale ORC technology and commercial growth can be a reliable alternative of energy production.

Recovery from internal combustion engines

Internal combustion engines are characterized by efficiencies up to 50% in the cases of very big installations, this efficiency is related to the amount of waste heat involved in the engine operations. The waste continue to be a challenge to the scientific community as a partial recovery if not all the thermal energy available both in the exhaust gases and cooling circuit for the production of mechanical work can increase the generated power thus the system efficiency. Among other technologies, ORCs appear to be the most prominent solution for such application. Yu et *al.* [50] present a study on ORC system (with R245fa as WF) that bottoms a diesel engine. They showed that about 75% of the waste heat from exhaust gas and about 9.5%

of the diesel engine water jacket could be recovered under the engine conditions ranging from the high to low loads. The expansion power obtained was 14.5kW with a recovery efficiency of up to 9.2% while the exergy efficiency registered was about 21%, they concluded by demonstrating that an overall thermal efficiency of a diesel engine could be improved up to 6.1% when combined with an ORC system. Zhang et *al.* [99] analyzed the characteristics of a light-duty diesel vehicle engine coupled in a dual loop ORC for the recovery of waste heat from the engine exhaust, intake air and coolant. They reported that the net power from the low temperature loop was higher than that of the high temperature loop and that the relative output power improved both in the peak effective thermal efficiency and the low load regions. Shu et *al.* [100] illustrated the application of a combined ORC system with an internal combustion engine for Waste Heat Recovery (WHR) and reported an economic and thermodynamic evaluation of a dual-loop ORC coupled to an internal combustion engine for waste heat recovery and a comparison between a Transcritical Organic Rankine Cycle (TORC) and a Subcritical Organic Rankine Cycle (SORC) cycles for waste heat recovery with R123 and R245fa as WF. Vaja and Gambarotta [101] presented a thermodynamic analysis of different architectures of bottoming ORC for a stationary ICE, a comparison was also done between a number of WFs and three different configurations for the bottoming cycle: a simple cycle recovering heat only from the ICE exhaust gases, a simple cycle with recovery from both the exhaust gases and the cooling water as thermal input (the latter used to preheat the WF before evaporation) and a regenerative cycle, capable of recovering only the thermal energy of the exhaust gases. The analysis concluded that the most significant enhancements in the performances of the system can be achieved in the cases of the preheated and the regenerated ORCs, with about 5 percentage points increase of the overall efficiency of the system. It is interesting to note that both these solutions are equivalent in terms of efficiency, though regeneration enhances the ORC efficiency, penalizes exploitation of the cooling water as a thermal source (due to its low temperature), causing an incomplete heat recovery from the ICE. This confirms that the internal regeneration in a heat recovery ORC does not always involve significant benefits in terms of performance. Bonafin et *al.* [102] studied a marine engine with a rated power of 5.7MW and an efficiency equal to 49%. They analyzed the effective load distribution of the ICE which often operates in off-design conditions by considering the average time and the corresponding load for which the engine was operated. From the findings, the authors compared four different configurations of bottoming cycles: a simple ORC, recovering energy only from the exhaust gases, a preheated ORC, exploiting also the cooling water waste heat, a regenerative cycle, which does not allow to use the cooling water as a thermal source, and a combination of two ORCs in

cascade, which recovers energy from both the exhaust gases and the cooling water and also exchanges energy between each other (the condensation heat of the upper cycle is used to start the evaporation of the fluid of the lower cycle). Considering only the design conditions, the authors showed that the regenerated cycle and the combination of two ORCs gave more or less the same performances, but after an off-design analysis, they recognized the regenerated ORC as the best configuration to be installed as bottoming cycle for the studied engine, since the large decrease in the cooling water temperature at partial loads affects significantly the performances of the combined cycle. Durmusoglu et *al.* [103] studied a two-stroke engine for marine applications taking into account also the ICE operation at partial load, they calculated that the installation, on a single ship, of a bottoming ORC would save approximately 1230 tons/year of fuel and would reduce the CO_2 emissions of about 54 tons/year. An application of ORCs on ground vehicles is described by Aumann et *al.* [104] where potential savings related to the use of a combined ICE-ORC propulsion system on a truck are presented. They also presented a comparison on fuel consumption of the considered system and the result was a net saving of 5.6% from an initial value of 34.0 l/100 km to 32.1 l/100km with the installation of a heat recovery ORC unit. In [105], Quoilin discusses the ORC applications in the automotive field and further suggests the expander types suitable for the applications: according to him, positive displacement machines: scroll, vane and pistons types are preferable while turboexpanders are preferable for trucks. Lion et *al.* [106] assessed the possibility of fitting an ORC system in a commercial agricultural tractor, recovering waste heat from a 300 kW brake power heavy duty diesel engine with a maximum fuel consumption reduction of 10.6% obtained using methanol as WF. Reference installations for micro-ORC are shown in Table 2.4, the table also include for every installation, the type of the Architecture (Arch), Application (App), the expander type, the Degree of Maturity (DoM), the WF, the thermal efficiency (η_t) and the expander efficiency (η_{exp}). The installations have been classified as mature (m), very promising (vp), promising (p), developing (dev).

2.3 The chosen WF for this study

R245fa already abundantly discussed in literature has been confirmed to be a suitable WF candidate for waste heat recovery (low grade heat) systems, chosen according to the selection criteria discussed above: heat source temperatures, system maximum pressure, safety, toxicity and the legislations imposed on the characteristics of a good WF. The detailed description of the fluid screening procedure has been presented by [55] who contributed largely in the design phase of the laboratory test facility. In the study, 13

Arch	Exp Type	App	DoM	WF	T_c [°C]	T_{evap} [°C]	η_{exp} [%]	η_t [%]	size [kW]	Reference
Power	Scroll	NRORC	m	R134a	n/a	80	65	n/a	1.5	[59]
Power	vane	NRORC	m	R11	20	99	30	n/a	1.4	[6]
Power	Scroll	NRORC	m	R245fa	n/a	120	70	n/a	1.5	[27]
Power	Scroll	NRORC	m	Steam	n/a	n/a	34	n/a	11.5	[117]
Power	Scroll	RORC	m	R123	37	160	49.9	92.3	0.3	[116]
Power	Scroll	n/a	m	R134a	n/a	n/a	77	n/a	1	[121]
Solar	Scroll	NRORC	dev	R113	35	136	65	42	0.45	[118]
Solar	Scroll	NRORC	dev	R123/R34a	n/a	150	68	56	7.3	[85]
Solar	Scroll	NRORC	dev	R245fa	n/a	150	70	75	3	[111]
Solar	Scroll	RORC	dev	R245fa	32.5	82.5	n/a	n/a	0.67	[124]
Solar	Turbine	RORC	dev	R245fa	30	137	75	n/a	100	[82]
Solar	Vane	n/a	dev	R11	n/a	n/a	55	n/a	5	[57]
Solar	Screw	n/a	dev	R245fa	n/a	121	n/a	80	50	[112]
WHR	Scroll	NRORC	vp	R245fa	30	85	70	n/a	1.7	[24]
WHR	Scroll	NRORC	vp	R123	n/a	n/a	83	n/a	2.96	[119]
WHR	Gerotor	NRORC	vp	R123	n/a	n/a	85	n/a	2.07	[119]
WHR	Turbine	NRORC	vp	R245fa	n/a	137	n/a	60	100	[31]
WHR	Scroll	NRORC	vp	R245fa	10	180	70	n/a	2	[109]
WHR	Scroll	NRORC	vp	R123	10	180	70	n/a	1.98	[109]
WHR	Scroll	n/a	vp	Air	n/a	n/a	69	n/a	3.5	[115]
WHR-ICE	piston	TORC	vp	steam	100	450	78	44.9	24	[110]
CHP	Scroll	NRORC	m	R245fa	26.6	97.5	75	n/a	2.1	[113]
CHP-Biomass	Turbine	RORC	m	Decane	100	345	70	86	0.76	[107]
CHP	Vane	RORC	m	HFE7000	46.2	123	53.92	61.1	0.861	[123]
CHP	Wanke	NRORC	m	Steam	n/a	170	65	n/a	20	[58]
CHP-Biomass	Turbine	RORC	m	Decane	100	337	70	86	5.02	[108]
CHP	Vane	NRORC	m	Steam	n/a	n/a	75	n/a	20	[57]
Desalination	Scroll	n/a	p	R134a	n/a	60	50	35	1	[95]
HVAC	Scroll	NRORC	p	R245fa	n/a	87.2	n/a	n/a	1	[122]
n/a	Scroll	NRORC	n/a	Helium/R123	n/a	165	68	n/a	1.82	[22]
n/a	Scroll	n/a	n/a	Ammonia	n/a	n/a	60	7.2	5	[114]
n/a	Scroll	n/a	n/a	R245fa	n/a	100	71.03	71.9	2.5	[120]

Table 2.4: reference Installations for micro-ORC.

substances were each optimized by simulating an ORC micro-cogenerator, using as heat source the temperature profile of a biomass boiler. The objective functions in the optimization were: the expander inlet temperature, the evaporation pressure, the condensing pressure, the degree of subcooling of the fluid at condenser outlet and the expander power. Considering this analysis as input, 6 fluids were selected and further examined using the simulation model for the ORC developed for this thesis. The model was im-

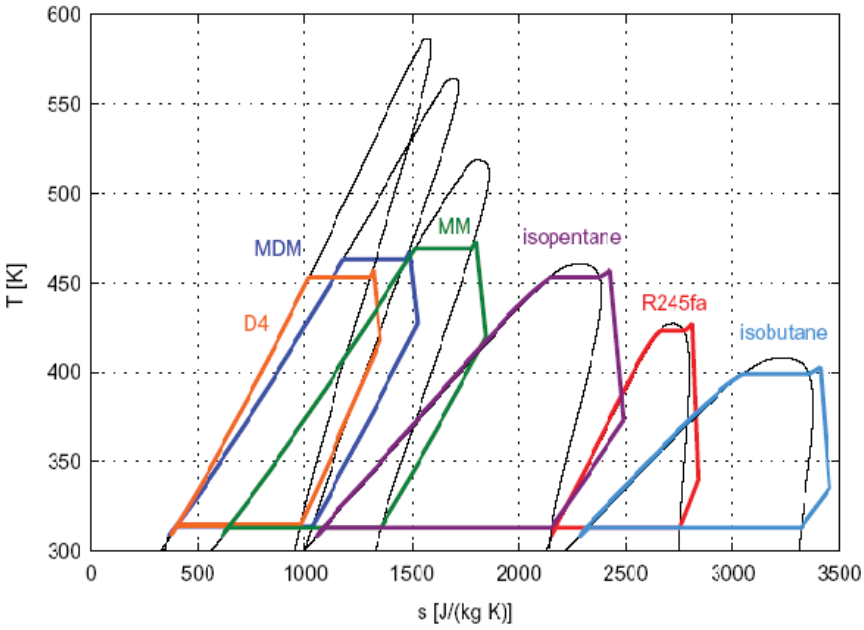

Figure 2.6: T-s diagram for WFs candidates low grade and waste heat recovery applications.

plemented both for a stand alone ORC system using electric heaters as heat source with diathermic oil as heat carrier, as well as a solar system with hot water by considering an evaporation, condensation temperatures and the evaporation pressure. The results are summarized in Figure 2.6 where it is visible the thermodynamic cycle diagram on the T-s plane for the WFs considered. Amongst these fluids Isopentane, R245fa and isobutane showed evaporation temperature within accepted limits, lower than 20 bar which is ideal for the applications of our interest. Furthermore, these fluids present critical temperatures within the range of heat carriers for low grade heat and waste heat systems.

2.4 Conclusion

In this chapter a literature review of ORC systems has been presented with focus on the WF selection criteria, heat source types and different fields of application. Indications have been provided for the degree of maturity for different ORC technologies as in Table 2.4, for micro systems of up to about 100kW plant sizes. Literature suggests the use of positive displacement type machines like the scroll as the expansion device for very small (<10kWe) applications while the screw and vane types expanders for small-medium size (10-100kW) ORC applications. Positive displacement pumps appear to be suitable for small scale ORCs because of low flow rates and high differential pressures required. This solution presents some drawbacks like low efficiency as the power consumption of the pump is an important fraction of that produced by the expander. Amongst the other components of an ORC are HEs, literature also suggests the use of PHEs for small size plants, instead of the shell and tube types suitable for big and medium size plants. Furthermore, no single fluid has been identified as optimal for ORC as the choice depends on the specific application and the working conditions. In terms of the applications, the review reveals that renewable sources such as solar, geothermal and biofuels leading the list, followed by waste heat recovered from industrial processes and internal combustion engines, as illustrated in Figure 2.7, are potential heat sources for ORC systems.

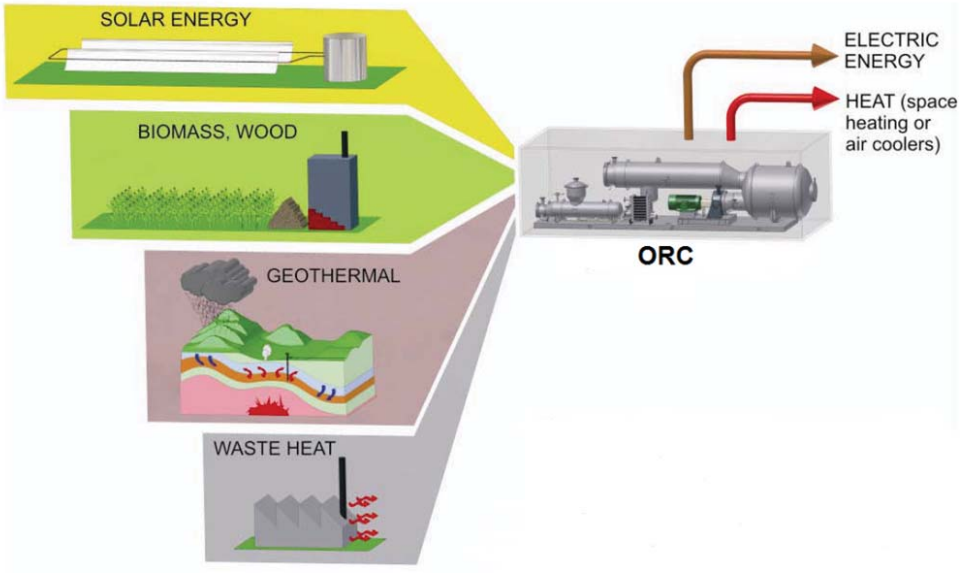

Figure 2.7: summary of the potential heat sources for ORC.

Chapter 3

System modeling

3.1 Overview

A process simulation model has been developed using the EES software to study the thermodynamic cycle of the ORC with R245fa as WF. The aim was to study the system behavior in different operating conditions and using different solutions for the plant components. A model of the solar power system was also developed using Trnsys platform to analyze the possibility of integration with the ORC prototype. Trnsys is a modular, component based simulator and it has widely been used to perform analytical simulations of heating and cooling systems providing the possibility to integrate other mathematical solvers such as MATLAB, SIMULINK AND EES. The models were later integrated to achieve a common platform for studying the combined solar-ORC system. The main objective of the simulation analysis was to study the system under real operation conditions, then to assess the influence of different parameters settings like the solar collector surface area and type, process pumps flow rate, auxiliary components consumption, evaporation and condensation temperature profiles in order to achieve the best result in terms of the electric power developed by the ORC expander. The aim of the model is to study a small scale ORC power plant with expander delivery power of about 4kW. The heat exchangers are sized with maximum thermal loads of 27 and 25 kW for the evaporator and condenser respectively while the regenrator is sized with a value of 9 kW. The maximum cycle temperature is lower the the critical temperature of the chosen fluid (R245fa), the condensation temperature, between 20-30°C. The feed pump selected can process the working fluid up to about 20 bar. The model has been developed based on these design specifications, while the choice of the components is based on the considerations presented in the previous chapter, matching the characteristics of each component with the desired application.

3.2 Engineering equation solver (EES)

EES is a commercial software for the solution of a set of algebraic equations. EES [125] can also solve differential equations, equations with complex variables, do optimization, provide linear and non-linear regression, generate publication quality plots, simplify uncertainty analyses and provide animations. There are two major differences between EES and existing numerical equation solving programs. First, EES automatically identifies and groups equations that must be solved simultaneously. This feature simplifies the process for the user and ensures that the solver will always operate at optimum efficiency. Second, EES provides many built-in mathematical and thermophysical property functions useful for engineering calculations. EES is particularly useful for design problems in which the effects of one or more parameters need to be determined. The program provides this capability with its Parametric Table, which is similar to a spreadsheet. The user identifies the variables that are independent by entering their values in the table cells. EES will calculate the values of the dependent variables in the table. The relationship of the variables in the table can then be displayed in publication quality plots. EES also provides capability to propagate the uncertainty of experimental data to provide uncertainty estimates of calculated variables.

3.3 ORC Simulation model

The ORC model was developed within the EES software environment to compute the thermodynamic analysis of the vapor cycle. The EES commercial software includes the National Institute of Standards and Technology (NIST) database that contains thermodynamic data for the organic fluid R245fa employed in the cycle [126]. The ORC mathematical model was called in the main Trnsys simulation using the "type 66" component. The EES model description is done with reference to the system layout of Figure 3.3 and thermodynamic diagram on the T-s plane in Figure 3.1.

3.3.1 Expander model

The expander considered in the model is a scroll expander type, a constant isentropic effiency η_{is}, of 65% was considered in the preliminary model, according to literature [127] and experimental data. The enthalpy at expander outlet (h_7) was computed according to (3.1):

$$h_7 = h_6 - \eta_{is}(h_6 - h_{7,is}) \tag{3.1}$$

Where the ideal isentropic expansion enthalpy ($h_{7,is}$) is the enthalpy at the end of an ideal isentropic expansion and h_6 the expander inlet enthalpy. h_6 is obtained considering a superheating of 2K on T_5. The electric power, $\dot{W}g$, generated by the expander considering a constant conversion efficiency, η_g, of 0.9, is given by:

$$\dot{W}_g = \eta_g \dot{m}_f (h_6 - h_7) \tag{3.2}$$

with $\dot{m}_f$ the WF flow rate.

3.3.2 Evaporator model

The vapor generator is modelled considering two sub blocks in order to handle both the liquid and the vapor phases of the fluid: the economizer, where the WF is in liquid state and the evaporator, where the fluid passes in the vapor state [128]. For the evaporator, a value of 5K was assigned for the pinch point difference (ΔT_{pp}), therefore:

$$\Delta T_{pp} = 5K \tag{3.3}$$

and

$$T_{h4} - T_4 = \Delta T_{ppe} \tag{3.4}$$

The WF power was calculated by computing a heat balance across the heat exchanger according to (3.5) thus obtaining the increase in the specific enthalpy of the fluid stream, hence the calculation of the WF flow rate, R245fa flow rate ($\dot{m}_f$) of the power fluid, R245fa.

$$\dot{m}_w c_{pw} \Delta T_w = \dot{m}_f \Delta H \tag{3.5}$$

where ΔH is the enthalpy rise in the evaporator from h_3 to h_5, $\dot{m}_w$ the collector water flow rate, ΔT_w temperature difference in the secondary circuit between T_{h3} and T_{h5}.

3.3.3 Condenser model

The condenser is a counter flow plate heat exchanger type and was modelled in a similar way as done for the evaporator and by performing the energy balance computation using (3.6):

$$\dot{m}_f \Delta H = \dot{m}_{cw} c_{pw} \Delta T_{cw} \tag{3.6}$$

where ΔH is the enthalpy change of the condenser WF, h_8 and h_1, $\dot{m}_{cw}$ is the cooling water flow rate, ΔT_{cw} is the temperature difference of the cooling water loop between inlet and outlet T_{c1} and T_{c8} respectively and c_{pw} is the cooling water specific heat capacity. The cooling water inlet temperature

is an input to EES obtained from an analogous energy balance analyses within the dry cooler. The pinch point temperature across the condenser was assigned the same value as for the evaporatoris and defined according to (3.7):

$$T_9 - T_{c9} = \Delta T_{ppc} \tag{3.7}$$

3.3.4 Regenerator model

The component has been modelled by imposing a temperature difference (ΔT_{reg}) of 10K between the fluid leaving the hot side T_8 and the fluid entering the cold side T_2 of the regenerator according to (3.8):

$$\Delta T_{reg} = T_8 - T_2 \tag{3.8}$$

By performing an energy balance between the two fluid streams, it is possible to calculate the regeneration efficiency ε_{reg} considering the relation in (3.9).

$$\varepsilon_{reg} = \frac{T_7 - T_8}{T_7 - T_2} \tag{3.9}$$

3.3.5 ORC feed pump model

The ORC pump was modeled using the thermodynamic state conditions at both inlet and outlet such as temperatures and pressures, hence the enthalpy change across the component. The electric power absorbed by the pump was calculated using (3.10):

$$\dot{W}_{PORC} = \frac{\dot{m}_f \Delta H}{\eta_p} \tag{3.10}$$

where, $\dot{W}PORC$ is the power absorbed by the pump, ΔH the enthalpy change across h_1 and h_2, and η_p the pump efficiency assigned as 70%.

3.3.6 Pressure drops

In the EES model, the pressure losses (losses due to pipe fittings, joints, tube convergence, divergence, elbows, surface roughness and other physical properties that will affect the pressure drop) have been considered proportional to the pressure at the inlet of the specific components. The thermodynamic cycle diagram for the WF employed in the system can be seen in Figure 3.1

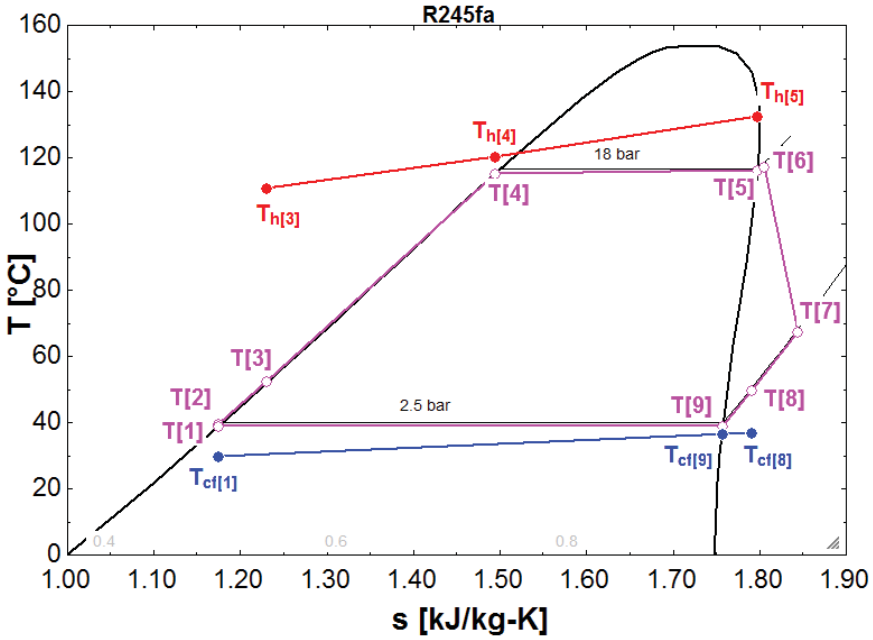

Figure 3.1: T-s diagram for R245fa: heat source temperature 130°C, fluid evaporation temperature 120°C, expander isentropic efficiency 0.65, pump efficiency 0.7, condensation temperature 24°C,

3.4 Trnsys software

Trnsys studio offers a complete and extensible simulation environment for the transient simulation of systems, including multi-zone buildings. It is used by engineers and researchers to analyze and validate new energy concepts, from simple domestic hot/cold water systems to the design and simulation of buildings and their equipment, including control strategies, occupant behavior, alternative energy systems (wind, solar, photovoltaic, hydrogen systems) etc. A Trnsys project is typically setup by connecting components graphically in the Simulation Studio shown in Figure 3.2. The choice of using this program lies in its simplicity to use, inserting components and control of the typical devices used in solar systems, such as panels, pumps and heat exchangers. If a component is missing or does not meet the requirements of our model, it is easy to build new blocks through the use of FORTRAN code or by inserting a call to an external application, such as MATLAB or EES. Trnsys uses a procedural language to define its simulation models and discrete time integration algorithm. Models can be encapsulated in so-called Types, which are FORTRAN routines with standardized arguments. Many Types implement their own mathematical solvers for differential and algebraic equations. The system model is then solved using either successive

substitution with relaxation or a differential equation solver that converts the system of differential equations to non-linear algebraic equations which it solves using Powell's method, a combination between steepest descent and Newton's method.

3.5 The solar plant model

The simulation software Trnsys 17 [129] was used to simulate the solar system and later used for the integration of the ORC unit modeled in EES by means of an external routine. The simulated model is built based on design know-how gained by working with both solar and ORC experimental facilities separately. The Trnsys simulation was performed for a whole year period with a simulation time step of one hour which allows flexibility of the meteorological conditions variability. The yearly weather data was provided by the Typical meteorological Year (TMY) format weather reader component "type 99" of the Trnsys library. The tolerance integration and convergence parameter have been set to 0.01. Energy balance calculations were computed to control the convergence and accuracy of the results. The graphic user interface of the simulation model can be seen in Figure 3.2.

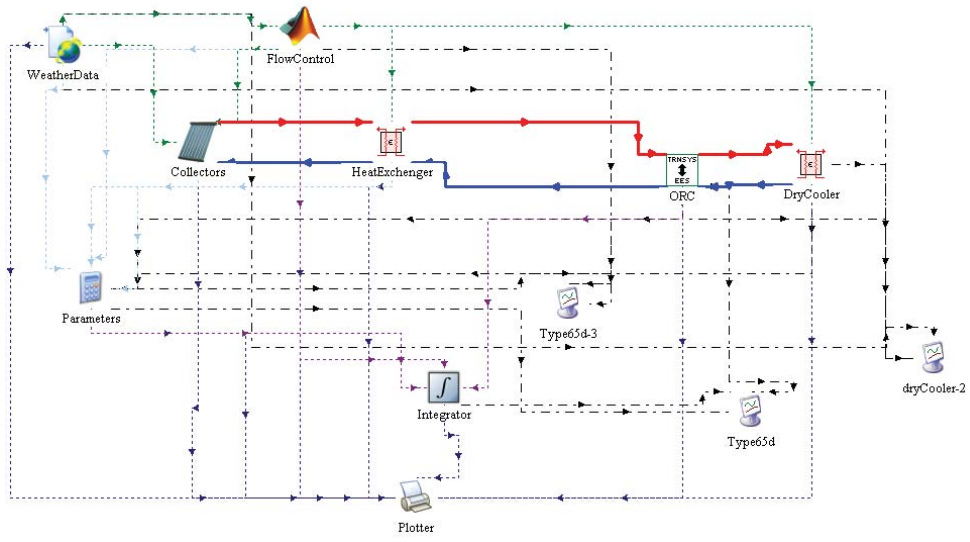

Figure 3.2: graphic user interface of TRNSYS simulation model.

3.5.1 Panel orientation and positioning

Weather data available in Trnsys are used to assess the operational profile of the plant in different period of the year. As visible in Table 3.1, the slope of the panels is needed to calculate the insolation on the tilted surface. In this model a value of 30° for horizontal is considered. The reason of this decision dwells in the fact that for the location considered, this slope guarantee the maximum benefits in terms of energy.

Parameter	value
location	Trieste
longitude	13° 48' 15" E
latitude	45° 38' 1" N
tracking mode	1-fixed surface
slope of surface	30°
azimuth of surface	0° pointing South
ground reflectance without snow	0.2
ground reflectance with snow	0.7

Table 3.1: input parameters for panel orientation.

3.5.2 Solar collector model

The Trnsys library preloaded "type 71" component was used to model the evacuated tube collectors, the complete simulation model has been presented by the author in [134]; the input parameters include collector inlet temperature, flow rate and efficiency coefficients are set by the user. This type simulates a solar field of many panels linked to each other, but for simplicity just one panel is shown in the layout though the surface area considered is the area of the total solar field. The layout of the combined solar ORC discussed above is visible in Figure 3.3. The thermal efficiency of a given solar collector can be calculated as a function of the incident solar radiation, the mean collector temperature, and the ambient air as specified in European standard EN 12972 [130] using the general formula in (3.11):

$$\eta = \eta_0 - C_1 \frac{(T_m - T_{amb})}{G} - C_2 \frac{(T_m - T_{amb})^2}{G} \tag{3.11}$$

where η is the collector efficiency, η_0 is the optical efficiency, C_1 and C_2 are respectively the first order and second order loss coefficients, obtained from manufacturer datasheet [131], G is the solar radiation, the ambient temperature T_{amb} and the collector mean temperature T_m are expressed as follows:

$$T_m = \frac{T_{h1} + T_{h2}}{2} \tag{3.12}$$

(3.11) can be rewritten as in [132]:

$$\eta = \eta_0 - C_1\frac{\Delta T}{G} - C_2\frac{(\Delta T)^2}{G} \tag{3.13}$$

where ΔT is the difference between the collector water mean temperature and the ambient temperature expressed as:

$$\Delta T = T_m - T_{amb} \tag{3.14}$$

The $\dot{Q}c$ is linked to the collector efficiency according to:

$$\dot{Q}_c = \eta G A \tag{3.15}$$

with A is the total surface area of the collector arrays. The useful energy transferred from the collectors to the fluid is given by:

$$\dot{Q}_c = \dot{m}_w c_p \Delta T_{sc} \tag{3.16}$$

with $\dot{m}_w$ is the flow rate in the collector, c_p the specific heat capacity, ΔT_{sc} the temperature difference across the collector.

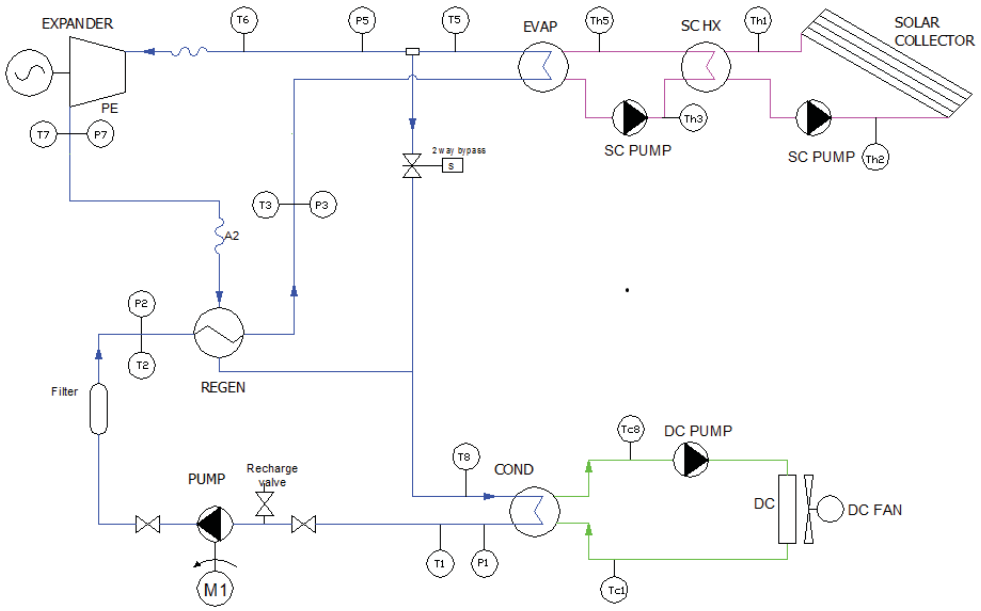

Figure 3.3: scheme of the solar thermal system.

3.5.3 Solar collector heat exchanger model

A constant efficiency heat exchanger, "type 91" from the Trnsys component library was used to model the heat exchanger named Solar Collector Heat Exchanger (SCHX) in Figure 3.3. The heat exchange within the component is computed according to the energy balance relation in (3.17)

$$\dot{m}_c c_{ps} \Delta T_{sc} = \dot{m}_w c_{pw} \Delta T_w \tag{3.17}$$

where collector water flow rate ($\dot{m}_c$), specific heat capacity primary circuit (c_{ps}) of the antifreeze solution in the primary circuit, specific heat capacity secondary circuit (c_{pw}), temperature difference across the collectors (ΔT_{sc}) in the secondary circuit, temperature difference in the secondary circuit (ΔT_w). The heat exchanger is considered to be adiabatic.

3.5.4 Circulating water pump model

The energy consumption of the circulation pumps (collector and cooling water) has been assessed considering the following equation (3.18):

$$\dot{W}_p = \frac{Hydraulicpower}{pumpefficiency} = \frac{\dot{m}_w g H}{\eta_p} \tag{3.18}$$

where collector water flow rate ($\dot{m}_w$) is the flow rate, acceleration due to gravity (g) the acceleration of gravity, head (H) the head, and pump efficiency (η_p) the pump efficiency chosen is 70%.

3.5.5 Dry cooler model

The dry cooler was modelled in the same manner as the collector heat exchanger and using the same library component type with the unique difference being that the heat exchange is between water and air. The effectiveness assumes the value 85%, the dry cooler inlet temperature ambient temperature (T_{amb}) is provided by the meteorological data available in Trnsys.

Dry cooler pump model

The energy consumption of the cooling water pump was computed in a similar manner as for the collector water pump circulation pumps (collector and cooling water) has been modeled as in (3.18):

Dry cooler air fan model

The Trnsys "type 91" component was used to model the air-dry cooler, the energy consumption of the dry cooler air fan has been assessed in a similar

manner like for the circulation water pumps:

$$\dot{W}_f = \frac{fanpower}{fanefficiency} = \frac{\dot{m}_a g H}{\eta_{fan}} \tag{3.19}$$

where $\dot{m}_a$ is the air flow rate, g acceleration of gravity, H the head, and the η_{fan} the fan efficiency chosen as 70%.

3.6 Flow rate control

A Matlab script has been developed and called as a subroutine from the Trnsys component library with "type 15" to handle the variation of:

- the flow rates of the solar collectors: the collector flow rate is dependent on the solar radiation and has been optimized to maximize the electricity production;
- the condenser cooling circuit: dry cooler air and liquid flow rates have been assessed taking into account the ambient conditions in order to minimize electricity consumption;

In both cases the pumps and dry cooler air fan switches on when there is solar radition and off as soon as the radiation is weak enough to produce hot water.
The flow rate of the ORC feed pump is determined by the temperature of the hot water from the solar collector and is computed according to the energy balance in the evaporator between the two streams: collector water and R245fa as in (3.5).

3.7 Efficiency calculations

The ORC efficiency ORC efficiency (η_{ORC}) is obtained as the ratio between the Net Energy produced by the ORC unit ($\dot{Q}_{net}$), and thermal energy absorbed by the collector ($\dot{Q}_c$) transferred from the collectors to the ORC WF according to (3.20):

$$\eta_{ORC} = \frac{\dot{Q}_{net}}{\dot{Q}_{coll}} \tag{3.20}$$

where $\dot{Q}_{net}$ is the difference between the power generated by expander ($\dot{W}_g$) and Energy absorbed by auxiliaries ($\dot{Q}_{aux}$). The latter term include the following components: the collector and cooling water pumps, power absorbed by water pump ($\dot{W}_p$), the ORC pump, power absorbed by ORC pump ($\dot{W}_{PORC}$), the dry cooler fan, power absorbed the dry cooler fan ($\dot{W}_f$) and the power consumed by the control system power absorbed by the control system ($\dot{W}_{CS}$). In a similar manner, we can have:

$$\eta_{coll} = \frac{\dot{Q}_{coll}}{\dot{Q}_{sol}} \tag{3.21}$$

with collector efficiency (η_{coll}), given as the ratio between $\dot{Q}_c$ and Solar energy made available to collectors ($\dot{Q}_s$). Finally,

$$\eta_{Overall} = \frac{\dot{Q}_{net}}{\dot{Q}_{sol}} \tag{3.22}$$

where system overall efficiency ($\eta_{Overall}$) is defined as the ratio between $\dot{Q}_{net}$ and $\dot{Q}_s$.

Chapter 4

Experimental activities

4.1 Overview

The first activities were done at the ENESYSLAB of the University of Trieste equipped with an ORC test facility together with a Pump test bench. The analyses involve laboratory experiments of the ORC prototype using electrical resistances to simulate the heat source. The Laboratory tests have formed the base for the development of ORC prototypes. The field test consists of the coupling of one of the ORC prototype to a Parabolic Trough solar collector system (combined solar ORC) installed at Florence-Italy. The field test results confirm the feasibility of the combined solar ORC system and the potential profits obtainable in such a combination in terms of electric and thermal generation.

4.2 Laboratory test

4.2.1 Test on ORC experimental facility

The laboratory at the University of Trieste is equipped with an ORC test bench connected to a set of electric resistances used to simulate the heat source.The heat transfer medium employed within the electric resistances is a treated vegetable oil (Paryol F57). The test bench is made of different subsystems that will be described here below:

- Heat source: a storage tank, two electric resistances with a thermal capacity of 41kW each in a parallel arrangement, a process pump for the circulation of the heat transfer fluid through the resistances where it is heated to a temperature defined by the operator and a second process pump used to drive the hot oil from the storage tank to the ORC evaporator where the heat exchange with the working fluid of

the vapor cycle (R245fa) takes place. An inverter is used to control the speed of the circulating pump hence the volumetric flowrate of the heat transfer fluid. A power control system is also available to activate the heating load hence the the temperature of the heat transfer fluid;

- ORC loop: the ORC test bench comprises, a diaphragm pump that pressurizes and circulated the working fluid (R245fa) through the circuit, the pump is coupled to an inverter that controls its speed and consequently the mass flow rate, a regenerator where the high pressure fluid from the pump is pre-heated using the expanded hot fluid, an evaporator where heating, evaporation and superheating of the working fluid takes place, the superheated fluid at the evaporator outlet expands in a scroll expander producing the mechanical work, the fluid returns into the regenerator before condensing in a water cooled condenser to close the circuit the fluid enters a sub cooler where condensation completes before suction by the pump start and the loop repeats;

- Heat sink: two solutions for heat removal from the ORC unit of the test bench. One of the solutions consited in supplying the cooling water by means of a watercourse in an open loop where the condensation temperature is imposed by adjusting the water flow rate by means of a manual control valve. The second solution was achieved by installing an air dry cooler unit Figure 4.13 with the cooling water running in a closed loop, the condensation temperature in this case was obtained by adjusting the air flowrate thus varying the fan motor speed;

- Electrical load: in order to dissipate the electricity produced by the ORC expander, an electric load (composed of three rheostats arranged in parallel used to apply the breaking torque on the expander) is directly coupled to the expander;

- Measurements and acquisition system.

The layout of the described laboratory facility is visible in Figure 4.1.

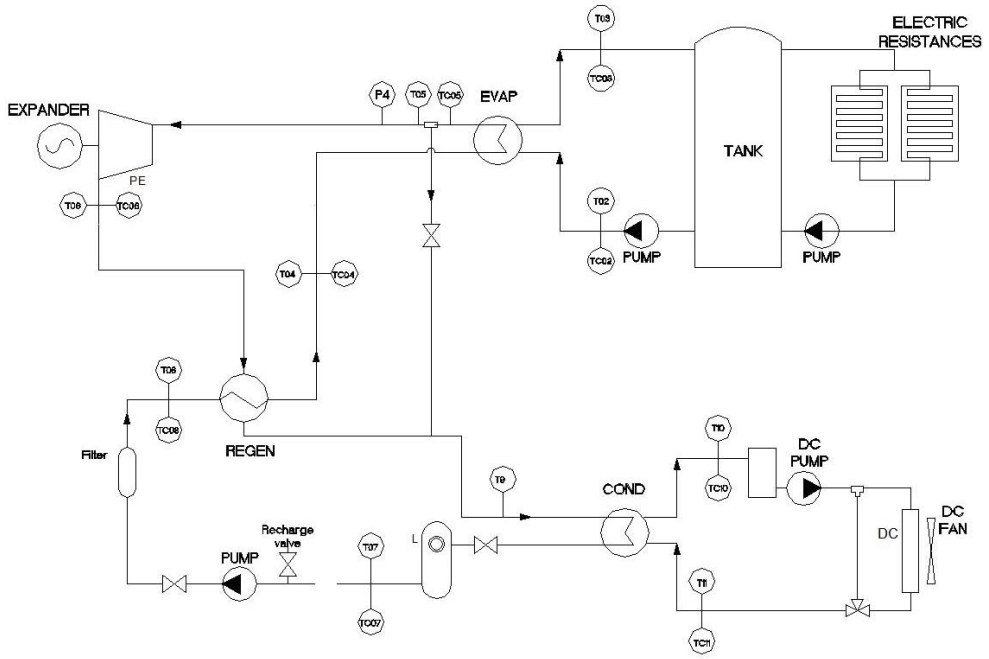

Figure 4.1: schematic representation of the test facility at the University of Trieste.

Test description

Our laboratory test bench can be considered to be of two distinctive architectures: the NRORC where the working fluid does not pass through the regenerator and the RORC where the fluid flows through the regenerator. To pass from one architecture to the other it is sufficient to close or open the by-pass valves that are situated at both entrances of the component thus deviating the working fluid to and from the regenerator. The data collected during the laboratory work include: the thermal oil and fluid mass flow rates, the electric power generated by the expander, temperatures and pressures of the fluid measured along the circuits. The electric power absorbed by the auxiliaries (the ORC feed pump, inverter and data acquisition system) are estimated by means of a power meter. The ORC test bench has been utilized to characterize the performance of the scroll expander used in the prototype as will be explained in the next chapter. A photo of the laboratory equipment is visible in Figure 4.2 The expander type installed on the test bench is a compressor derived scroll. Values of expansion ratio, net produced power and isentropic efficiency have been obtained by testing the expander whose displacement volume is $9.1cm^3$, using R245fa as working fluid.

Figure 4.2: the ORC test facility at the University of Trieste.

The tests have shown that the maximum overall expander isentropic efficiency η_{is}, (about 62%) is achieved for an expansion ratio of the scroll machine equal to about four. Such a value of efficiency can also be found in literature, as in [118], although higher values (up to 68-70%) have been reported in [30]. The expander isentropic efficiency η_{is} obtained experimentally from the test bench is presented in Figure 4.3 as function of the expansion ratio for different expander rotational speeds. In many cases, however, the value of efficiency measured in actual operating conditions is too small to achieve a good performance of the power cycle and multiple expanders systems can be considered [133]. In Figure 4.3, where the expander efficiency is shown as a function of the expansion ratio, it is possible to see that when high expansion ratios are imposed, the expander efficiency is much lower than its maximum value. It is also possible to see in Figure 4.4 the trend in the expander electric power generated as a function of the expansion ratio. In the experimental tests the temperature of the heat source has been regarded to vary in the range 90-150°C. This range can be typical for geothermal applications and medium temperature solar thermal collectors. In particular, the latter applications can be of interest if a solar cooling system is included as well.

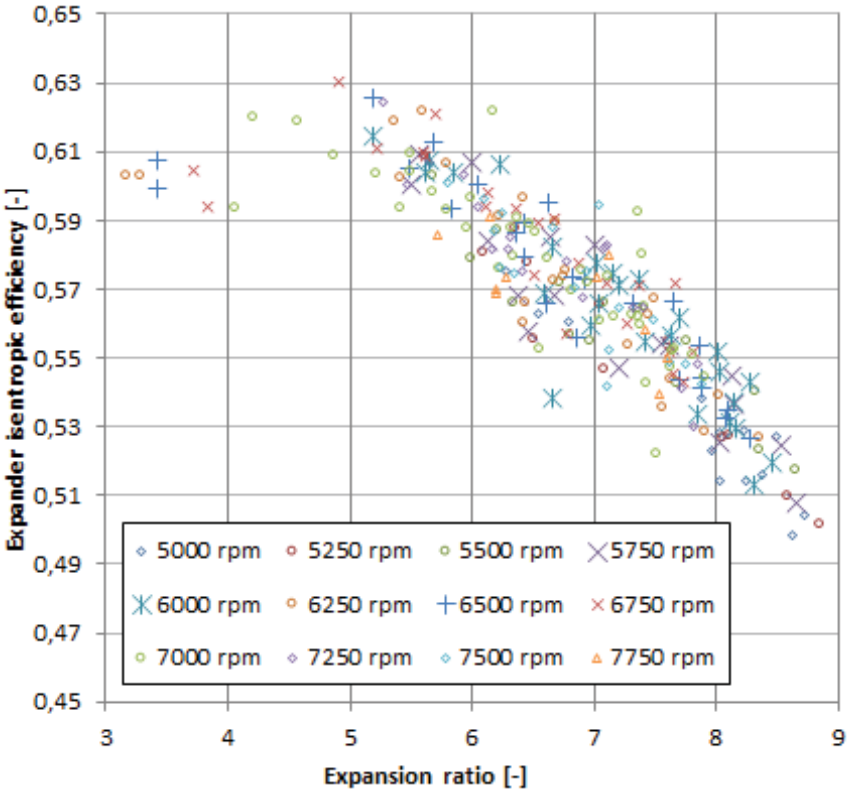

Figure 4.3: expander efficiency η_{is} vs. the expansion ratio at various rotational speeds.

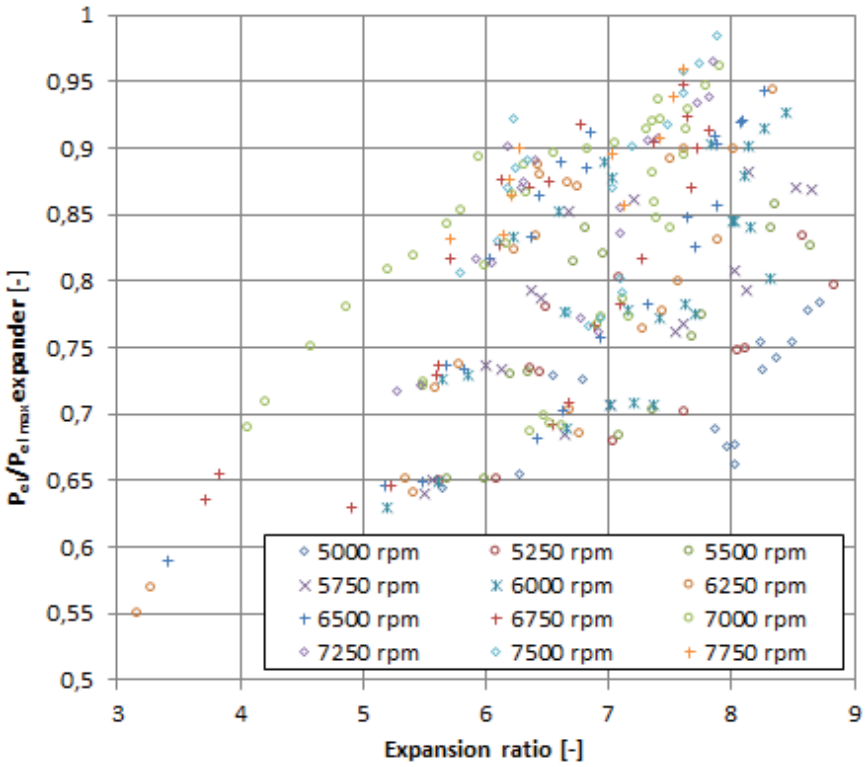

Figure 4.4: expander electric power vs. the expansion ratio at various rotational speeds.

4.2.2 Technical description of the components of the ORC test bench

A focus on the technical description of the main components: mechanical, electrical and instrumentations used for measurement and data acquisition, on the ORC test bench is presented in this section.

Expander

The expander is adapted from a scroll compressor designed for use in air conditioning systems. The scroll is a positive displacement machine essentially formed by two identical spiral shaped wraps fixed on back plates. One wrap has a hole in the back plate and is held fixed, while the other can orbit. If the machine is used as an expander, the working fluid enters the central chamber through the fixed back plate hole, then it moves towards the external endings of the wraps and exits. The drawbacks of this kind of solution are mainly two: the low fixed volumetric expansion ratio and the small displacement volume, that are not always well-suited for the requirements of power producing ORC. The expander as seen in Figure 4.5, looks

Figure 4.5: the scroll expander installed in the lab facility.

very compact. Referring to the illustration one can notice the dimensions

of the collectors which are 10 mm and 16 mm referring to the inlet and discharge sides respectively. The geometry of the expander can be assimilated to a cylinder about 20 cm high with a diameter of 12 cm which houses the alternator coils at the bottom and the spirals at the top. The machine can be opened for cleaning through a flange allowing to remove the upper casing revealing the scrolls, which are shown below in Figure 4.6. Some characteristics of operation are provided in Table 4.1 below.

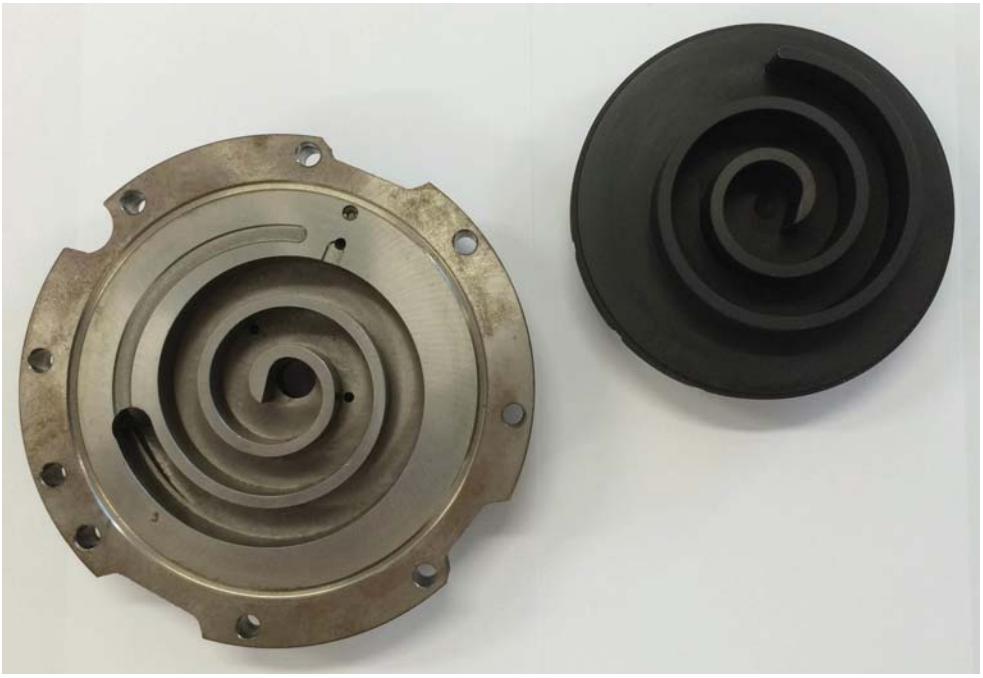

Figure 4.6: spirals of the fixed and mobile scrolls.

parameter	units	value
min rotation speed	[rpm]	8000
max rotation speed	[rpm]	9000
max fluid temperature at inlet	[°C]	150
max fluid temperature at outlet	[°C]	100
max surrounding temperature	[°C]	60
max fluid pressure at inlet	[bar]	17
lubrification	-	required

Table 4.1: technical specifications of the scroll expander.

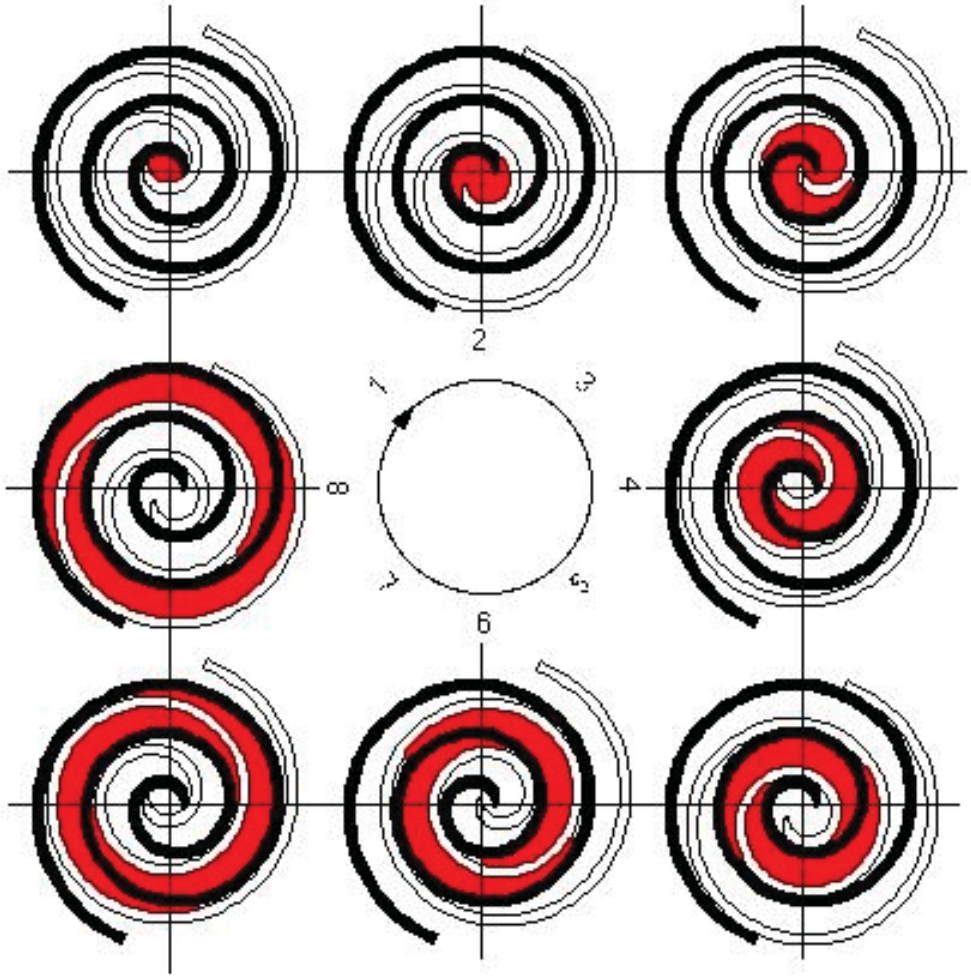

Figure 4.7: working principles of the scroll expander.

Feed pump

The pump used is the G03 series membrane type pump produced by Hydra cell Industrial pumps. The pump is characterized by a sealless pumping chamber and hydraulically balanced diaphragm, guaranteeing a perfect sealing between chamber and external ambient, with high compression ratios suitable for processing fluids over a wide range of pressures and flows. They generally consist of a piston that follows a reciprocating motion. The rotational motion of the electric motor is converted using the shaft-connecting rod mechanism, with the deformation of the elastic membrane causing the variation of the internal volume allowing fluid suction and discharge/delivery processes. The pump rotational speed is varied by means of an inverter thus the variation of the fluid flow rate [135]. Figure 4.8 shows the characteristic curves of the diaphragm pump while Table 4.2 shows the manufacturer's for the diagpragm pump.

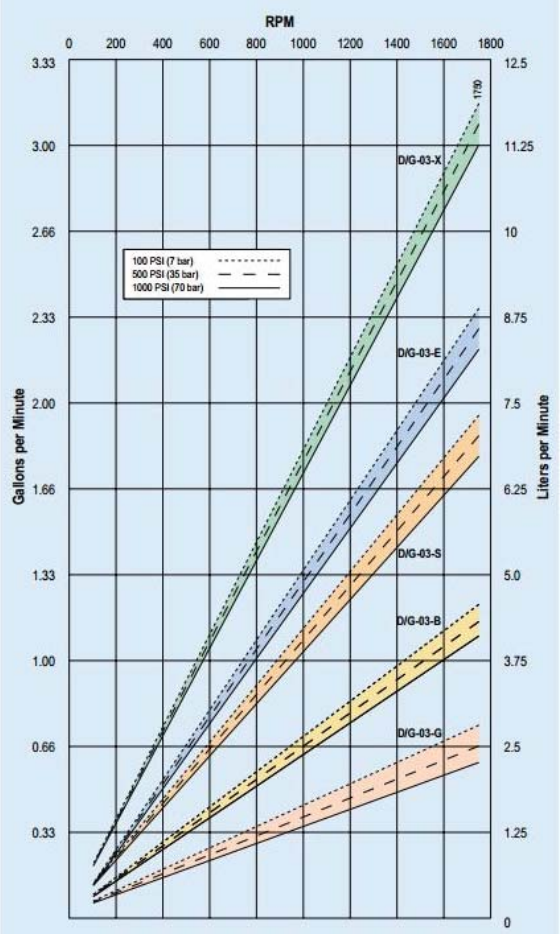

Figure 4.8: characteristic curves for the diaphragm pump. [135]

parameter	units	value
Flow rate ar 1750 rpm	[l/min]	8.3
max suction pressure	[bar]	17.3
max delivery pressure	[bar]	83
max differential pressure	[bar]	66
max casing temperature	[°C]	121
weight	[kg]	12.7

Table 4.2: technical specifications of the diaphragm pump.

Heat exchangers

The HEs installed on both the test bench and ORC prototypes are designed and constructed by SWEP and are classified as AISI 316, employing as materials, a combination of stainless steel or Mo-steel alloy, brazed with either copper or Nickel rated for standard or higher pressures according to the specific application. The flow pattern in the HE is illustrated in Figure 4.9, the technical specifications of each HE are summarized in Table 4.3. The

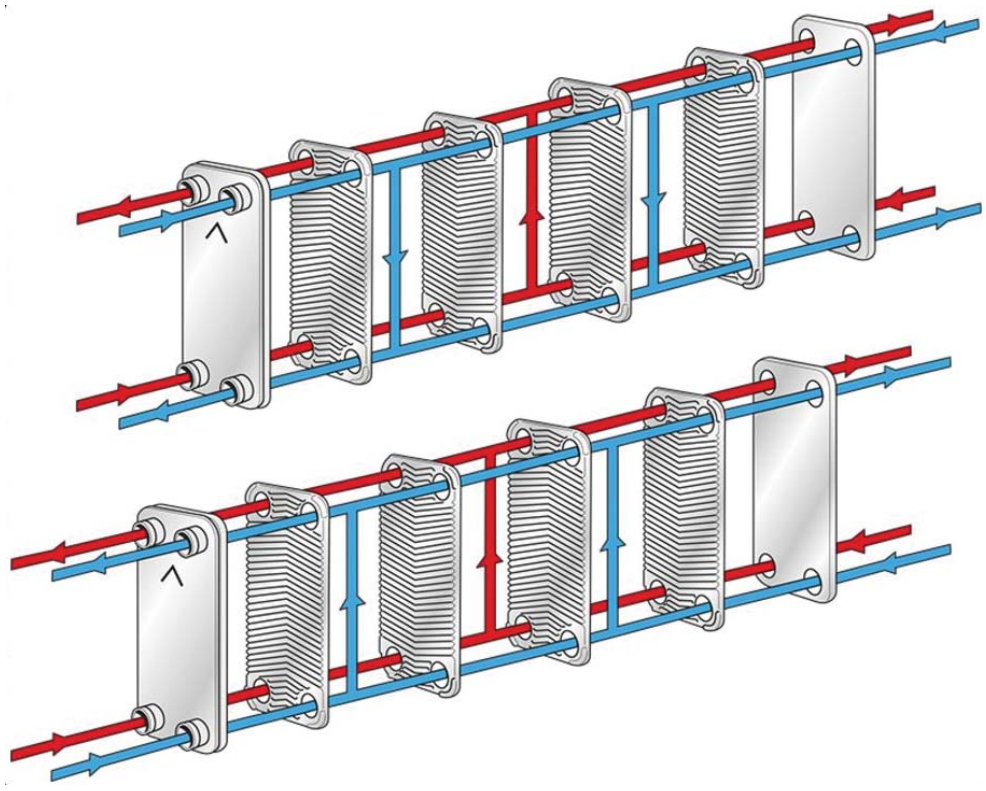

Figure 4.9: flow pattern of the plate heat exchangers PHEs.

denomination of the HE is of the form

$BUH - V - (X)(Y) - (Z)$
where U is the size or length of the HE, V the total number of plates, X the alloy type (Stainless steel or Mo-steel), Y the brazing material (copper or nickel) and Z the rating pressure (standard or High).

Evaporator

The HE used as evaporators on both systems are produced by SWEP as earlier said and belongs to the B25 series, it is made with stainless steel, copper brazed and rated for high pressure. The fluids involved across the evaporator are: the R245fa and thermal oil (hot water in the case of the field test on ORC prototype), in both cases the fluids flow in a counter-current configuration. All three phases of the fluid: heating, evaporation and superheating occur within the evaporator. The scheme of the evaporator is shown in Figure 4.10 with the technical data of exchanger size.

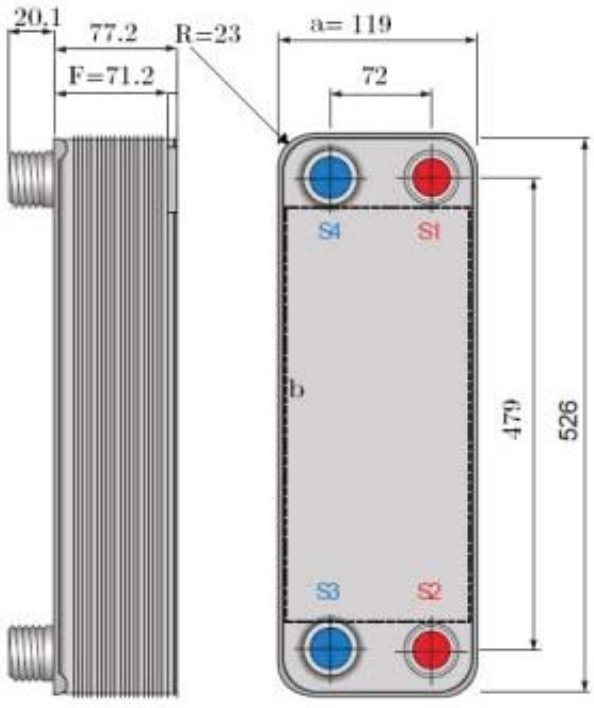

Figure 4.10: scheme of the evaporator HE.

Regenerator

The HE used for the regenerator is very similar to that used for the evaporator, both designed by SWEP. R245fa flows in both channels of the regenerator, in one channel the fluid is in the liquid state and in vapor state in the other channel. The datasheet of the regenerator is shown in Figure 4.11.

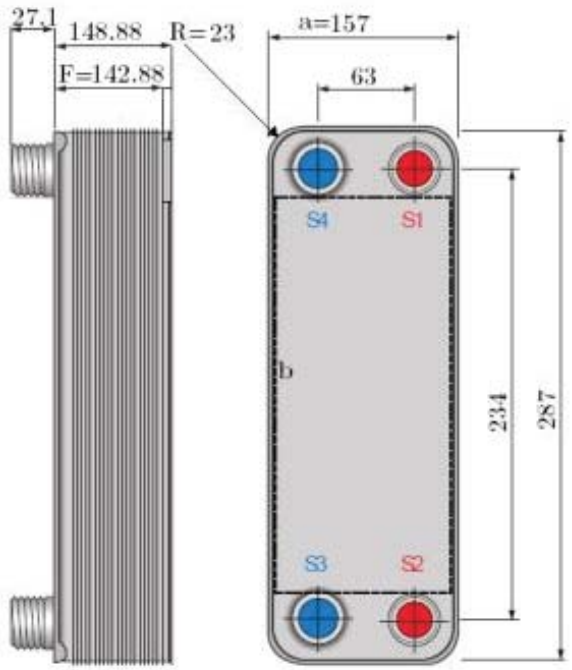

Figure 4.11: scheme of the regenerator HE.

Condenser

For the condenser, a similar HE as the previous two described above have been used with the main difference being in the size and the fluids that flow through, the heat exchange is between: R245fa in one channel and water in the other, in a counter-current flow arrangement. For the ORC test bench, the heat sink is an open loop water flow. Regarding the prototype, heat removal from R245fa during the laboratory was obtained as for the test bench, while for the field test a dry cooling unit was installed, thus, the heat removal was obtained in two steps; the first using water followed by air. In Figure 4.12 and Table 4.3 it is possible to find the technical specifications of the condenser.

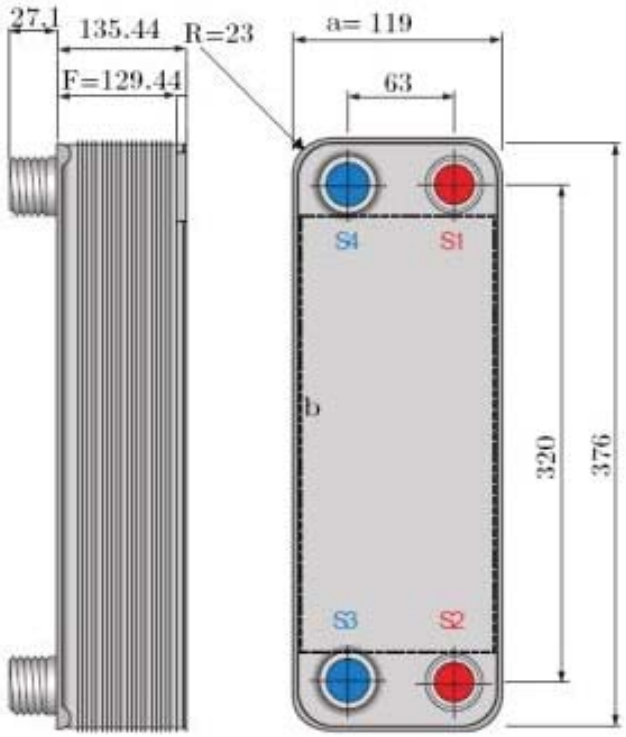

Figure 4.12: scheme of the condenser HE.

Parameter	units	evaporator	regenerator	condenser
Max flow rate	$[m^3/h]$	9	17	17
Max working pressure at 155 °C	[bar]	45	31	31
Max working pressure at 255 °C	[bar]	36	27	27
Min working temperature	[°C]	-196	-196	-196
Test pressure	[bar]	69	50	45
Number of plates	-	20	36	56
Number of inner channels	-	9	17	27
Number of outer channels	-	10	18	28
plate area	$[m^2]$	0.065	0.028	0.04
Total heat transfer area	$[m^2]$	1.134	0.952	1.2
channel volume	$[dm^3]$	2.07	0.063	0.082
Plate thickness	[mm]	0.3	0.28 0.3	
holdup volume inner circuit	$[dm^3]$	1	1.07	1.23
holdup volume outer circuit	$[dm^3]$	1.11	1.134	1.312
Total weight of plates	[kg]	5.7	5.76	5.57
Plate pack height	[mm]	75	88.6	75.7
a	[mm]	526	287	376
b	[mm]	119	117	119
F	[mm]	48.8	88.64	129.44

Table 4.3: technical specifications of the HE.

Dry cooler

The dry cooler installed in the system for heat dissipation, is a liquid to air HE, and a fan blows the ambient air over finned tubes containing water. The installed dry cooler, produced by Alfa-Laval model DG501, is shown Figure 4.13

Figure 4.13: view of the dry cooler.

max cooling capacity	[kW]	29
water temperature inlet/outlet	[°C]	29.6/25
nominal flow rate	$[m^3/h]$	5.9
max operating pressure	[bar]	4
air temperature inlet/outlet	[°C]	22.7/26.4
air flow	$[m^3/h]$	24000
pressure loss at max flow	[mbar]	290
max absorbed power	[kW]	0.54
power supply	[V, Hz]	230, 50/60
unloaded weight	[kg]	42

Table 4.4: main characteristics of the dry cooler [136].

Electric Load

As already explained at the beginning of this chapter, an electric load made of three rheostats connected in parallel have being used to dissipate the electric power generated by the scroll expander. The RC model linear slider rheostats used are produced by Italohm, and consists of one or more cylindrical porcelain tubes with an alloy wire resistive winding together with a sliding contact used to adjust the resistence thus the breaking load of the expander [137]. One of the rheostats is shown in Figure 4.14.

Figure 4.14: image of the rheostat.

Measuring Instruments

The instruments used for measuring the physical quantities of the test bench will be in the following described.

Thermocouples

A total of ten T-type thermocouples have been installed on the test bench. The thermocouples have an accuracy of ±1° C [138]

Pressure measurement

The JUMO DELOS SI with a 4-20mA analog output pressure transmitters have been used for measuring the pressures at different points along the circuit of the test bench. The sensor measures pressure ranging from 400 mbar to 60 bar with a ±0.1% accuracy at full scale [139].

Flowmeters

Two mass flow meters are installed on the test bench: one on the ORC loop and the other on the hot oil loop. The flowmeter on the R245fa loop is a Coriolis type produced by the KOBOLD Group. Some advantages offered by the instrument are that besides the mass flow measurement, they also allow the simultaneous monitoring of densities and temperatures. The design max flow rate in the ORC loop is 400 kg/h [140]. On the diathermic oil circuit, a diaphragm flowmeter is used and a JUMO dTRANS p20 DELTA, type 403022 differential pressure transmitter with HART® interface is installed. The max flow rate in the hot oil loop is 800 kg/h [141]. Both the Coriolis and the JUMO dTRANS flow meters are of high precision with ±0.1% and ±0.07% accuracy at full scale respectively.

System monitoring and data acquisition

The variables measured on the test bench including the temperatures, pressures and mass flow are mornitored then recorded using a data acquisition system developed within the Labview environment. The developed system includes a computer Graphical User Interface (GUI) that allows the operator to control the test bench: start and stop operations, set points for the flow rates (hot oil and R245fa) and the temperature either of the heat carrier or that of the R245fa. The recorded data is obtained by:

- An ABB PLC connected to the computer using a Modbus protocol

- A NI cDAQ connected to the computer by means of a USB cable: uses the NI 9214 module with 16 channels for the thermocouple measurements and the NI9208 32 channel current for the pressure.

The developed code displays graphs of the acquired variables (temperatures, pressures), the thermodynamic condition of the R245fa on a P-H plane, besides, it provides computed values for:

- Heat duties of the HE's.
- Absorbed power by the electric resistances, circulation and ORC feed pumps.
- Electric power generated by the expander (current, voltage and frequency).
- System efficiency.

4.2.3 ORC pump test bench

Description of the test bench

A specific test bench for pump testing is available at the laboratory of the University of Trieste and it has been designed to characterize different pump types that could be suitable for a micro ORC system. The test bench has been used to assess the performance of the pump used in the ORC prototype with fluids of different viscosity. A scheme of the piping's and instrumentations installed on the facility can be seen in Figure 4.15. The fluid in the

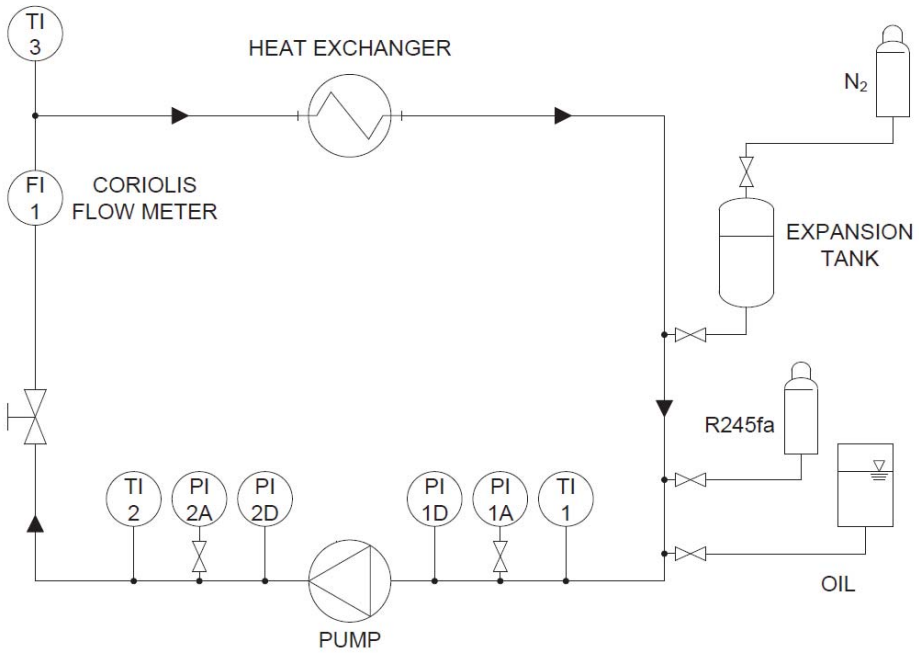

Figure 4.15: scheme of the ORC pump test facility.

system runs in a closed loop made of the following components:

- an air HE
- a pump
- an expansion vessel
- a control valve

The heat exchanger installed is a fin tube type and used to dissipate the excess heat of the fluid, therefore maintaining the heat balance within the circuit. The exchanger is adopted with a centrifugal fan thus facilitating

the heat rejection process. The element that has been used as expansion vessel is a membrane hydro pneumatic accumulator. The device consists of a steel tank divided into two volumes by an elastic membrane: one of the volumes is filled by the liquid mixture of the working fluid (R245fa or gasoil) and oil, while the other is charged with nitrogen or compressed air at controlled pressure. In this way, in addition to compensating for any thermal expansions or any leakage of the working fluid to environment, the accumulator can be used to pre-charge the system by setting the pressure of nitrogen or the compressed air. The manual adjusting valve is used to dissipate the energy possessed by the fluid at the pump delivery. The set up of the test bench is visible in Figure 4.16.

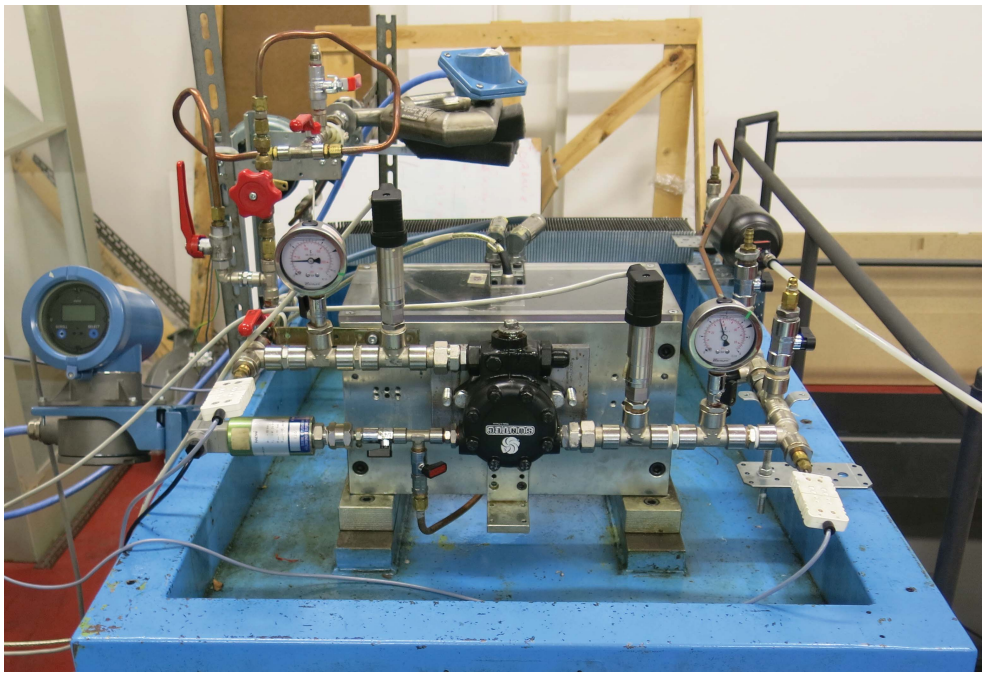

Figure 4.16: view of the pump test facility experimental setup.

The test facility is completed with a series of sensors for the measurements of different thermodynamic quantities during the test for example, each side of the pump is adopted with a piezoresistive pressure transducer for pressure measurements, PI1D and PI2D respectively, while two analog pressure manometers (PI1A and PI2A) are equally installed on the same pipes in order to allow the monitoring of pressure. The suction and delivery side temperatures are measured with two resistance thermometers (marked by TI1 and TI2). The last sensor installed on the system for the acquisition of the flow rate in the circuit is a Coriolis type flow meter placed between the control valve and the HE indicated with FI1. The sensor has been arranged with axis lying in a horizontal plane, in such a way as to prevent the possible

occurrence of two phenomena that would affect the flow measurement:

- Oil return blockage since it has a greater density compared to the organic fluid in the test conditions, which might occur if the meter is installed in a vertical arrangement with uprising pipe downwards and in the case there is no separation between the two fluids that make up the test mixture;
- Formation of steam bubbles, which could occur in the case the meter is installed in a vertical arrangement with uprising pipe upwards and both mixtures are simultaneously in a two phase state.

Test description

Several researches on different pump types have been carried out in search of the best match between cost and performance for the small scale plants amongst which the gear, diaphragm and screw types. The pump tested in the present work is a gear type SUNTEC TA2C model [142] specially designed for industrial heating applications using light or heavy oils and kerosene, its main features, derived from the technical data sheets, can be seen in Table 4.5. In the experiments, the working temperatures and pressure were maintained between the ranges 15°C to 50°C and 1 to 20 bar respectively, values contained within the limits as indicated in the technical sheet by the manufacturer. The kinematic viscosity of the selected fluid is approximately equal to $0.3mm^2/s$. This value is about 10 times lower than the minimum limit indicated by the manufacturer for proper operations ($3mm^2/s$ Table 4.5. For this reason, one of the objectives of the laboratory tests on the pump is to check the general performance with the particular fluid, actually a mixture of the working fluid with a lubricant before mounting the pump on the prototype. The fluids considered are R245fa and gasoil, results of the test on are discussed in chapter five.

characteristics	units	performance
max delivery pressure	[bar]	40
operating temperature	[°C]	0-150
Kinematic viscosity	$[mm^2/s]$	3-75
nominal speed	[rpm]	2850
maximum speed	[rpm]	3600
Nominal torque @ 40rpm	[Nm]	0.3
weight	[kg]	5.4

Table 4.5: manufacturer's datasheet for gear pump.

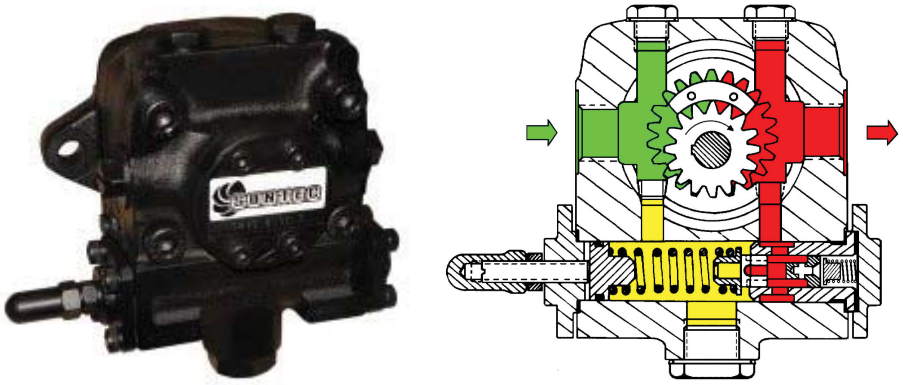

(a) (b)

Figure 4.17: suntec TA2 pump

.

4.3 Field test on ORC prototype

The ORC prototype has been installed in Florence (Italy) in an existing solar field facility, developed by the University of Florence, composed principally of two different types of collector strings connected in series for a total of $96m^2$. Both collector types are Parabolic Trough Concentrator (PTC). The first collector type is a one axis tracking trough PTC1800 produced by Solitem [143] with a tracking precision of 0.1°, covering an area of $54m^2$, the second type is a prototype panels developed by FeroTech [144] with 0.2° tracking precision with a tracking area of 42 $42m^2$. Orientation of all the collectors is NS 21°. A summary of the characteristics of the different collector types installed is shown in Table 4.6. Both collectors use water as the heat transfer medium. Other components included in the system are: an Air Treatment Unit (ATU), an air dry cooler, a hot water storage tank and two adsorption chillers. A simplified layout of the system can be seen in Figure 4.18.

Once the installation of the ORC prototype was completed, the first field tests were carried out in November 2015 and the preliminary results obtained are discussed in chapter five. The plant is visible in Figure 4.18: the solar collectors are shown on the left, the ORC prototype is seen on the right, together with the dry cooler while Table 4.6 shows the characteristics of the different collector types installed.

The solar ORC combined plant was installed at the end of summer (November 2015) thus the amount of data collected was quite low, furthermore, the schedule for the preliminary tests was not very favorable as solar radiations were very low and it was not possible to collect experimental data

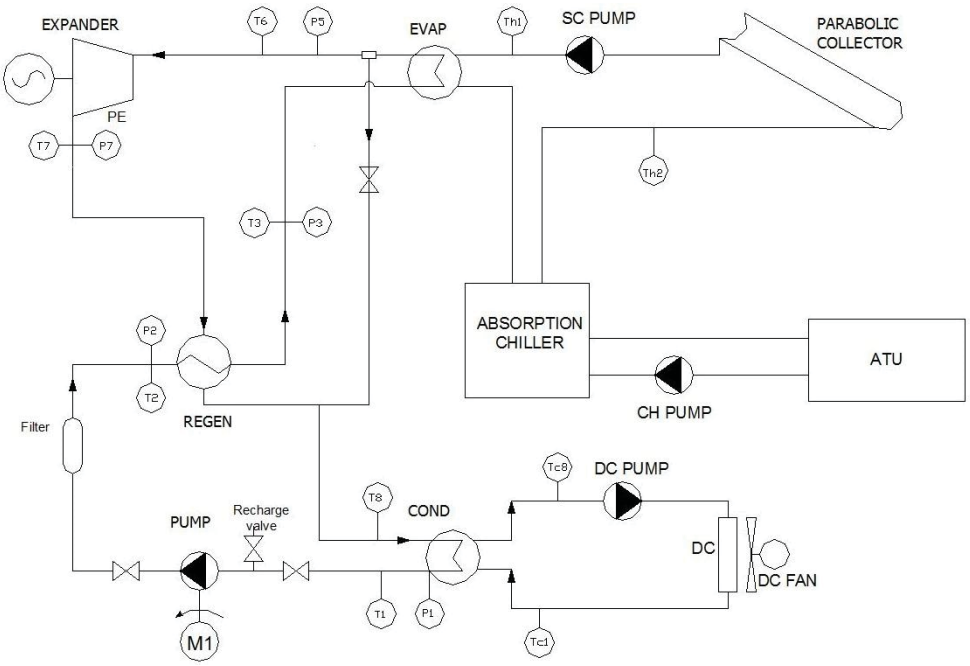

Figure 4.18: layout of the solar ORC system.

Figure 4.19: solar-ORC: left solar collector and tracking system, right ORC prototype and the dry cooling unit.

model	aperture m^2	η_0 [-]	C_1 $[W/m^2K]$	C_2 $[W/m^2K^2]$	References
Solitem PTC1800	54	0.6833	0	0.0033	[143]
Fero PTC1600	42	n/a	n/a	n/a	[144]

Table 4.6: technical data of solar collectors.

covering all the operation range of the ORC prototype. A selection of the collected data is shown in Table 5.3 and discussed in section 5.5.

To complete the characterization of the system, the field tests were repeated in August 2016 and some of the significant data collected from the installation is shown in Table 5.4. The average values for solar radiation and power consumed by auxiliaries throughout the test period were approximately 1100 W/m^2 and 300 W respectively. Peak registered temperatures of the hot water at the collector outlet temperature (T_{out}) inlet collector inlet temperature (T_{in}) were 164 °C and 156 °C respectively at a flow rate $\dot{m}_c$ of 4200 kg/h. For the ORC loop, the super heating temperature (T_{SH}) was close to 120 °C, the T_{SC} 27°C, Evaporation pressure (p_{evap}) 15.4 bar. Other system parameters provided in the table are T_{out}, T_{SH}, pump speed (n_{pump}), expander speed (n_{exp}) and $\dot{W}_g$.

Chapter 5

Results and discussion

5.1 Overview

In this chapter the results obtained both for the developed model as well as those obtained experimentally will be presented and commented.

5.2 Numerical Simulation Analysis

5.2.1 Solar collectors efficiency

The efficiency coefficients and curves of the collectors considered are presented in Table 5.1 and Figure 5.1, and oriented with the specifications; solar incidence angle 0°, collector slope 30°. The surface area considered for both collector types is $100m^2$. The characteristic of the collector according to the manufacturer's datasheet are presented in Table 5.1:

collector (type)	aperture m^2	η_0 [-]	C_1 $[W/m^2K]$	C_2 $[W/m^2K^2]$
CPC type1:(model N/A)[128]	100	0.680	0.40	0.004
CPC type2:Thermics 10 DTH[131]	100	0.675	1.41	0.0033

Table 5.1: technical data of the collectors considered in the simulation.

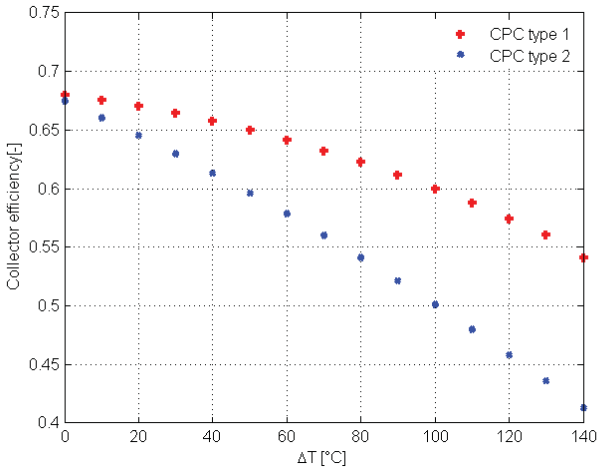

Figure 5.1: collectors efficiency curves, the coefficients of the curves are as in Table 5.1

5.2.2 ORC generated power

The Trnsys-EES simulation model estimates a maximum power of about 5kW for the hours of the day that are rich of solar radiation. The corresponding ORC efficiency is also visible in Figure 5.2 with a maximum efficiency value close to 10%. This value is however comparable with those obtained in literature for plants of this size.

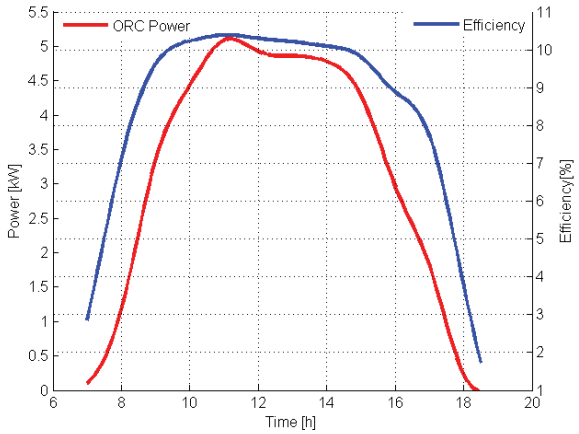

Figure 5.2: generated electric power and corresponding ORC efficiency for a typical sunny day of July: expander isentropic efficiency 0.65, pump efficiecncy 0.7.

5.2.3 Solar-ORC thermal profile

Just like in the case of the ORC power generated, the code was used to compute other system parameters such as the temperature profile of the solar collector as shown in Figure 5.2 for a typical sunny day of July. The trend of the temperature time profile of the collector outlet and the ORC evaporator inlet is seen in Figure 5.3.

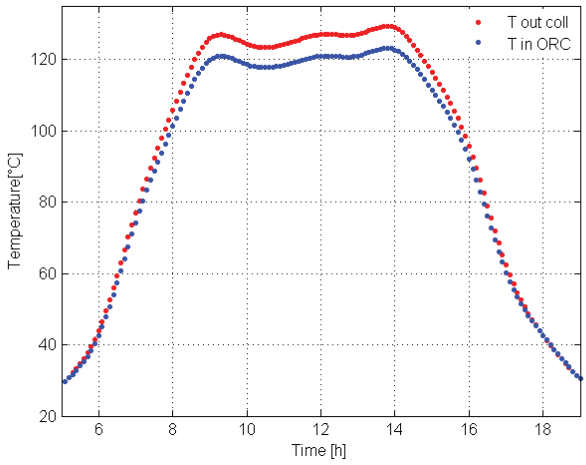

Figure 5.3: collector outlet and ORC inlet temperature profiles.

5.2.4 ORC condensation temperature

Considering the possibility of producing hot water for thermal heating, the electric power generated has been evaluated by varying the condensation temperatures in the range 15°C - 60°C, as expected there is a significant decrease in electrical power generation as the condensation temperature increases with significant benefits in hot water production. According to the priority, the user can choose to produce maximum electricity, compromising hot water production for heating and vice versa or operate on moderate electric power generation alongside hot water production.

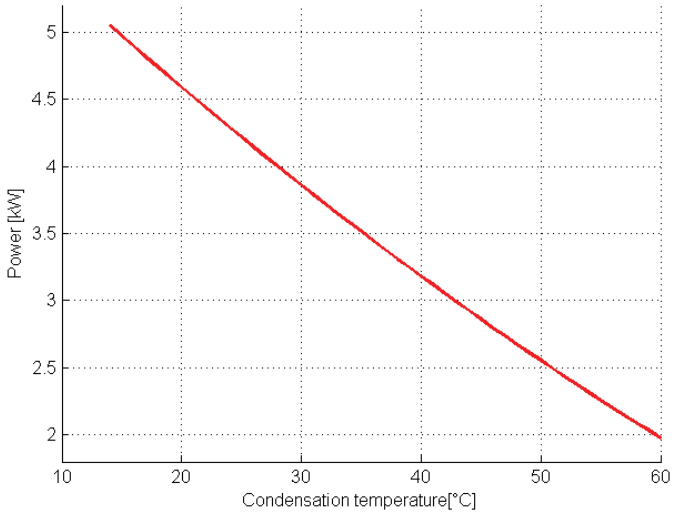

Figure 5.4: ORC power as function of condensation temperature: expander isentropic efficiency 0.65, pump efficiency 0.7, T_{SC} varies between 15-60°C

5.2.5 Comparison of collector types

The two types of collectors presented in Table 5.1 have been compared in terms of electricity production. The results obtained, for example, for the month of July are presented in Figure 5.5. As expected, the results of the analyses show better performance for the type 1 collector over type 2, the value of optical efficiency (η_0) for collector type 1 is slightly greater than that for collector 2: this difference is very significant as η_0 is a key parameter for the choice of collector type during design.

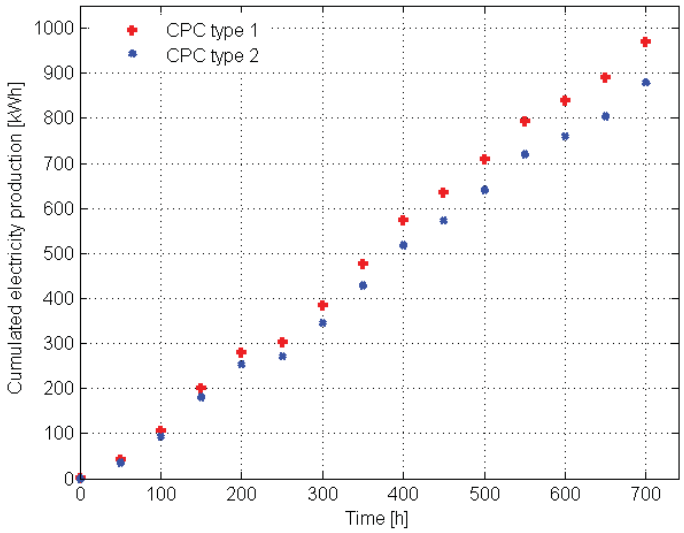

Figure 5.5: cumulated electrical energy for the two collectors examined in July: specifics of collector curves are found in Table 5.1

5.2.6 Power consumed by auxiliaries

In order to compute the net power production of the system, the electric power consumed by the auxiliaries have been estimated and the data for a typical day of July are presented in Figure 5.6. From the diagram, it can be observed that the ORC feed pump consumes the greatest share of the total power absorbed by the auxiliaries. The efficiency assumed for the pump model in the simulation is 70% though the measured value for the pump installed on the prototype is close to 40% as the pump and the electric motor are not optimized for this specific application.

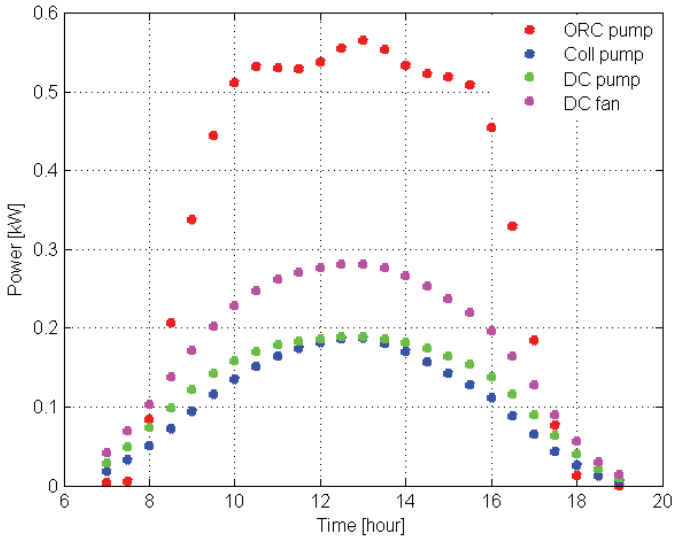

Figure 5.6: power consumption of auxiliary components for a typical day of July.

5.2.7 Cumulated power curve

During the design phase of the system it is important to choose the ORC power output that offers the best compromise in terms of costs and energy production. In Figure 5.7 the cumulated power profile over one year is shown. As observed, the number of hours for which the power output is higher than 4 kW is small (less than 500h), therefore it could be more convenient to choose an ORC power output that does not reach the power peak, and exploit the additional energy using a thermal storage. Integrating a thermal storage is a good solution however though it leads to an increase in the total plant cost, thus the initial cost, but makes the system more reliable and guarantees continuity.

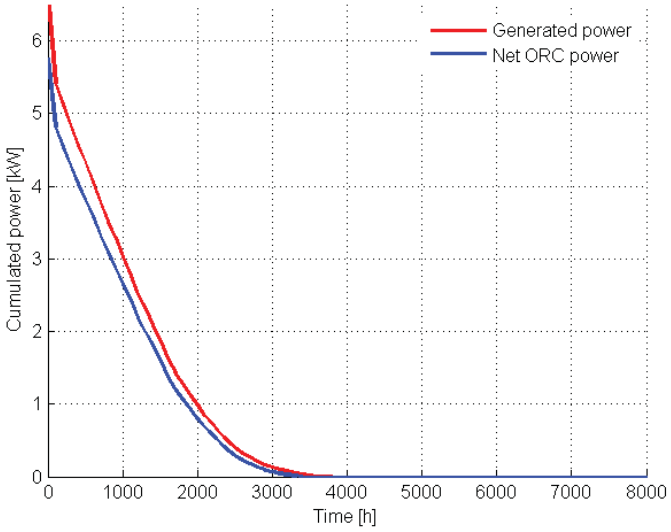

Figure 5.7: power curve for the solar ORC system considered in the simulation model.

5.3 Summary of model results

The global results of the simulation are presented on an annual base while the detailed results are referred to a typical summer day. In Table 5.2 it is visible the amount of $\dot{Q}_s$, the amount converted into useful energy by the collectors $\dot{Q}_c$, the amount converted into electric energy ORC energy ($\dot{Q}_{ORC}$), $\dot{Q}_{aux}$, and $\dot{Q}_{net}$ for each month of the year. It is also possible to see the efficiency parameters of the considered system such as: η_{ORC}, η_{coll} and $\eta_{Overall}$. The last row presents the sum total for the energy terms and average values for the efficiencies.

month	$\dot{Q}s$ [kWh]	$\dot{Q}_c$ [kWh]	$\dot{Q}ORC$ [kWh]	$\dot{Q}aux$ [kWh]	$\dot{Q}net$ [kWh]	η_{ORC} [%]	η_{coll} [%]	$\eta_{Overall}$ [%]
Jan	6269	2254	219	42	177	35.95	9.72	2.82
Feb	8159	3107	331	53	278	38.08	10.66	3.41
Mar	11523	4679	510	74	436	40.61	10.89	3.78
Apr	14085	6051	658	90	568	42.96	10.88	4.03
May	17020	7596	92	109	683	44.63	10.43	4.02
Jun	18136	8251	840	88	752	45.49	10.18	4.15
Jul	19439	9153	912	125	788	47.08	9.97	4.05
Aug	18181	8590	858	117	741	47.25	9.99	4.07
Sep	14830	6829	699	96	603	46.05	10.24	4.07
Oct	10852	4466	448	70	378	41.16	10.04	3.49
Nov	8004	3034	313	53	261	37.90	10.33	3.25
Dec	4782	1562	149	33	115	32.66	9.52	2.42
Tot/Ave	151279	5570	6731	951	5780	41.65	10.24	3.63

Table 5.2: results of the simulation model on an annual basis.

5.4 Results of experimental tests

5.4.1 Characterization of the ORC test bench

The experiments where carried out using both the regenerative RORC and the non regenerative NRORC ORC layouts [145]. A total of 240 sets of data has been collected, the operative conditions in which the data were collected is summarized below:

- the expander speed has been varied in the range 5000-8000 rpm with steps of 250 rpm;
- the working fluid R245fa flow rate in the ORC circuit in the range 200-300 kg/h with steps of 25 kg/h;
- two values of the heat carrier flow rate were considered: 400 and 450 kg/h;
- two condensation temperatures were considered for the R245fa: 24 and 30 °C;
- the temperature of the heat carrier varied in the range 135,6 and 147,1 °C with an average value of 140,2°C as it was not possible to control the temperature during the tests;

Expander generated electric power

The main aim of the analysis is to study the main differences between the RORC, the NRORC and the influence of the operating parameters on the system performance. The results of the performed tests are presented in terms of the generated expander power as function of the expander rotational speed while varying the working fluid flow rate $\dot{m}_f$. Results will be shown for two different heat carrier flow rate ($\dot{m}_{hc}$): 400 and 450 kg/h and for two different values of the T_{SC}: 24 and 30°C. The generated electric power is expressed as a function of the expander speed, the expander speed was varied by means of the electric load in the range:5000-8000 rpm. The first value in the legenda is refered to the working fluid flow rate, the second is the heat transfer media flow rate and the last is the condensation temperature at which the data was registered. From the test results, it can be noted that the expander speed seems to have little influence on the generated electric power, on the other hand, the generated power increases with increasing $\dot{m}_f$ and decreases with increasing T_{SC}. On comparing the cycle performance for the different architectures, it was found that the electric power generated was higher for the RORC (Figure 5.8) respect to the NRORC (Figure 5.9).

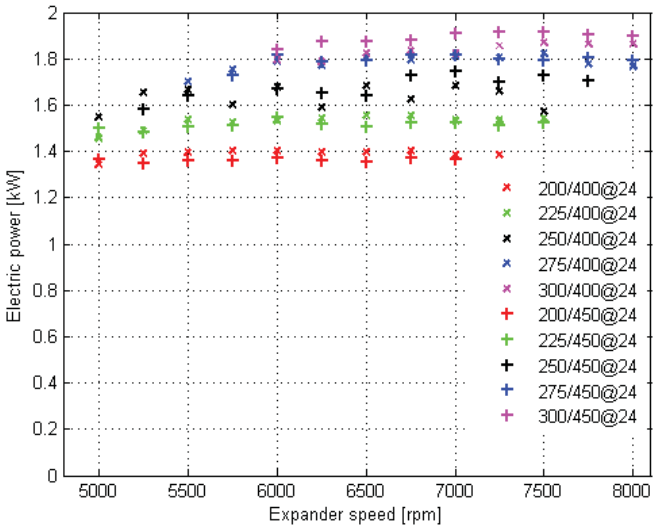

Figure 5.8: generated electric power for the RORC as function of expander speed at T_{SC}: 24 °C.

The maximum generated power for the NRORC was 1788 W at the following conditions: $\dot{m}_f$ and $\dot{m}_{hc}$ of 300 and 450 kg/h respectively, n_{exp} of 7000 rpm and T_{SC} of 24°C. In the case of the RORC, the maximum generated power was 1918 W at the following conditions: $\dot{m}_f$ and $\dot{m}_{hc}$ of 300 and 450 kg/h respectively, n_{exp} of 7250 rpm and T_{SC} of 24° C. The generated electric power is expressed as a function of the expander speed, the expander speed was varied by means of the electric load in the range:5000-8000 rpm. The first value in the legenda is refered to the working fluid flow rate, the second is the heat transfer media flow rate and the last is the condensation temperature at which the data was registered.

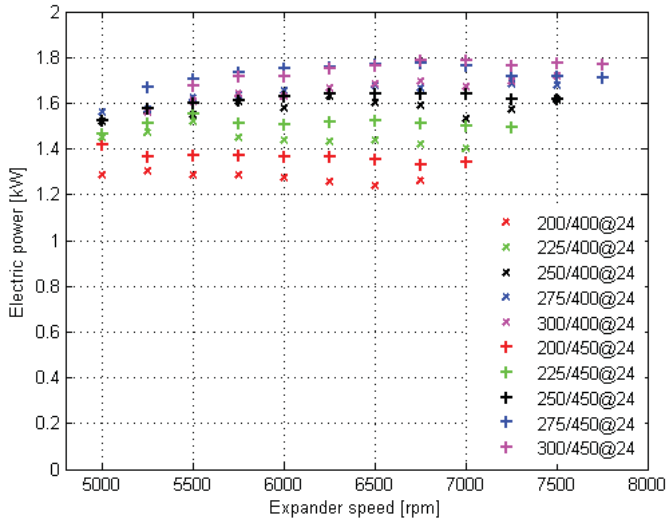

Figure 5.9: generated electric power for the NRORC as function of expander speed at T_{SC}: 24 °C.

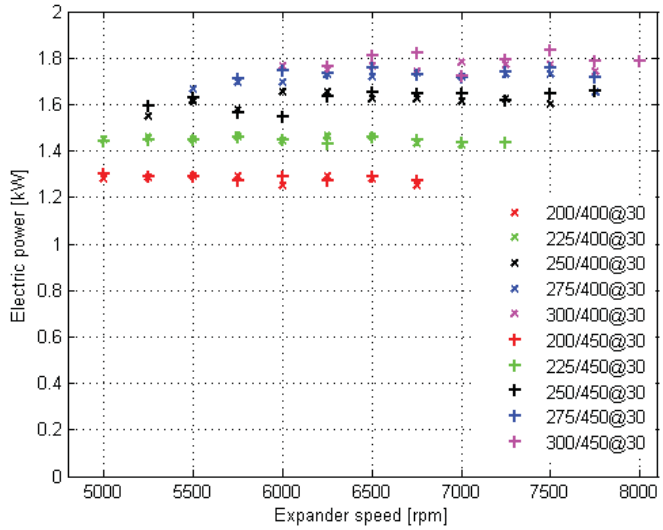

Figure 5.10: generated electric power for the RORC as function of expander speed at T_{SC}: 30 °C.

The influence of the heat carrier $\dot{m}_{hc}$ on the system performance was also considered by running the experiments for two values of the $\dot{m}_{hc}$, varying the $\dot{m}_f$ in the same range (200-300kg/h) at the fixed T_{SC} 24 and 30°C, the result for both cases RORC and NRORC is that the generated electric power significantly increases with $\dot{m}_{hc}$ as expected, this can be seen in Figure 5.10 and Figure 5.11 shows always the electric power for the RORC and the NRORC for other two hot fluid flow rates (400 and 450 kg/h). The generated

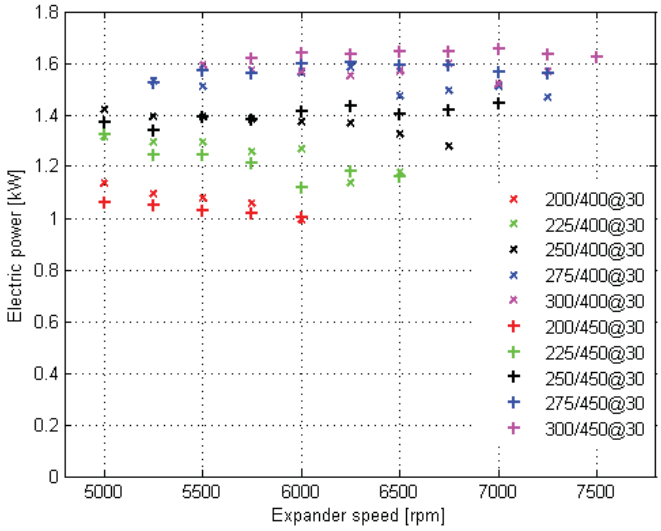

Figure 5.11: generated electric power for the NRORC as function of expander speed at T_{SC}: 30°C.

electric power is expressed as a function of the expander speed, the expander speed was varied by means of the electric load in the range:5000-8000 rpm. The first value in the legenda is refered to the working fluid flow rate, the second is the heat transfer media flow rate and the last is the condensation temperature at which the data was registered.
In terms of the expander isentropic efficiency, the trend initially increases then decreases with increasing condensation temperature, with a peak value of 62.0% at 42.2 °C for the RORC, while for NRORC cycle the maximum is equal to 62.2% at 48.1 °C as in Figure 5.12. This trend confirms that the expander efficiency depends on the expansion ratio.

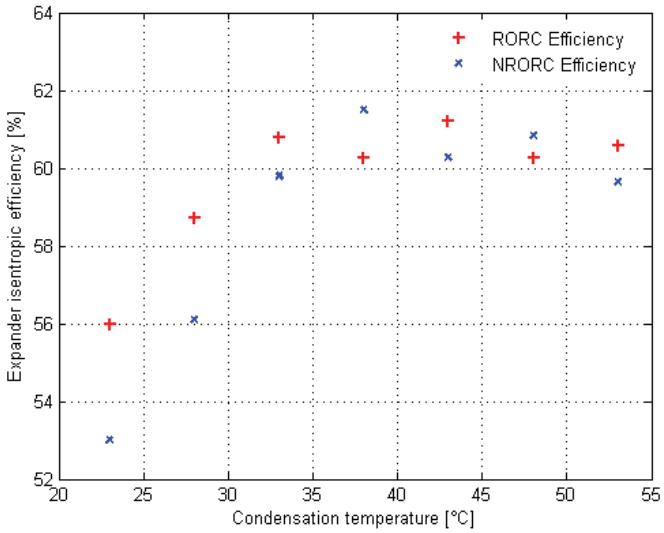

Figure 5.12: expander isentropic efficiency for both RORC and NRORC. $\dot{m}_f$: 275 kg/h, $\dot{m}_hc$: 400 kg/h, n_{exp}: 7000rpm.

Expander electrical efficiency

A similar analysis has been done for the electrical efficiency (η_{el}); the efficiency remained almost constant, varying only a few tenth of percentage point at different n_{exp} and showed almost no remarkable dependency with the $\dot{m}_f$. An important aspect of the analysis is the decrease in η_{el} with increasing condensation temperature, this difference is very evident for lower $\dot{m}_f$.
In terms of the plant architecture, the η_{el} show higher values for the RORC respect to the NRORC in virtue of the fact that the high enthalpy contained in the fluid (at the hot side) is used to preheat in the regenerator the compressed fluid (in the cold side) prior to its entry into the evaporator. This efficiency was higher for the test at $\dot{m}_{hc}$ of 400kg/h over that at 450 kg/h. The results for the RORC with $\dot{m}_{hc}$ of 400kg/h at T_{SC} of 24°C has been chosen and presented in Figure 5.13 for simplicity even though the analysis has been considered too at T_{SC} of 30°C as well as $\dot{m}_{hc}$ of 450kg/h at T_{SC} of 24 and 30°C.
Obviously the benefits obtained for the RORC respect to the NRORC in terms of performance is compensated with a possible loss of the condenser thermal duty that could favor hot water production in case the system was seen to operate in cogeneration asset as the heat content in the expanded fluid is partially lost in the regenerator before getting into the condenser. With these considerations, we can thus deduce that: the RORC architecture is preferred if the system is designed for power generation (exclusive power

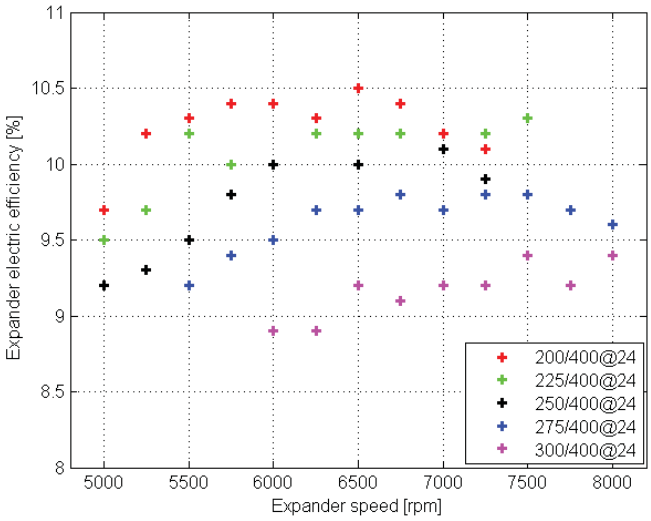

Figure 5.13: expander electric efficiency for the RORC as function of expander speed at T_{SC}: 24°C, $\dot{m}_h c$: 400 kg/h.

generation) while the NRORC is preferable if the system is designed for cogeneration allowing the use of the condenser dissipation for other thermal applications such as hot water production. The first solution is beneficial as it permits to obtain a high electric efficiency and an overall cycle efficiency greater than 10%, the second solution is more beneficial and flexible as it allows the complete exploitation of the available heat in the hot source and the production of hot water in the case of the cogeneration plant.
To summarize, the maximum value reached for the overall η_{el} for the RORC was 10.5% at $\dot{m}_f$ and $\dot{m}_{hc}$ of 200 and 400 kg/h respectively, n_{exp} 6500 rpm, T_{SC} of 24°C. For the NRORC, the maximum value reached for η_{el} was 8.1% at $\dot{m}_f$ and $\dot{m}_{hc}$ of 200 and 450 kg/h respectively, n_{exp} 5000 rpm, T_{SC} of 24°C.

System performance in cogeneration mode

The opportunity of generating thermal power taking advantage of the heat dissipated by the condenser has also been evaluated for both the RORC and NRORC cycles, this was achieved by running the system at different condensing temperatures of the cycle in a wide range, on so doing it was possible to assess the significant parameters of the system if intended to operate in cogeneration mode. As seen in the previous subsection, the system power and electric efficiency are less sensible to both the expander rotational speed and heat carrier flow rate. At the same time the electric power increases with increasing R245fa flow rate though the cycle efficiency slightly decreases. Given the context, all the other parameters have been left constant and the system behavior monitored by varying only the condensation

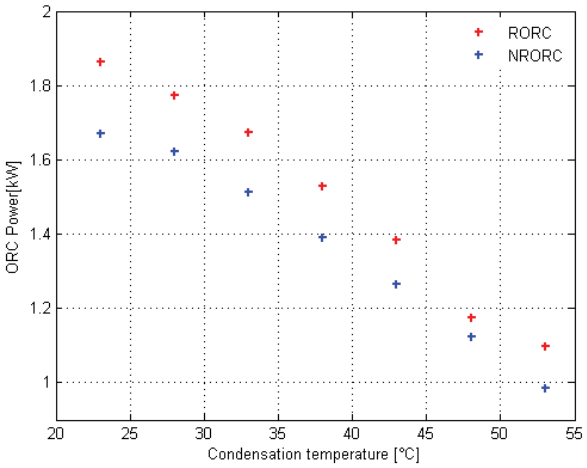

Figure 5.14: electric power for both RORC and NRORC. $\dot{m}_f$: 275 kg/h, $\dot{m}_h c$: 400 kg/h, n_{exp}: 7000rpm.

temperature: it thus follows that 275kg/h and 400kg/h were kept constant for R245fa and heat carrier mass flows respectively while the expander rotational speed was also kept at 7000 rpm. The condensing temperature was made to vary by acting on the cooling water flow rate. It is possible to see the graphs Figure 5.14 of some parameters of interest (generated electrical power, cycle efficiency, isentropic efficiency of the expander) in function of condensation temperature, obtained by running the tests by varying the condensation temperature between 23°C up to 55 °C. From the graphs above a comparison can be made for both the RORC and NRORC cycles, in fact, it is noted that the electric power produced by this system has a decreasing trend with increasing condensing temperature, for the RORC cycle the curve drops from 1.864 kW at 23.0 °C to 1.090 kW at 52.5 °C, while for the NRORC cycle the electric power curve drops from 1.670 kW for at 24.1°C to 1.004 kW at 54.0 °C. The electrical power is still higher for RORC cycle with respect to the NRORC. In terms of overall cycle efficiency, it is possible to note a decreasing trend with increasing condensation temperature: for the RORC, a peak value of 9.0% at 24.1 ° C dropping to 6.0% at 52.5 °C, while for the NRORC the value drops from 7.5% at 24.1 °C to 4.6% at 54.0 °C as visible in Figure 5.15. Even in this case the efficiency is higher for the RORC compared to the NRORC cycles, though the two cases is reduced with increasing condensation temperatures.

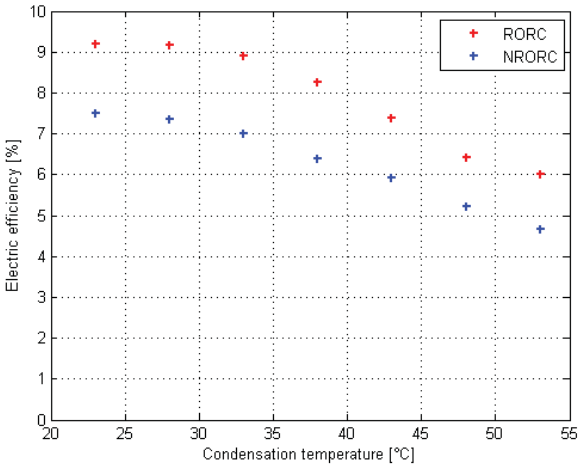

Figure 5.15: electric efficiency for both RORC and NRORC. $\dot{m}_hc$: 400 kg/h, n_{exp}: 7000rpm

Expansion Ratio

The expansion ratio expansion ratio (β), defined as the ratio between the expander inlet and outlet pressures has been analyzed for both the regenerative and non regenerative case as a function of the condensation temperature. The trend for β is seen to decrease with increasing condensation temperature as in Figure 5.16 for both cases. Higher values for β are obtained for condensation temperatures in the range 23-25°C with minimum values at temperature above 50°C. The heat carrier temperature and mass flow rate were fixed at 140°C and 400 kg/h respectively while the R245fa flow rate was kept fixed at 275 kg/h. The generated electric power has as well been analyzed as a function of the expansion ratio considering both the regenerative and non regenerative cycles and shown in Figure 5.17, as can be observed, there is an increasing trend with increased expansion ratio up till a threshold value for each case (7 and 6 respectively) above which the generated power is almost constant.

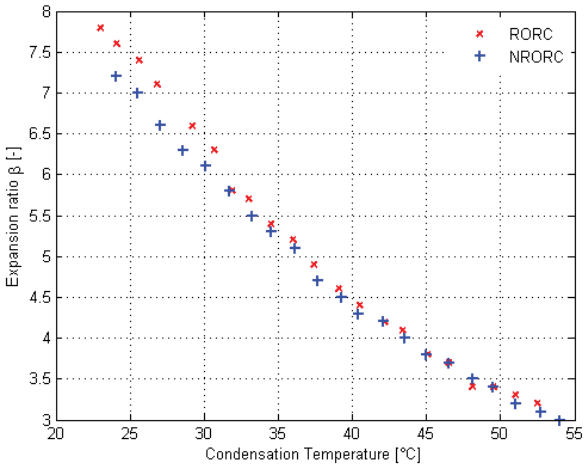

Figure 5.16: trend of the expansion ratio β as function of the condensation temperature for both RORC and NRORC. Condensation temperatures ranges between 23-55°C, $\dot{m}_f$: 275 kg/h, $\dot{m}_h c$: 400 kg/h, n_{exp}: 7000rpm

It was also seen in an earlier analysis that the maximum values of the expander isentropic efficiency (63%) occurred at relatively lower expansion ratios (say 4) compared to the generated power, it can thus be inferred that the expander's performance values do no match. A possible explanation to this fact could be that, the expander is not designed for this particular applications.

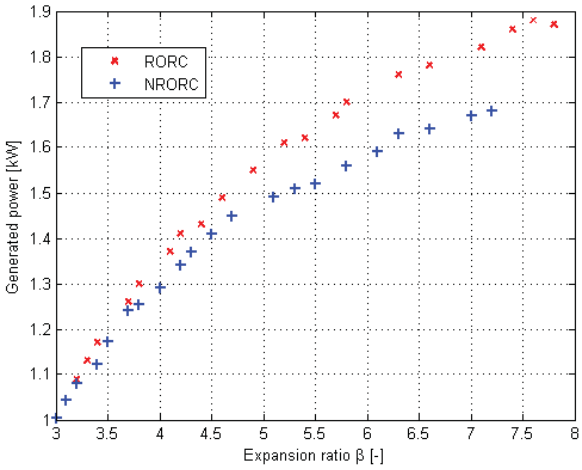

Figure 5.17: generated power as function of the expansion ratio β for both RORC and NRORC.$\dot{m}_f$: 275 kg/h, $\dot{m}_hc$: 400 kg/h, n_{exp}: 7000rpm.

5.4.2 Characterization of the ORC feed pump

The diagram in (Figure 5.18) shows the volumetric flow rate of the pump as a function of the Differential pressure (ΔP) between suction and delivery for both fluids considered. The flow rate across the pump is seen to decreases with increasing pressure. The pressure difference developed by the pump could reach 14 bar with a corresponding flow rate of 0.14kg/s at the design speed.

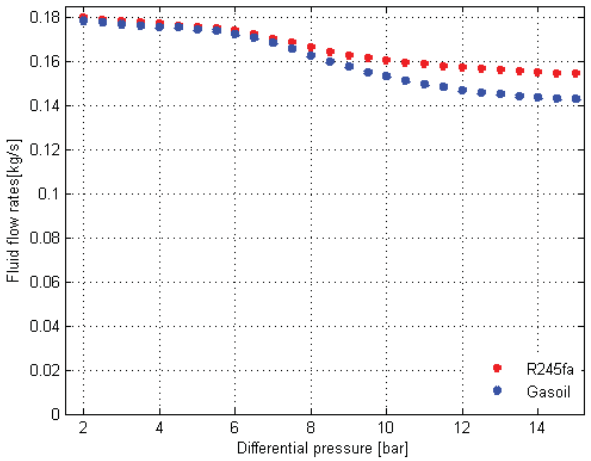

Figure 5.18: gear pump characteristics with gasoil and R245fa.

The results obtained show that the pump meets the performance (flow rate and discharge pressure) required for a proper operation of the power cycle 300kg/h and 15 bar respectively and to work with a moderate global efficiency. More relevant is the fact that the power absorbed by the pump could reach about 20% of the power generated by the expander thus reducing the overall performance of the system. The test was initially performed with gasoil then with R245fa and a comparison of the results between the two fluids tested show a slight difference for the flow rates at higher differential pressure. It can be noticed the difference between the curve for the test with gasoil and that of R245fa, this marked difference can be explained by the difference in the viscosity of the fluids. Data show, as expected, that the flow rate is reduced with R245fa as the viscosity is lower.

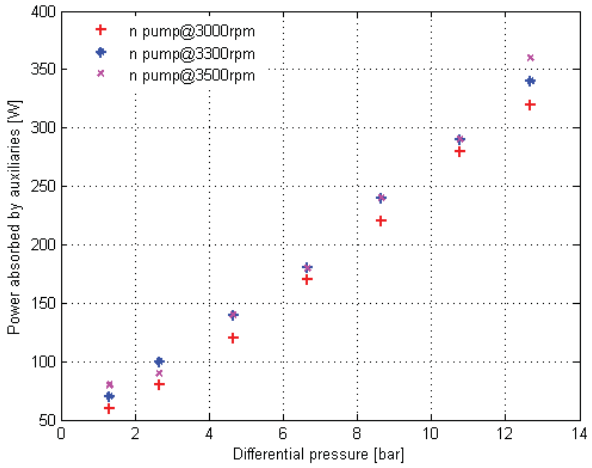

Figure 5.19: power absorbed by pump for different pump speeds.

The power consumed by the auxiliaries (pump inverter and electric motor) was also analyzed and shown in (Figure 5.19) for different pump speeds. It can be noticed that the trend is almost constant for the three rotational speeds considered: 3000, 3300, and 3500 rpm.

5.4.3 Characterization of the ORC prototype in the laboratory

This sub section describes the test carried out on the ORC prototype in the laboratory during the design phase. Once all the components were assembled and the prototype connected to both the heat source and sink some preliminary tests were made to verify its functionality. The very first test regards the test for leakage. The ORC loop was filled with air raised to the cycle design pressure and left for 24h. The loop was then filled with R245fa with a 5% in mass mixture of lubricating oil. At this point the first test was carried out and the performance registered in terms of electric power generation. The trend in generated power as function of the expander speed is presented in Figure 5.20.

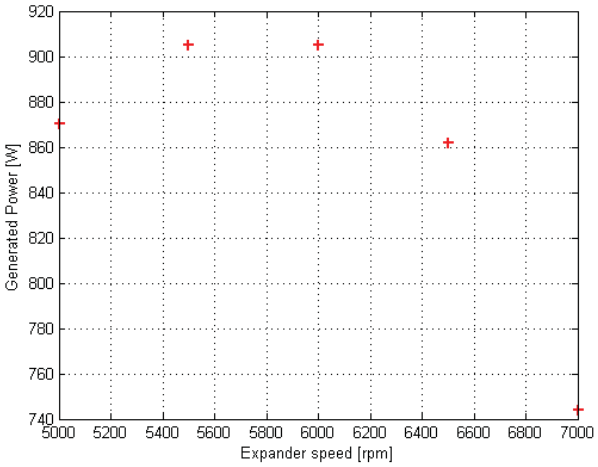

Figure 5.20: characterization of prototype in the laboratory. $\dot{m}_f$: 300 kg/h, $\dot{m}_hc$: 500 kg/h, n_{exp}:5000-7000rpm

Another analysis carried out on the prototype was that of the power consumed by the auxiliary components as this aspect is very important for the calculation of the system efficiency, the components include: the pump, the inverter and the data acquisition system. The trend of the consumed power has been presented as a function of the expander speed as in Figure 5.21. From the analysis, it was found that the share of the power consumed by the auxiliaries accounts for about 40% of the power generated by the expander, this share cannot thus be neglected and becomes objective function for optimization.

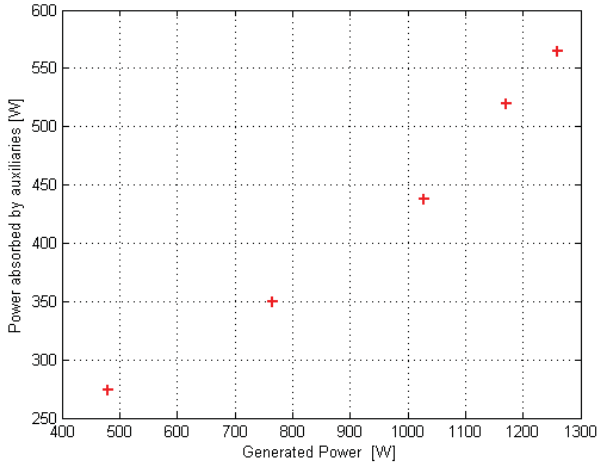

Figure 5.21: power absorbed by the auxiliary components.

5.4.4 Field test on ORC prototype

Preliminary field test results

The preliminary field tests were performed in the month of November 2015, in which two sets of tests were carried out: in the first case, a set of data was registered at a constant expander speed (6000 rpm) and collector water flow rate of 4200 kg/h. In the second case, the test was run run at constant collector water flow rate (1800kg/h) at different expander speeds within the range (4000-6000 rpm). In both cases the R245fa flow rate was kept constant and the peak value registered for the solar radiation was $590 W/m^2$ with corresponding ambient temperatures of 19°C. The data collecyed is visible in Table 5.3 where it is possible to see for the ORC circuit the Expander power (P_{exp}), p_{evap}, Evaporation Temperature (T_{evap}) and the n_{exp} while for the solar collector circuit one can see the: the imposed flow rate $\dot{m}_c$, T_{in}, and T_{out}, the $\dot{Q}_c$ of the collector and the instantaneous solar radiation. The peak

ORC-R245fa circuit			Solar collectors circuit				
P_{exp}	T_{evap}	n_{exp}	$\dot{m}_c$	T_{out}	T_{in}	$\dot{Q}_c$	G
W	°C	rpm	kg/h	°C	°C	W	W/m^2
670	82.5	6000	4200	100.4	88.1	8100	590
280	76.9	6000	1800	95.2	82.5	7700	490
400	75.4	5000	1800	94.1	80.7	9600	497
434	74.7	4500	1800	91.3	79.8	6100	532
395	72.7	4000	1800	90.4	77.8	8100	508

Table 5.3: field test preliminary results

ORC power was 670 W. This power output has been obtained with a solar radiation of $590 W/m^2$ and a collector outlet temperature of 100.4°C, hot water supplied at ORC evaporator inlet at 88.1°C with corresponding ORC fluid T_{evap} of 82.5°C at the evaporator outlet and a condensation temperature of 32.2°C. The data show that the electric power output is low but very low is the evaporation temperature as well. Therefore, overall, the result seems to be promising. Moreover, a significant thermal loss has been measured on the solar collector outlet to the ORC evaporator inlet (more than 10°C over a pipe length of about 15m). This loss can be reduced by adopting an appropriate insulation and, thus, improving system efficiency. The power curve of the preliminary test is shown in Figure 5.22.

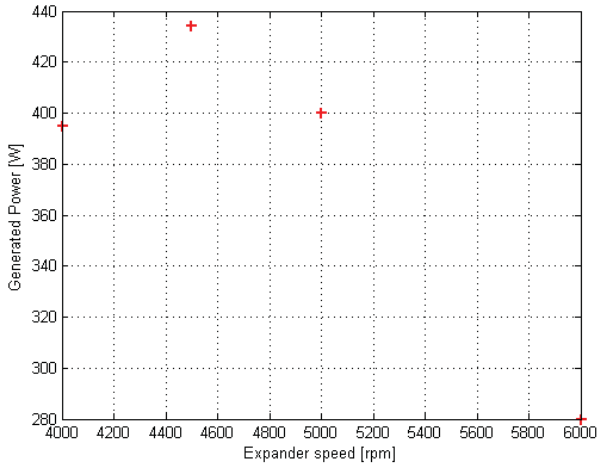

Figure 5.22: generated power as function of expander rotational speed, test conditions shown in Table 5.3.

Field test results

The field test was repeated in summer (August) of 2016, the data collected are visible in Table 5.4 and presented in this sub section. Before the data was registered, a preliminary test to verify system functionality and leakages was performed. The outcome brought to modification of the configuration of the system, a watercourse in an open loop for heat removal from the condenser was adopted instead of the air dry cooler initially installed on the prototype. This modifications followed the damage of the cooler unit as was not emptied at the end of summer 2015 with the consequent freezing of the water contained in its' circuits. Three sets of tests were carried out: in the

collector water loop			R245fa loop			performance parameters		
$\dot{m}_c$	T_{in}	T_{out}	T_{SH}	T_{SC}	p_{evap}	n_{pump}	n_{exp}	$\dot{W}_g$
l/min	° C	°C	°C	°C	bar	%	rpm	W
60	143	148	109.4	26.9	12.2	80	7000	870
70	156	164	119.3	25.0	15.2	100	6500	1340
70	150	157	117.2	25.0	15.4	100	6000	1240
60	143	147	108.8	26.9	13.2	80	5500	1075
60	143	147	109.4	27.2	13.5	80	5000	1070

Table 5.4: field test results

first case the data was registered at a constant expander speed and collector water flow rate at 6000 rpm and 3600 kg/h respectively while varying the pump between 900-1500 rpm thus the flow in the R245fa circuit the performance curve for the test is visible in Figure 5.23.

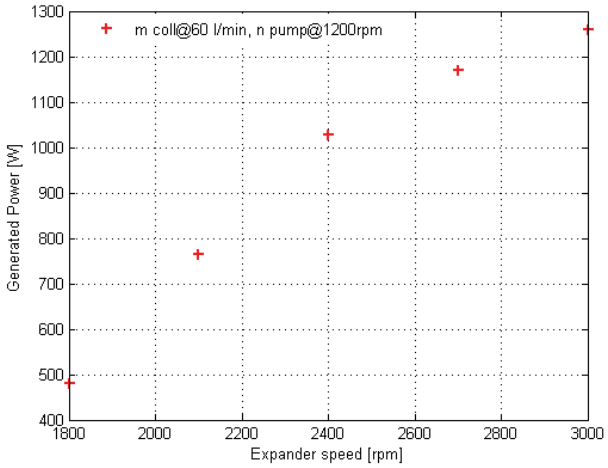

Figure 5.23: characterization of the solar-ORC system: expander power as a function of expander speed, test conditions shown in Table 5.4.

In the second case, both the pump speed and collector flow rate were kept constant at 1500 rpm and 3600 kg/h respectively while varying the expander speed through 5000-7000 rpm. In the last case, the collector water was varied through 2400-4200 kg/h while both the expander and pump speeds were kept constant at 6000 and 1500 rpm respectively. For the collector water circuit, a maximum temperature of 164°C at collector outlet was reached while the temperature gradually decreased to 134°C at ORC inlet. For the R245fa circuit, the temperature at evaporator outlet T_{evap} was 119°C at 15.2 bar, expander output of 1340 W and condenser outlet of 25°C. The peak expander power was obtained at solar radiation of approximately $1100 W/m^2$ with corresponding ambient temperatures of 33°C Figure 5.24.

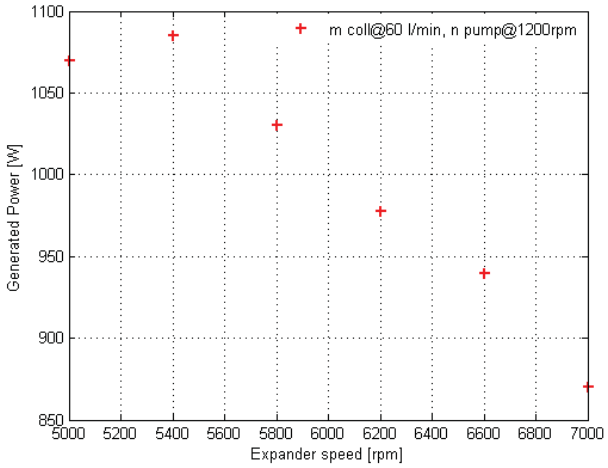

Figure 5.24: generated power as function of expander rotational speed.

Even in this case (as well as in the case of the preliminary field test), significant thermal losses were encountered on the collector circuit as a temperature difference of about 30°C was measured between the collector outlet and ORC evaporator inlet. A plot of the power generated by the expander

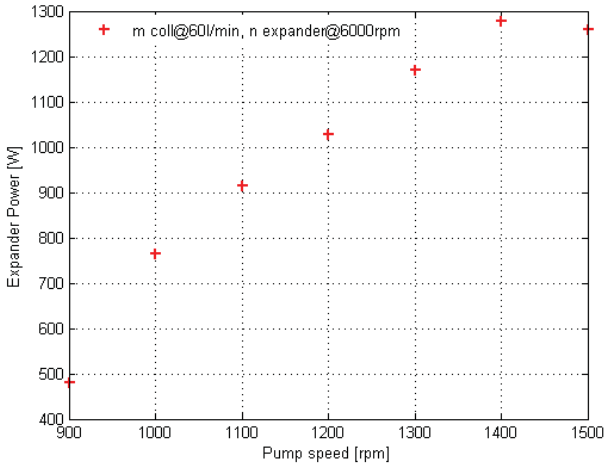

Figure 5.25: generated expander power as function of pump speed.

as function of the pump speed has also been plotted as shown in Figure 5.25. The generated power is initially seen to increase with increasing pump speed thus fluid flow rate, at some value considered as optimal for the pump type, increasing the flow rate no more influences the generated power.

5.5 Concluding remarks

According to this study, for the proper design of an efficient micro ORC using R245fa as working fluid and scroll expander, the following considerations could be of interest especially if the generator is seen to be employed in low grade heat systems: for the analyzed working fluid R245fa and the chosen expander type for this study, according to the analyses on the laboratory experiment, typical maximum temperatures of the working fluid, in this case R245 can range between 130-150°C, this being the temperature above which the chemical properties of R245fa degrade, while minimum evaporation temperatures should not be below 90-100°C. Condensation temperature should lie within the range 20-60°C with corresponding dry or water cooler can be conveniently used for sanitary hot water production or space heating systems.

Chapter 6

Economic analyses

6.1 Overview

In this chapter, some basic concepts and analytical tools usually employed in engineering economics and management will be briefly presented with the aim of providing a preliminary design estimate and the evaluation of the costs and benefits involved in the integration of a solar ORC. In particular, the italian incentive scheme for solar power plants are considered in addition to saving and sales of the electricity produced. The parameters considered in the cost analyses will be discussed first followed by the estimate of the systems costs including the auxiliaries and the maintenance cost and finally a sensitivity analysis will be presented.

6.2 Investment evaluation

In this section an assessment of the value of a solar-ORC plant in economic terms is presented, some indicators of performances for the possible investment for a solar power plant are presented. The objective of the economic analysis can be viewed as the determination of the least cost method of meeting the energy need, considering both solar and non-solar alternatives. For solar energy processes, the problem is to determine the size of the solar energy system that gives the lowest cost combination of solar and auxiliary energy. To simplify the analyses, we define the plant lifetime to be 25 years, this is the time for the considered investment or the time for which the incentive tariff are applied to the plant. Different approaches of doing economic evaluations, with emphasis on the life-cycle savings method will be discussed. This latter considers the time value of money and allows detailed consideration of the complete range of costs. It is introduced by an outline of cost considerations, note of economic parameters of merit (design crite-

ria), and comments on design variables which are important in determining system economics.

6.2.1 Economic parameters of merit

Net present Value (NPV) or Net present Worth (NPW)

In finance, the NPV or NPW are defined as the sum of the present values of the incoming and outgoing cash flows over a period, in other words both terms are referred to the difference between costs and income or returns over a period. The time value of money dictates that time has an impact on the value of cash flows. The decrease in the current value of future cash flows is based on the market dictated rate of return. More technically, cash flows of nominal equal value over a time series result in different effective value cash flows that makes future cash flows less valuable over time. The NPV is determined by calculating the costs (negative cash flows) and benefits (positive cash flows) for each period of an investment. The period is typically one year. After the cash flow for each period is calculated, the present value (PV) of each one is achieved by discounting its future value at a periodic rate of return. NPV is the sum of all the discounted future cash flows. Because of its simplicity, NPV is a useful tool to determine whether a project or investment will result in a net profit or a loss. A positive value for the NPV results in a profit and the investment is worthwhile, while a negative value results in a loss thus, the investment will not yield the desired return as represented by the discount rate employed in the present worth calculation. The NPV measures the excess or shortfall of cash flows, in PV terms, above the cost of funds. In a theoretical situation of unlimited capital budgeting a company should pursue every investment with a positive NPV. However, in practical terms a company's capital constraints limit investments to projects with the highest NPV whose cost cash flows, or initial cash investment, do not exceed the company's capital [149]. NPV is a central tool in Discount Cash Flow (DCF) analysis and is a standard method for using the time value of money to appraise long-term projects. It is widely used throughout economics, finance, and accounting. The concepts over mentioned can be formulated mathematically using (6.1):

$$NPV = \frac{R_t}{1 + i^t} \tag{6.1}$$

NPV represents the cash inflow or outflow discounted back to its PV, then they are summed. Therefore, NPV is the sum of all the terms given in (3.5).

$$NPV(i, N) = \sum_{t=0}^{N} \frac{R_t}{1 + i^t} \tag{6.2}$$

where length of the analysis period (N), Net cash flow (R_t) over the period (t) and Discount Rate (i).

Internal Rate of Return (IRR) or Economic Rate of Return (ERR)

The IRR or ERR is a rate of return used in capital budgeting to measure and compare the profitability of investments. It is also called the discounted cash flow rate of return (DCFROR). In the context of savings and loans, the IRR is also called the effective interest rate. The term internal refers to the fact that its calculation does not incorporate environmental factors (e.g., the interest rate or inflation). The internal rate of return on an investment or project is the "annualized effective compounded return rate" or rate of return that makes the net present value of all cash flows (both positive and negative) from a particular investment equal to zero. It can also be defined as the discount rate at which the present value of all future cash flow is equal to the initial investment or in other words the rate at which an investment breaks even. In more specific terms, the IRR of an investment is the discount rate at which the net present value of costs (negative cash flows) of the investment equals the net present value of the benefits (positive cash flows) of the investment. It can be formulated as in (6.3):

$$\sum_{t=0}^{N} \frac{R_t}{1 + IRR^t} = 0 \tag{6.3}$$

Pay Back Period (PBP)

The PBP in capital budgeting refers to the period required to recover the funds spent in an investment, or to reach the break-event point. All else being equal, shorter payback periods are preferable to longer payback periods. Payback period is popular due to its ease of use. The term is also widely used in other types of investment areas, often with respect to energy efficiency technologies, maintenance, upgrades, or other changes. Although primarily a financial term, the concept of a payback period is occasionally extended to other uses, such as energy payback period (the period over which the energy savings of a project equals the amount of energy absorbed since project inception); these other terms may not be standardized or widely used. In the considered context, the payback period can be expressed as in (6.4) by [132]:

$$\sum_{t=0}^{PBP} \frac{R_t}{1 + i^t} = 0 \tag{6.4}$$

Least Cost Solar Energy (LCSE)

The Least cost solar energy method is suitable for systems in which solar energy is the only energy resource. The system yielding least cost can be defined as that showing minimum owning and operating cost over the life of the system, considering solar energy only. However, the optimum design of a combined solar plus auxiliary energy system based on minimum total cost of delivering energy will generally be different from that based on least cost solar energy, and the use of least cost solar energy as a criterion is not recommended for systems using solar in combination with other energy sources.

Life Cycle Cost (LCC)

The LCC is the sum of all the costs associated with an energy delivery system over its lifetime or over a selected period of analysis, in today's currency, and considers the time value of money. The basic idea of life-cycle costs is that anticipated future costs are brought back to present cost (discounted) by calculating how much would have to be invested at a market discount rate to have the funds available when they will be needed. A life-cycle cost analysis includes inflation when estimating future expenses. This method can include only major cost items or as many details as may be significant.

Annualized Life Cycle Cost (ALCC)

The ALCC is the average yearly outflow of money (outgoing cashflow). The actual flow varies with year, but the sum over the period of an economic analysis can be converted to a series of equal payments in today's currency that are equivalent to the varying series. The same ideas apply to an ALCC.

6.3 Costs

The cost shall be analyzed separately for both systems, the overall estimate of the solar-ORC plant has been studied using an approach similar to that presented by Bocci et *al* in [150]. The cost for the ORC has been estimated using design know-how gained by working on the experimental facility, while that of the solar system has been estimate with reference to the standards of solar process economics according to which; the buying and installation of a solar power system include the delivered price of the equipments such as collectors, pipings (pipes, ducts and fittings), storage unit, heat exchangers, blowers, controls as well as the components of the ORC loop such as: pumps, expander, heat exchangers and the related pipings. In evaluating the cost of the system, we must also include the cost of installation as well as the cost

of maintenance, cost of structures to support collectors. The installation cost of a plant can be considered as the sum of two terms; one proportional to the collector area, and the other independent of the collector area as in (6.5) see [132]:

$$C_S = C_A A + C_E \tag{6.5}$$

where Total installation cost (C_S) in € , cost of area dependent equipment (C_A) €/m^2 include purchase and installation of the collector and storage system, collector surface Area (A) collector area in m^2 and cost of non area dependent equipment (C_E) in € includes costs of controls, construction or erection equipments' to the installation site. Operating costs are also included, these consists of auxiliaries and costs of operating the pumps and blowers generally defined as cost for parasitic energy already include in the calculation of the net produced energy in the particular case.

6.3.1 Cost of the ORC unit

Estimating a market price for a small scale ORC is not easy due to the absence of reference installations. Generally, ORC producers have in stock only groups of larger dimensions (medium size plants) used to recover the surplus heat produced from industrial processes which is usually in the range of 400 and 1500kW. In the case, of powers up to 10 kWe, the producers, today, rarely have such options in production. From our experience in developing ORC prototypes, it is estimated that an average price for low power ORC can be fixed at 5000€/kW, this include the cost of the single components generally obtainable from the HVAC sector: pump, expander, HE and auxiliaries like pipings, inverter and the control board. This price is quite high, but it is reliable if considered the industrial development of such technology. With an eye on the future it is easy to understand that if the low power generators will be required by the market extensively, for example as a main component of a small scale solar power system, the prices will have a considerable reduction.

6.3.2 Cost of the solar collectors

The overall price of the solar collectors cover most of the total price of the plant. Depending on the particular technology adopted, the panels have a wide range of possible market prices. Our choice to use evacuated tubes with a high efficiency curve leads to an average price of 400€/m^2.

6.3.3 Cost of dry cooler and auxiliaries

The cost of the auxiliaries includes the heat exchanger of the solar circuit, the circulation pumps and the dry cooler. It is possible to estimate an overall price of 2500€ for those components. Different is the case when thought of an auxiliary boiler and thermal storage, in this case, the cost of the auxiliaries should be re-evaluated.

6.3.4 Maintenance cost

The typology of plant adopted does not need an excess of maintenance work per year, but a minimal revision and some stops during the activity is indispensable. Generally, if properly respected, ordinary maintenance schedule will be sufficient to keep the system operational yearly. An overall cost for maintenance of 200€/*year* is considered reasonable for this application.

6.3.5 Total plant cost

Summing the costs of materials and installation it is possible to consider an overall cost of the plant of 67500€. In this context, it is important to take in account that the Italian legislation consider a deduction in case of energy upgrading of buildings, and for solar panels installation. Taking advantage of this deduction, it is possible to save in taxes the 65% of the plant costs. The savings are returned to the administrator in the form of 10 equal rates distributed one per year for 10 years. In the specific case, this means that it is possible to receive a reduction in taxes of 4380€ a year for 10 years, considering that the cost of the plant would be of 43875€.

6.4 Incentives for solar power plants

In Italy, the incentives for solar power plants were regulated by the decree Ministerial decree of 11 April published 30 April 2008, titled "Criteri e modalità per incentivare la produzione di energia elettrica da fonte solare mediante cicli termodinamici" [151]. The decree defines the modality and entity of the resources made available to produce electricity from solar energy through thermodynamic cycles. The application of the incentives is demanded to the Gestore dei Servizi Energetici (GSE). The GSE is an Italian corporation, controlled by the Ministry of Economy and Finance, which provides economic incentives to produce electricity from renewable sources and provide information to promote the culture of energy use compatible with sustainable needs of the environment. The GSE also plays a central role in fostering and development of renewable sources in Italy.

6.4.1 Access policies to incentives

As explained in [152], the incentive tariffs are available only for solar thermal plants, including hybrid, of new construction. There are therefore no subjects of the incentives power plants already existing or existing plants upgraded. The tariffs can be added to the selling price of electricity. The maximum capacity eligible for incentives, including the solar part of the hybrid plants, it corresponds to $2500000m^2$ of cumulative intercepting surface. In case of hybrid plants the tariff covers only the fraction of production corresponding to solar generation. Hybrids are considered the power plants that produce electricity from a variety of sources even different than solar one, they can be renewable or not. For the installations whose only source is solar thermal power, or whose integration fraction of solar energy is less than 15%, the incentive energy is the net power output of the plant, expressed as:

$$P = P_{net} = P_g - W_{aux} \tag{6.6}$$

where Net power generated (P_{net}), gross Energy (P_g) and Work done to drive the auxiliaries (W_{aux}).

6.4.2 The tariffs

The incentive mechanism rewards with special tariffs the net electricity generated for a period of 25 years. Rates remain constant in currency throughout the incentive period. The incentives are recognized only for the net production of electricity due to the solar power P, calculated by subtracting from the total production the part attributable to other sources of energy, whichever greater than 15% of the total as in Table 6.1. If instead the integrative fraction is less or equal to 15% the fee is paid for the total production.

Surface (m^2)	Integration fraction (%)	Tariff (€/kWh)
s < 2500	< 15	0.36
	15 < x < 50	0.32
	x> 50	0.30
s > 2500	< 15	0.32
	15 < x < 50	0.30
	x > 50	0.27

Table 6.1: incentive tariffs based on total surface used.

Where s is the cumulative intercepting surface of the solar collectors and x the fraction of production corresponding to solar generation. In the considered case, it is possible to assume an incentive of $0.36€/kWh$ for a period of 25 years as gain to sum to the saving of the unpurchased electricity and the eventual sold surplus.

6.5 Cost of electricity

The saving of electricity due to the production and self-consumption can be calculated using the average cost of electricity for private clients. This value is a statistical parameter calculated year by year. The most values for the case of Italy were presented at the assembly of Senators in a memorial available on the web site of the *Autorità per l'energia elettrica il gas e il sistema idrico* [153]. The data for Italy and for the other UE country members are elaborated by the Eurostat, a work group of the European commission with the task of elaborating independent statistics of interest for each European country. According to Eurostat, the price the final user would pay for electricity in Italy has been summarized in Table 6.2 for the year 2014 (elaborated from [153]) . For our purpose the final price for electricity used is $0.23€/kWh$. With a similar procedure, it is possible to decide a price to the sold part of net energy not used. In our case the energy production sold to the energy national system can be considered priced at $0.13€/kWh$.

consume (kWh/yr)	tax free (€/kWh)	taxed (€/kWh)
< 1000	0.207	0.292
$1000 < \& < 2500$	0.143	0.211
$2500 < \& < 5000$	0.150	0.239
$5000 < \& < 15000$	0.182	0.297
> 15000	0.209	0.331

Table 6.2: cost of electricity in €/kWh produced.

6.6 Thermal energy production

So far, the only valuable output of the plant considered is the electricity produced by theORC cycle. It is to consider that the heat dissipated from the condenser could have a value for the user if a need of medium-low temperature water is required like hot water production for both ambient heating and sanitary water. In this case, the system can be considered to operate in cogeneration mode. In the case considered it has been ssumed that all the heat is recovered and consumed. A value of $0.05€/kWh$ for the thermal energy has been considered.

6.7 Cash flow analyses

In the following section the cash flows for the investment are calculated using (6.4). Three scenarios have been considered for the incoming cash flow: in the first case, all the produced electricity is self consumed, in the second case, all the electricity produced is sold and an intermediate case where part of the produced electricity is self consumed in a 50% ratio of the total. In the analysis, the thermal energy is considered as valuable with a price of $0.05€/kWh$. The considered time of the investment is 25 years. In this analysis, the discount rate chosen is 1.17%, this value is the present interest rate on government bonds. In the following table the gains for each month are presented in Table 6.3.

month	Net prod [kWh]	Thermal energy [kWh]	Incentive [€]	Price for thermal prod [€]
Jan	50.88	1056.63	18.32	52.83
Feb	81.98	1570.98	29.51	78.55
Mar	172.96	2542.81	62.27	127.14
Apr	235.1	3304.13	84.63	165.21
May	287.43	4217.42	103.48	210.87
Jun	308.36	4607.24	111.01	230.36
Jul	342.68	5149.36	123.37	257.47
Aug	322.72	4837.94	116.18	241.90
Sep	258.29	3801.18	92.98	190.06
Oct	146.43	2530.56	52.72	126.53
Nov	95.76	1690.57	34.47	84.53
Dec	31.10	942.64	11.20	47.13
Tot	2333.68	36251.45	840.13	1812.57

Table 6.3: annual plant energy production and cash flow.

By producing 2334 kWh/year of electric energy it is possible to consider the benefit in self-use of electricity, the selling or an intermediate situation. The savings for self-consumption amounts to $537€/kWh$, in case of total sale, $303€/kWh$, while the case of half self-consume and half sale results to $420€/kWh$ savings [154]. For the three cases the total income cash flow are presented in Table 6.4.

parameter	consumption	sold	consumption-sold 50%
PBP	9	10	10
NPV	38430	33900	36165
IRR	0.076	0.070	0.073

Table 6.4: cash flow analyses for the reference plant.

6.8 Sensitivity analysis

In this section a sensitivity analysis has been carried out to analyze the influence of the variability of some of the main design parameters on other representative indicators of energy efficiency and economic feasibility. In particular, the sensitivity analysis would consider the following scenarios.

- variation of plant cost
- variation of collector efficiency
- variation of plant location

6.8.1 Variation of plant cost

To consider the variability of market prices for the components over the time, two different situations are considered. An increase of the overall cost of the plant of 10% and a reduction of the same entity are considered. The importance of this analysis dwell in the contribution to understand the importance of the evolution of the prices in the long-term investment. In Table 6.5 the plant costs are presented.

parameter	unit	cost	consumption	sold	consumption-sold 50%
+10% ref cost	[€]	74250	3166.11	2956.08	3061.09
PBP	[year]	-	+ 1	0	0
NPV	[%]	-	-5.36	-6.04	-5.68
IRR	[%]	-	-11.20	-11.63	-11.40
-10% ref cost	[€]	60750	3166.11	2956.08	3061.09
PBP	[year]	-	0	-1	-1
NPV	[%]	-	+5.09	+5.69	+5.37
IRR	[%]	-	+11.93	+12.30	+12.10

Table 6.5: annual cash flow analyses and economic parameters as plant cost is varied.

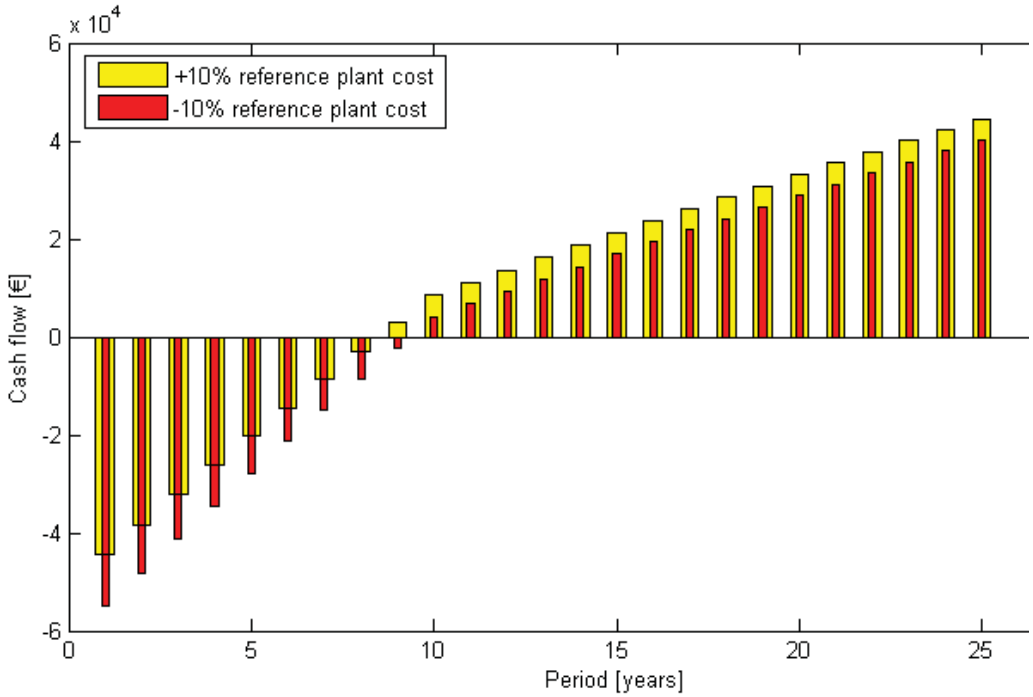

Figure 6.1: comparison of the cumulated cash flow considering plant cost variation.

6.8.2 Variation of collector efficiency

The main characteristic of a solar panel is its efficiency and this can be correlated to a temperature difference for each value of global irradiance according to the following formula:

$$\eta = \eta_0 - C_1 \frac{(T_m - T_{amb})}{G} - C_2 \frac{(T_m - T_{amb})^2}{G} \tag{6.7}$$

Where η_0, C_1 and C_2 are respectively; the intercept efficiency, the first and second order efficiency coefficients. Their values are a characteristic of the particular panel and are calculated experimentally by the producer. A variation of the coefficients is equivalent to altering the characteristic curve of the panel. In particular, parameter η_0 graphically represents the intercept of the efficiency curve with the ordinate axis. An alteration of η_0 represents a shift of the whole curve vertically, meaning an equivalent modification of the efficiency. For this analysis, it is chosen to improve the panel efficiency by 10% by considering a +10%. Doing so, means to change the panels and substitute them with more efficient ones. Being more efficient also means being expensive, in other words, a more efficient solar system will be more

expensive. For the reference case, an initial value of η_0 equal to 0.675 has been considered, then modified to 0.775.

month	Net prod [kWh]	Thermal energy [kWh]	Incentive [€]	Price for thermal prod [€]
Jan	73.54	1116.54	26.48	55.83
Feb	127.99	1781.41	46.08	89.07
Mar	230.38	2904.42	82.94	145.22
Apr	310.36	3777.88	111.73	188.89
May	379.35	4815.97	136.57	240.80
Jun	406.81	5264.42	146.45	263.22
Jul	450.78	5886.42	162.28	294.28
Aug	424.46	5538.19	152.81	276.91
Sep	340.04	4356.92	122.41	217.85
Oct	197.77	2874.99	71.20	143.75
Nov	130.70	1921.83	47.05	96.09
Dec	55.87	985.65	20.11	49.28
Tot	3128.07	41223.90	1126.11	2061.19

Table 6.6: annual plant energy production and corresponding savings for collector type variation.

parameter	unit	consumption	sold	consumption-sold 50%
+10% η_0	[€/kWh]	3875.48	3593.95	3731.71
Difference	[%]	22.41	21.58	22.01
PBP	[year]	-1	-1	-1
NPV	[%]	+37.33	+37.27	+32.44
IRR	[%]	+28.46	+28.47	+20.40

Table 6.7: annual cash flow analyses in the case collectors of different efficiency are considered.

In Figure 6.2, it is possible to see the difference between the two panels efficiency for irradiance of 1000 W/m^2. As expected, the performance of the improved collectors are higher in particular there is a net improvement of productivity especially in the colder month of the year. The overall productivity of net energy increases from a starting value of the reference simulation of 2333 kWh/year through 3128 kWh/year see Table 6.6. From the economic point of view, there is a net advantage in terms of cash flows higher than 20% points for all the considered cases in favor of the higher efficiency panel, regarding the PBP; all three cases present a one year gain for the PBP. For the other two performance parameters, the NPV presents a net difference higher than 30% points while the IRR presents a difference higher than 20% points for all three cases. Table 6.7

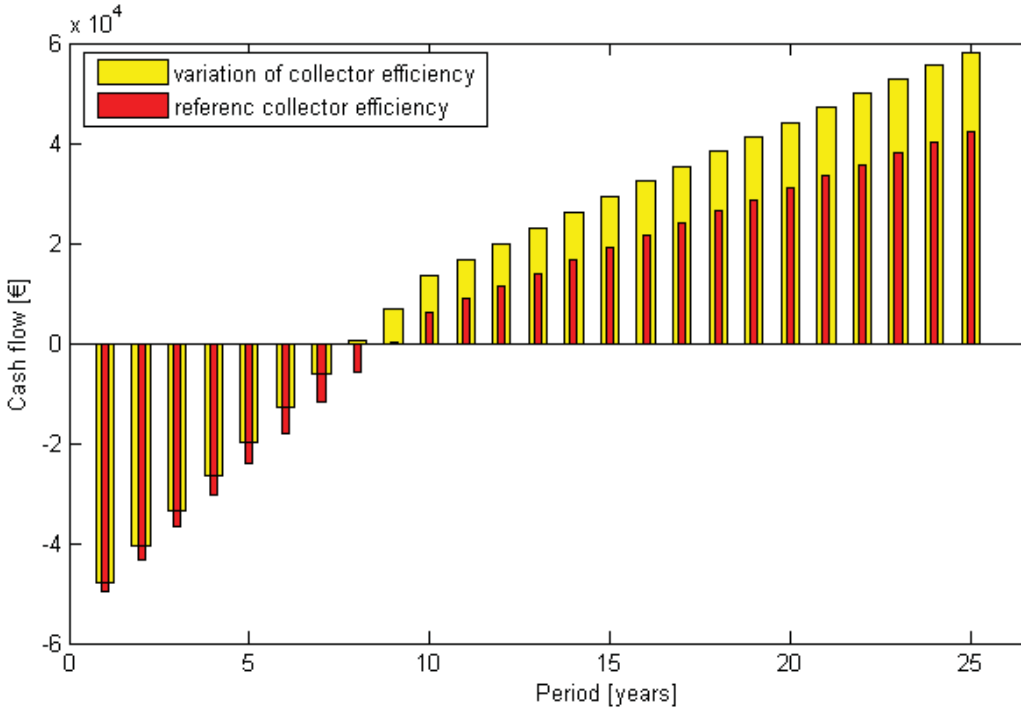

Figure 6.2: comparison of the cumulated cash flow considering collectors of different efficiency.

6.8.3 Variation of plant location

This analysis aims at assessing the influence on the system location like the weather conditions (radiation and temperature) on the overall energy and economic performance as they are proportionally related to the generated electric power. In the following simulation, it has been chosen to use weather data of Sicily with solar radiation 20% higher than the reference location (Trieste)the analyses in terms of energy production and the relative savings are shown in Table 6.8. From Table 6.8, it can be observed as ex-

month	Net prod [kWh]	Thermal energy [kWh]	Incentive [€]	Price for thermal prod [€]
Jan	104.34	1721.94	37.56	86.10
Feb	170.20	2368.73	61.27	118.44
Mar	257.90	3401.83	92.85	170.09
Apr	311.86	4081.13	112.27	204.06
May	334.68	4523.67	120.49	226.18
Jun	360.37	5048.90	129.73	252.44
Jul	332.78	5057.18	119.80	252.86
Aug	315.46	4836.10	113.57	241.81
Sep	306.13	4287.41	109.85	214.37
Oct	226.46	3395.51	81.52	169.78
Nov	146.63	2262.93	52.79	113.15
Dec	100.92	1730.11	36.33	86.51
Tot	2966.74	42715.43	1068.03	2135.77

Table 6.8: annual plant energy production and corresponding savings as plant location is varied.

pected that, the higher the solar radiation available (Sicily), the higher the amount of thermal energy produced by solar thermal collectors, the higher the net energy produced by the ORC generator. As visible in Table 6.9, the difference in terms of energy produced and efficiency is not negligible. The correct location of any kind of plants using solar energy is a parameter of prime importance. From the economic point of view, there is a net advantage in terms of cash flows for both indexes (NPV and IRR) with values higher than 20% points, on the contrary, regarding the PBP; the case of the self-consumed energy presents almost no significant variation while, the remaining two cases present a one year gain in the payback time. In the table, the header for example, $\triangle\eta_{coll}$ is referred to the difference in collector efficiency between the case of Sicily and that of Trieste. The same holds for the other parameters $\triangle\eta_{ORC}$ and $\triangle\eta_{Overall}$.

$$\triangle\eta = \eta_{Sicily} - \eta_{Trieste} \tag{6.8}$$

parameter	unit	consumption	sold	consumption-sold 50%
+20% irradiance	[€/kWh]	3856.48	3589.47	3722.98
Difference	[%]	21.80	21.43	21.62
PBP	[year]	0	-1	-1
NPV	[%]	+20.81	+21.08	+20.94
IRR	[%]	+24.60	+25.04	+24.80

Table 6.9: annual cash flow analyses as plant location is varied.

From the economic point of view, there is a net advantage in terms of cash flows for both indexes (NPV and IRR) with values higher than 20% points, on the contrary, regarding the PBP; the case of the self-consumed energy presents almost no significant variation while, the remaining two cases present a one year gain in the payback time. Table 6.10 expresses

month	$\triangle\eta_{coll}$ [%]	$\triangle\eta_{ORC}$ [%]	$\triangle\eta_{Overall}$ [%]
Jan	15.56	29.36	59.80
Feb	12.58	29.14	63.59
Mar	8.65	6.32	20.30
Apr	4.84	4.54	12.20
May	1.23	6.11	9.35
Jun	4.04	4.33	10.60
Jul	0.46	0.55	1.44
Aug	0.45	1.64	2.43
Sep	3.37	2.70	7.83
Oct	8.89	8.67	24.64
Nov	10.91	6.88	26.15
Dec	23.14	39.50	94.97
Ave	7.96	11.28	27.13

Table 6.10: difference in performance (efficiencies) as plant location is varied.

the differences in percentages, in efficiencies between the reference location (Trieste) and compared location (Sicily).

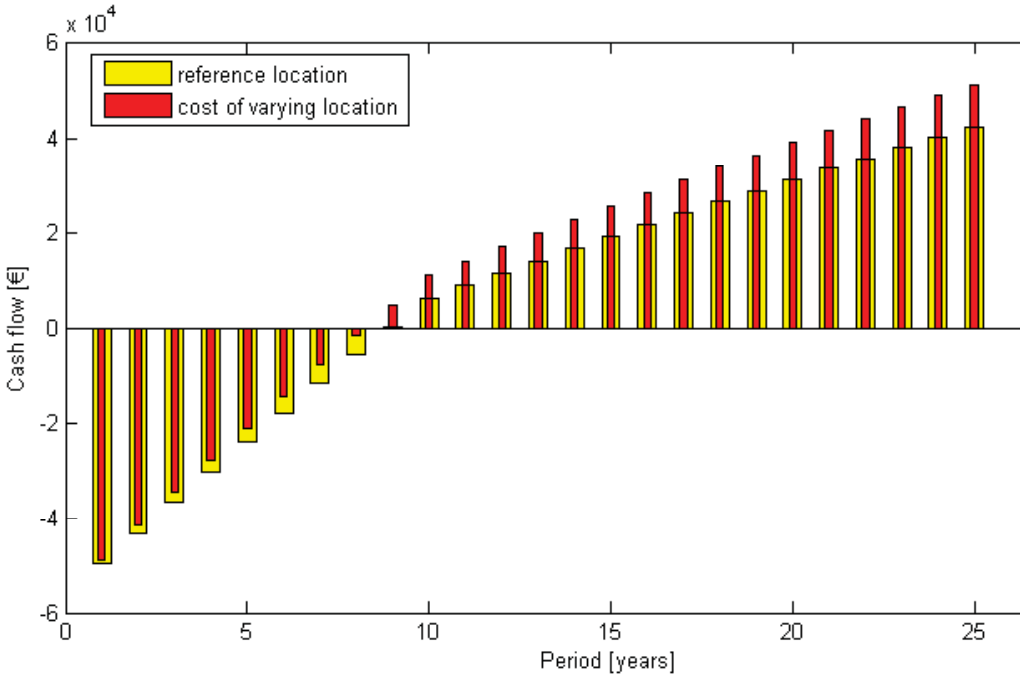

Figure 6.3: comparison of the cumulated cash flow as plant location is varied.

6.9 Concluding remarks

As earlier discussed, solar panel have a wide market price, the high efficiency evacuated tube solar collectors considered in study have an average price of $400€/m^2$ while the ORC module is estimated at $5000€/kW$. The overall proposed solar-ORC plant cost results to be quite consistent especially if intended solely for power generation, in this case, an ORC module with generation capacity in the range 10-15 kW may be quite interesting. In particular, the cost of the ORC could be realistic (less than $5000€/kW$) if we consider industrial production. This cost could be more realistic if we consider a high volume industrial production of its components (heat exchanger, pumps and expanders: available in the HVAC field). For the ORC modules of power range lower than 5 kW as the case studied, the prospective of operating in cogeneration mode: combining electricity production with a medium temperature thermal production finds maximum benefits if there is a substantial demand in this range of temperatures, such as for the heating of swimming pools or other domestic needs in low-temperature. The system efficiency can be further increased if operated in trigeneration mode, the use of the hot water returning from the ORC still at high enough temperature to feed an absorption machine thus reducing system cost by including the sav-

ings in refrigeration that can be relevant. From this analysis we can confirm that solar-ORC systems with electric efficiencies of about 10% can allow to achieve economic savings of about 15% and can be attractive only with the adoption of incentive schemes as in th e case of fuel cost reduction.

CONCLUSION

In the present study, the ORC has been employed as the conversion technology for the exploitation of low grade heat as primary energy source, which, like industrial waste heat are more often unexploited for the generation of electricity. Although the ORC is not a new technology for energy conversion, its application for micro size systems are presently found either as experimental or laboratory prototypes yet to gain technological maturity. To contribute to the development and feasibility of these systems: the state of the art on ORC has been analyzed, a simulation model has been developed to study the system, experimental activities have been performed on some key components that make up the system as well as on an ORC prototype, the prototype has been integrated to a solar field then tested and, an economic evaluation has been carried out providing indications on the possible economic savings achievable with ORC for energy production from renewable souces.

From the study, it emerges that ORC's can be used to exploit in a convenient manner low grade heat sources that are generally not exploited by other traditional technologies. In particular, more interesting is the coupling of an ORC module to renewable energy sources, a prospective that is supported by environmental issues given the present global scenario with increasing consumption of fossil fuels as primary sources of energy. Furthermore, the reduction of CO_2 emissions resulting from the energy will render energy generation sustainable. Other than exploiting low grade heat, small ORC's can conveniently be used for heat recovery from industrial waste as well as waste heat from internal combustion engines ICE. In the case of low grade heat exploitation, the critical components (pumps, expanders) of the ORC should be properly designed for the specific application in order to obtain higher conversion efficiencies. In the case of waste heat recovery, the temperatures of the heat source are generally higher, as such even by employing devices directly derived from the automotive and the HVAC field or conventional components, the maximum achievable efficiencies can be obtained.

According to the literature analyzes carried out in this thesis considering systems between 1-10kWe power range discussed in chapter two, the choice of the working fluid varies from case to case and depends on the particular ap-

plication and conditions in which the system operates. The scroll expander has been seen to be suitable for very small systems generally <10kWe production while the screw and vane type expanders are preferable for systems up to a 100kWe. In terms of the HE, the analyzes suggests the use of PHEs for small size plants, while the shell and tube types could be suitable for medium and large size plants and regarding applications, renewable sources such as solar, geothermal and biofuels as well as waste heat from industrial processes and internal combustion engines are potential heat sources for a micro power ORC.

After the theoretical analyses carried out, a process simulation model of a micro ORC system and its integration in a solar thermal plant has been implemented and discussed in chapter three, a preliminary model developed in EES for the simulation of the ORC has been used to predict the performance of the system and behavior at different operating conditions. The model can be conveniently exploited to study the system behavior in a reliable manner in the most different operating conditions without having to conduct each of the experimental tests that can sometimes be lengthy and difficult to perform.

For the integration of the ORC to a real application a specific model has been developed to study the coupling of the prototype to a solar field implemented in a combined simulation solver Trnsys - EES platform. The model developed for the solar - ORC has been used to show the dependency of electricity production on the amount of solar irradiance available at the collector surface. The model can be used at the design phase to evaluate the solar energy available for any desired geographical plant location and provides a useful tool for the evaluation of how much of this available energy can be transformed into electricity as well as the amount of hot water that can be produced for heating purposes.

The results of the experimental analyses performed on the laboratory prototype presented in chapter five have allowed the characterization of some key components and the ORC prototype itself. The tests were organized to verify the maximum yields obtainable from the ORC prototype for a given heat source by considering a wide temperature range for the heat source. So far, from the measurements on the test bench presented in chapter five, the generated electric power obtained is close to 2kW with an electrical efficiency of about 10% (for the RORC architecture) in line with microgeneration plants of similar size that exploit low grade heat. The tests have also enabled to understand the system response at different operating conditions thus enhancing the design of the optimized system.

The laboratory test carried on the pump test bench has also been useful for the characterization of the pumps. The results of the tests have also allowed to calculate the pump efficiency and to compute the power absorbed by the

pump and the electric motor, this element is fundamental, given its effect on the system overall efficiency.
The result obtained from testing the built ORC prototype, coupled with a system of solar collectors for electricity production allow assessment of the potentiality of the technology for micro electric power generation from a low temperature heat source. From the experimental measurements, though the expander designed nominal power was not achieved, the peak electric power obtained was about 1.4 kW, the possibility of achieving it seems to be feasible by improving the prototype design. The conversion efficiency of thesolar-ORC reached was slightly above 4%, a quite low value compared to the simulated efficiency (12%) as well as the laboratory test efficiency (10%), a possible cause to this loss could be the non neglible thermal losses about 30°C measured across the collector pipings.
Finally, an economic analysis has been presented evaluating the cost of installing a solar - ORC. According to the analysis, the time to recover the investment of an installed system is 10 years considering the Italian scheme of incentives as the plan of investment. The analysis reveals that the cost of the plant is consistent and that its reduction is one of the points of focus to retract the return time of the investment in a value of greater interest, especially, if compared with other competing technologies like solar photovoltaics with slightly higher system efficiencies. Nevertheless, if operated in cogeneration mode, solar thermal plants could be interesting. The production of hot water at low temperature is a strength of the system which finds the maximum benefit if there is a substantial demand in this range of temperatures, such as for the heating of swimming pools or other needs in low-temperature.
In the future it can be expected to study ORC systems of larger sizes considering the results presented in the thesis as a starting point, it will also be interesting to study their behavior in coupling with other renewable sources (like geothermal or biomass boiler) or even installing the ORC prototype to recover heat from an internal combustion engine. The solar-ORC facility can be improved by integrating a supplementary heater, for example, a biomass boiler, and thermal storage in order to guarantee continuity thus covering the hours of the day that are short of solar radiation. The system could, as well, be thought of operating in trigeneration mode by supplying an absorption chiller with the high temperature water in the ORC cooling circuit for ambient cooling, thus, improving overall system efficiency. The simulation model could be improved by considering: the operation of the expander in off design conditions and a more detailed model of the heat exchangers.
Apart from selecting a suitably designed expander for small ORC, the pumping element should be selected taking into consideration especially the compatibility of the pump material and the viscosity of the working fluid which

usually result to leakage through the pump sealings. With the improvements highlighted, higher efficiencies are expected to be obtained with the prototype as well as with similar ORC of the size range. It will also be interesting to perform a second principle (exergy) analysis to better evaluate the real efficiency of the system. This approach could address potential improvements of the ORC system, identifying the components where energy is actually degraded

To conclude, the discussions presented in the work are going to contribute to the diffusion and maturity of this technology, furthermore, the research highlights the potentials of the ORC for the exploitation of low grade heat and energy recovery from thermal wastes allowing achievable environmental as well as economic benefits. Nevertheless, more is yet to be done in order that the ORC gains technological maturity.

NOMENCLATURE

A collector surface Area

ALCC Annualized Life Cycle Cost

ALT Atmospheric Life Time

App Application

Arch Architecture

ATU Air Treatment Unit

C_1 collector first order loss coefficient

C_2 collector second order loss coefficient

C_A cost of area dependent equipment

C_E cost of non area dependent equipment

CFC Chlorofluorocarbons

CH_4 methane

CHP Combined Heat and Power

CO_2 Carbon Dioxide

c_p specific heat capacity

c_{ps} specific heat capacity primary circuit

c_{pw} specific heat capacity secondary circuit

C_S Total installation cost

dev developing

DCF Discount Cash Flow

DoM Degree of Maturity

EES Engineering Equation Solver

ERR Economic Rate of Return

g acceleration due to gravity

G solar radiation

GHG Green House Gas

GSE Gestore dei Servizi Energetici

GUI Graphical User Interface

GWP Global Warming Potential

h_1 enthalpy at pump inlet

h_2 enthalpy at pump outlet

h_3 enthalpy at evaporator inlet

h_5 enthalpy at evaporator outlet

h_6 enthalpy at expander inlet

h_7 enthalpy at expander outlet

$h_{7,is}$ ideal isentropic expansion enthalpy

H_2O Water

H_2S Hydrogen Sulphide

H_2 Hydrogen

H head

HC Hydrocarbons

HCFC Hydrochlorofluorocarbons

HE Heat Exchanger

HFC Hydrofluorocarbons

HFE Hydrofluoroethers

HTF Heat Transfered Fluid

HVAC Heating Ventilation and Air Conditioning

i Discount Rate

ICE Internal Combustion Engine

IRR Internal Rate of Return

LCSE Least Cost Solar Energy

LCC Life Cycle Cost

m mature

MED multi effect distillation

MSF multi stage flash

NIST National Institute of Standards and Technology

N length of the analysis period

N_2 Nitrogen

NH_3 Ammonia

n_{exp} expander speed

n_{pump} pump speed

NPV Net present Value

NPW Net present Worth

NRORC Non Regenerative Organic Rankine Cycle

ODP Ozone Depleting Potential

OECD Organization for Economic Cooperation and Development

OFC Organic Flash Cycle

ORC Organic Rankine Cycle

p promising

PBP Pay Back Period

p_{evap} Evaporation pressure

P_{exp} Expander power

P_{net} Net power generated

P_g gross Energy

PFC Perfluorocarbons

PHE Plate Heat Exchanger

p_{max} maximum cylinder pressure

PTC Parabolic Trough Concentrator

PV present value

Q_s Solar energy made available to collectors

RO Reversed Osmosis

RORC Regenerative Organic Rankine Cycle

R_t Net cash flow

SCHX Solar Collector Heat Exchanger

SORC Subcritical Organic Rankine Cycle

t period

TMY Typical meteorological Year

T_{evap} Evaporation Temperature

TCC Transcritical Cycle

TLC Trilateral Cycle

TORC Transcritical Organic Rankine Cycle

T_1 pump inlet temperature

T_2 pump outlet temperature

T_4 fluid temperature at evaporation start

T_7 Regenerator inlet temperature at the hotside

T_8 Regenerator outlet temperature at the hotside

T_9 fluid temperature at condensation start

T_m collector mean temperature

T_{amb} ambient temperature

T_{c1} cooling water inlet temperature

T_{c8} cooling water outlet temperature

T_{c9} cooling water temperature at condensation start

T_{h3} heat exchanger inlet temperature

T_{h4} hot water temperation at evaporation start

T_{h5} heat exchanger outlet temperature

T_{h1} collector outlet temperature

T_{h2} collector inlet temperature

T_{out} collector outlet temperature

T_{in} collector inlet temperature

T_{SH} super heating temperature

T_{SC} sub cooling temperature

Trnsys Transient Simulation System

vp very promising

W_{aux} Work done to drive the auxiliaries

WF Working Fluid

WHR Waste Heat Recovery

List of Symbols

β expansion ratio

ΔT_{sc} temperature difference across the collectors

ΔT_{w} temperature difference in the secondary circuit

ΔT_{cw} temperature difference in the cooling circuit

ΔT_{pp} pinch point difference

ΔT_{reg} temperature difference

ΔP Differential pressure

ΔH enthalpy change

η collector efficiency

η_0 optical efficiency

η_{fan} fan efficiency

η_p pump efficiency

η_g generator efficiency

η_{is} expander isentropic efficiency

η_{el} electrical efficiency

η_{vol} volumetric efficiency

η_m mechanical efficiency

η_t thermal efficiency

η_{exp} expander efficiency

η_{ORC} ORC efficiency

η_{coll} collector efficiency

$\eta_{Overall}$ system overall efficiency

$\dot{m}$ flow rate

$\dot{m}$ mass flow rate

$\dot{m}_f$ R245fa flow rate

$\dot{m}_a$ air flow rate

$\dot{m}_{cw}$ cooling water flow rate

$\dot{m}_c$ collector water flow rate

$\dot{m}_w$ collector water flow rate

$\dot{m}_{hc}$ heat carrier flow rate

$\dot{Q}_c$ thermal energy absorbed by the collector

$\dot{Q}_s$ Solar energy made available to collectors

$\dot{Q}_{ORC}$ ORC energy

$\dot{Q}_{aux}$ Energy absorbed by auxiliaries

$\dot{Q}_{net}$ Net Energy produced by the ORC unit

$\dot{W}_{CS}$ power absorbed by the control system

$\dot{W}_f$ power absorbed the dry cooler fan

$\dot{W}_g$ power generated by expander

$\dot{W}_e$ expander power

$\dot{W}_{net}$ Net energy production

$\dot{W}_p$ power absorbed by water pump

$\dot{W}_{PORC}$ power absorbed by ORC pump

ε_{reg} regeneration efficiency

Bibliography

[1] U. S. Department of Energy. *Industrial technologies program*, 2008.

[2] M.J. Moran. Engineering Thermodynamics. vol 181, 1958.

[3] U. S. Energy Information Administration. International Energy Outlook 2016. *Technical Report*, 2016.

[4] E.Macchi and M. Astolfi. Organic Rankine Cycle (ORC) Power Systems. 2016.

[5] Organic Rankine Cycle power plant for renewable energy resources.

[6] T. A. Davidson. Design and analysis of a 1 kW Rankine power cycle, employing a multi-vane expander, for use with a low temperature solar collector. *Bachelor's Thesis, Massachusetts Institute of Technology*, 1977.

[7] G. Hnat, J. S. Patten, L. M. Bartone, J. C. Cutting. Industrial Heat Recovery With Organic Rankine Cycles. *Proceedings of the Fourth Industrial Energy Technology Conference*, 524–532, 1982.

[8] K. K. Srinivasan, P. J. Mago, S. R. Krishnan. Analysis of exhaust waste heat recovery from a dual fuel low temperature combustion engine using an Organic Rankine Cycle. *Energy*, 35:2387–2399, 2010.

[9] S. Lecompte, H. Huisseune, M. van den Broek, B. Vanslambrouck, M. De Paepe. Review of organic Rankine cycle (ORC) architectures for waste heat recovery. *Renewable and Sustainable Energy Review*, 47:448–461, 2015.

[10] B. F. Tchanche, M. Pétrissans, G. Papadakis. Heat resources and organic Rankine cycle machines. *Renewable and Sustainable Energy Review*, 39:1185–1199, 2014.

[11] D. Ziviani, A. Beyene, M. Venturini. Advances and challenges in ORC systems modeling for low grade thermal energy recovery. *Applied Energy*,121:79–95, 2014.

[12] H. H. Dow. Diphenyl oxide bi-fluid power plants. *Journal of the American Society for Naval Engineers*, 38:940–950, 1926.

[13] S. K. Ray, G. Moss. Fluorochemicals as working fluids for small Rankine cycle power units. *Advanced Energy Conversion*, 36:89–102, 1966.

[14] H. M. Curran. Use of organic working fluids in Rankine engines. *Journal of Energy*, 5:218–223, 1981.

[15] E. H. Wang, H. G. Zhang, B. Y. Fan, M. G. Ouyang, Y. Zhao, Q. H. Mu. Study of working fluid selection of organic Rankine cycle (ORC) for engine waste heat recovery. *Energy*, 36:3406–3418, 2011.

[16] G. Angelino, M. Gaia, E. Macchi. Review Of Italian Activity In The Field Of Organic Rankine Cycles.*Proceedings of the International VDI Semina*:465–482, 1984.

[17] H. Chen, D. Y. Goswami, E. K. Stefanakos. A review of thermodynamic cycles and working fluids for the conversion of low-grade heat. *Renewable and Sustainable Energy Review*, 14: 3059–3067, 2010.

[18] C. Guo, X. Du, L. Yang, Y. Yang. Organic Rankine cycle for power recovery of exhaust flue gas. *Applied Thermal Engineering*, 75:135–144, 2015.

[19] E. Cayer, N. Galanis, H. Nesreddine. Parametric study and optimization of a transcritical power cycle using a low temperature source. *Applied Energy*, 87:1349–1357, 2010.

[20] S. Lecompte, H. Huisseune, M. van den Broek, S. De Schampheleire, M. De Paepe. Part load based thermo-economic optimization of the Organic Rankine Cycle (ORC) applied to a combined heat and power (CHP) system. *Applied Energy*, 111:871–881, 2013.

[21] O. Badr, P. W. O'Callagham, M. Hussein, S. D. Probert. Multi-vane expanders as prime movers for low grade energy organic Rankine cycle engines. *Applied Energy*,16:129–146, 1984.

[22] V. Lemort, S. Quoilin, C. Cuevas, J. Lebrun. Testing and modeling a scroll expander integrated into an Organic Rankine Cycle. *Applied Thermal Engineering*, 29:3094–3102, 2009.

[23] S. Clemente, D. Micheli, M. Reini, R. Taccani. Energy efficiency analysis of Organic Rankine Cycles with scroll expanders for cogenerative applications. *Applied Energy*, 97:792–801, 2012.

[24] J. Chang, C. Chang, T. Hung, J. Lin. Experimental study and CFD approach for scroll type expander used in low-temperature organic Rankine cycle. *Applied Thermal Engineering*, 73:1444-1452, 2014.

[25] S. Y. Cho, C. H. Cho, K. Y. Ahn, Y. D. Lee. A study of the optimal operating conditions in the organic Rankine cycle using a turbo-expander for fluctuations of the available thermal energy. *Energy*,64: 900–911, 2014.

[26] J. Wang, Z. Yan, M. Wang, S. Ma, Y. Dai. Thermodynamic analysis and optimization of an (organic Rankine cycle) ORC using low grade heat source. *Energy*, 49:356–365, 2013.

[27] R. Bracco, S. Clemente, D. Micheli, M. Reini. Experimental tests and modelization of a domestic-scale ORC (Organic Rankine Cycle). *Energy*, 58:107–116, 2013.

[28] J. Wang, Z. Yan, M. Wang, S. Ma, Y. Dai. Thermodynamic analysis and optimization of an (organic Rankine cycle) ORC using low grade heat source. *Energy*, 62:379–384, 2013.

[29] G. Pei, Y. Li, D. Wang, J. Ji,J. Li. Energetic and exergetic investigation of an organic Rankine cycle at different heat source temperatures. *Energy*, 38:85–95, 2012.

[30] S. Quoilin, R. Aumann, A. Grill, A. Schuster, V. Lemort, and H. Spliethoff. Dynamic modeling and optimal control strategy of waste heat recovery Organic Rankine Cycles. *Applied Energy*, 88:2183–2190, 2011.

[31] D. Wei, X. Lu, Z. Lu, J. Gu. Dynamic modeling and simulation of an Organic Rankine Cycle (ORC) system for waste heat recovery. *Applied Thermal Engineering*, 28:1216–1224, 2008.

[32] I. Vaja, A. Gambarotta. Dynamic model of an organic rankine cycle system. part I - mathematical description of main components. *Proceedings of the 23rd International Conference ECOS 2010*, 3:35–42, 2010.

[33] M. O. Bamgbopa, E. Uzgoren. Quasi-dynamic model for an organic Rankine cycle. *Energy Conversion Management*,72:117–124, 2013.

[34] B. Peris, J. Navarro-Esbrí, F. Molés, R. Collado, A. Mota-Babiloni. Performance evaluation of an Organic Rankine Cycle (ORC) for power applications from low grade heat sources. *Applied Thermal Engineering*: 1–7, 2014.

[35] Gary Zyhowski Andrew Brown. Low Global Warming Fluids for Replacement of HFC-245fa and HFC-134a in ORC Applications Honeywell. *A History of Innovation CFCs HCFCs HFCs HFOs*, 2014.

[36] B. T. Liu, K. H. Chien, C. C. Wang. Effect of working fluids on organic Rankine cycle for waste heat recovery. *Energy*, 29:1207–1217, 2004.

[37] B. Saleh, G. Koglbauer, M. Wendland, J. Fischer. Working fluids for low-temperature organic Rankine cycles. *Energy*, 32:1210–1221, 2007.

[38] Q. Chen, J. Xu, H. Chen. A new design method for Organic Rankine Cycles with constraint of inlet and outlet heat carrier fluid temperatures coupling with the heat source. *Applied Energy*, 98:562–573, 2012.

[39] F. Heberle, M. Preißinger, D. Brüggemann. Zeotropic mixtures as working fluids in Organic Rankine Cycles for low-enthalpy geothermal resources. *Renewable Energy*, 37:364–370, 2012.

[40] J. Bao, L. Zhao. A review of working fluid and expander selections for organic Rankine cycle. *Renewable and Sustainable Energy Review*, 24:325–342, 2013.

[41] K. Yang, H. Zhang, Z. Wang, J. Zhang, F. Yang, E. Wang, B. Yao. Study of zeotropic mixtures of ORC (organic Rankine cycle) under engine various operating conditions. *Energy*, 58:494–510, 2013.

[42] P. Garg, P. Kumar, K. Srinivasan, P. Dutta. Evaluation of isopentane, R-245fa and their mixtures as working fluids for organic Rankine cycles. *Applied Thermal Engineering*, 51:292–300, 2013.

[43] M. Chys, M. van den Broek, B. Vanslambrouck, M. De Paepe. Potential of zeotropic mixtures as working fluids in organic Rankine cycles. *Energy*, 44:623–632, 2012.

[44] B. F. Tchanche, G. Lambrinos, A. Frangoudakis, G. Papadakis. Low-grade heat conversion into power using organic Rankine cycles - A review of various applications. *Renewable and Sustainable Energy Reviews*, 15:3963–3979, 2011.

[45] S. Quoilin, M. Van Den Broek, S. Declaye, P. Dewallef, V. Lemort. Techno-economic survey of Organic Rankine Cycle (ORC) systems. *Renewable and Sustainable Energy Review*, 22:168–186, 2013.

[46] J. Xu, C.Yu. Critical temperature criterion for selection of working fluids for subcritical pressure Organic Rankine Cycles *Energy*, 74:719–733, 2014.

[47] L. Dong, H. Liu, S. Riffat. Development of small-scale and micro-scale biomass-fuelled CHP systems – A literature review. *Applied Thermal Engineering*, 29:2119–2126, 2009.

[48] R. A. Victor, J. K. Kim, and R. Smith. Composition optimisation of working fluids for organic rankine cycles and kalina cycles. *Energy*, 55:114–126, 2013.

[49] H. Tian, G. Shu, H. Wei, X. Liang, L. Liu. Fluids and parameters optimization for the organic Rankine cycles (ORCs) used in exhaust heat recovery of Internal Combustion Engine (ICE). *Energy*, 47:125–136, 2012.

[50] G. Yu, G. Shu, H. Tian, H. Wei, L. Liu. Simulation and thermodynamic analysis of a bottoming Organic Rankine Cycle (ORC) of diesel engine (DE). *Energy*, 51:281–290, 2013.

[51] Ozone Depletion Potential, Wikipedia

[52] United Nations Environment Programme. The Montreal protocol on substances that deplete the ozone layer. *International Protocol*, 1987.

[53] Global Warming Potential, Wikipedia

[54] Green House Gas, Wikipedia

[55] Stefano Clemente. Small Scale Cogeneration Systems Based On Organic Rankine Cycle Technology. *PhD Thesis*, University of Trieste, 2013.

[56] S. Clemente, D. Micheli, M. Reini, R. Taccani. Performance Analysis And Modeling Of Different Volumetric Expanders For Small-Scale Organic Rankine Cycles. *Proceedings of the ASME 5th International Conference on Energy Sustainability*:1–10, 2011.

[57] O. Badr, S. Naik, P. W. O'Callaghan, and S. D. Probert. Expansion machine for a low power-output steam Rankine-cycle engine. *Applied Energy*, 39:93–116, 1991.

[58] R. Zanelli. Experimental Investigation of a Hermetic Scroll Expander-Generator. 1994.

[59] T. Yanagisawa. M. Fukuta, Y. Ogi, T. Hikichi. Performance of an oil-free scroll-type air expander. *International Conference on Compressors and their Systems*:167-174, 2001.

[60] B. Aoun. Micro combined heat and power operating on renewable energy for residential building. *PhD Thesis*, Ecole Nationale Supérieure des Mines de Paris, 2008.

[61] S. H. Kang. Design and experimental study of ORC (organic Rankine cycle) and radial turbine using R245fa working fluid. *Energy*,41:514–524, 2012.

[62] J. E. McCullough, F. Hirschfeld. Scroll Machine-An Old Principle With A New Twist. *Mechanical Engineering*, 101:46–51, 1979.

[63] J. J. Brasz, G. Holdmann. Power production from a Moderate - Temperature geothermal resource. *Conference Proceedings in Transactions - Geothermal Resources Council*, 29:729–733, 2005

[64] G. Haiqing, M. Yitai, L. Minxia. Some design features of CO2 swing piston expander. *Applied Thermermal Engineering*, 26:237–243, 2006.

[65] X. D. Wang, L. Zhao, J. L. Wang, W. Z. Zhang, X. Z. Zhao, W. Wu. Performance evaluation of a low-temperature solar Rankine cycle system utilizing R245fa. *Solar Energy*, 84:353–364, 2010.

[66] G. Pei, Y. Li, J. Li, J. Ji. Performance evaluation of a micro turboexpander for application in low-temperature solar electricity generation. *Journal of Zhejiang University Science*,12:207–213, 2011.

[67] M. Farrokhi, S. H. Noie, A.A. Akbarzadeh. Preliminary experimental investigation of a natural gas-fired ORC-based micro-CHP system for residential buildings. *Applied Thermal Engineering*,69:221–229, 2014.

[68] B. Yang, X. Peng, Z. He, B. Guo, Z. Xing. Experimental investigation on the internal working process of a CO2 rotary vane expander. *Applied Thermal Engineering*,29:2289–2296, 2009.

[69] X. Jia, B. Zhang, L. Pu, B. Guo, X. Peng. Improved rotary vane expander for trans-critical CO2 cycle by introducing high-pressure gas into the vane slots. *International Journal of Refrigeration*,34:732–741, 2011.

[70] Z. Miao, J. Xu, X. Yang, J. Zou. Operation and performance of a low temperature Organic Rankine Cycle. *Applied Thermal Engineering*, 1–11, 2014.

[71] E. J. Bala, P. W. O'Callaghan, S. D. Probert. Influence of organic working fluids on the performance of a positive-displacement pump with sliding vanes. *Applied Energy*, 20:153–159, 1985.

[72] A. D. Reid. Low Temperature Power Generation using HFE-7000 in a Rankine cycle. *San Diego State University*, 57, 2010.

[73] S. Quoilin. Experimental Study and Modeling of a Low Temperature Rankine Cycle for Small Scale Cogeneration. *Master thesis*. University of Liege, 2007.

[74] C. L. Ong, J. R. Thome. Flow boiling heat transfer of R134a, R236fa and R245fa in a horizontal 1.030mm circular channel. *Experimental Thermal and Fluid Science*, 33:651–663, 2009

[75] D. Walraven, B. Laenen, W. D'Haeseleer. Comparison of shell-and-tube with plate heat exchangers for the use in low-temperature organic Rankine cycles. *Energy Conversion Management*, 87:227–237, 2014.

[76] J. Wang, M. Wang, M. Li, J. Xia, Y. Dai. Multi-objective optimization design of condenser in an organic Rankine cycle for low grade waste heat recovery using evolutionary algorithm. *International Communication in Heat and Mass Transfer*, 45:47–54, 2013.

[77] V. Donowski, S. Kandlikar. Correlating evaporation heat transfer coefficient of refrigerant R-134a in a plate heat exchanger. *Proceedings of Boiling. 2000 Phenom*, pp. 1–18, 2000.

[78] D. Micheli, S. Alessandrini, R. Radu, I. Casula. Analysis of the outdoor performance and efficiency of two grid connected photovoltaic systems in northern Italy. *Energy Conversion Management*, 80:436–445, 2014.

[79] R. Singh and J. Srinivasan. Modified Refrigerant Compressor As A Reciprocating Engine For Solar Thermal Power Generation. *Journal of Energy Resources*, 12:69–74, 1988.

[80] V. Siva Reddy, S. C. Kaushik, K. R. Ranjan, and S. K. Tyagi. State of the art of solar thermal power plants. a review. *Renewable and Sustainable Energy Review*, 27:258–273, 2013.

[81] W. W. Husband, A. Beyene. Low-grade heat-driven Rankine cycle, a feasibility study. *International Journal Energy Resources*, 32:1373–1382, 2008.

[82] A. M. Delgado-Torres L. García-Rodríguez. Preliminary design of seawater and brackish water reverse osmosis desalination systems driven by low-temperature solar organic Rankine cycles (ORC). *Energy Conversion Management*, 51:2913–2920, 2010.

[83] J. L. Wang, L. Zhao, X. D. Wang. A comparative study of pure and zeotropic mixtures in low-temperature solar Rankine cycle. *Applied Energy*, 87:3366–3373, 2010.

[84] L. Jing, P. Gang, J. Jie. Optimization of low temperature solar thermal electric generation with Organic Rankine Cycle in different areas. *Applied Energy*, 87:3355–3365, 2010.

[85] Y. A. M. Kane, D. Larrain, D. Favrat. Small hybrid solar power system. *Energy*,28:1427–1443, 2003.

[86] Impianti solari termodinamici ibridi: tecnologie disponibili e potenziale applicativo in Italia. *Technical report*, 2013.

[87] E. Barbier. Geothermal energy technology and current status: an overview. *Renewable and Sustainable Energy Revision*, 6:3–65, Jan. 2002.

[88] A. Franco, M. Villani. Optimal design of binary cycle power plants for water-dominated, medium-temperature geothermal fields. *Geothermics*, 38:379–391, 2009.

[89] A. Borsukiewicz-Gozdur and W. Nowak. Comparative analysis of natural and synthetic refrigerants in application to low temperature Clausius-Rankine cycle. *Energy*, 32:344–352, 2007.

[90] F. Heberle, D. Brüggemann. Exergy based fluid selection for a geothermal Organic Rankine Cycle for combined heat and power generation. *Applied Thermal Engineering*, 30:1326–1332, 2010

[91] M. Astolfi, M. C. Romano, P. Bombarda, E. Macchi. Binary ORC (Organic Rankine Cycles) power plants for the exploitation of medium–low temperature geothermal sources – Part B: Techno-economic optimization. *Energy*, 66:435–446, 2014.

[92] R. S. El-Emam I. Dincer. Exergy and exergoeconomic analyses and optimization of geothermal organic Rankine cycle. *Applied Thermal Engineering*, 59:435–444, 2013.

[93] G. Raluy, L. Serra, J. Uche. Life cycle assessment of MSF, MED and RO desalination technologies. *Energy*, 31:2361–2372, 2006.

[94] A. Schuster, S. Karellas, E. Kakaras, H. Spliethoff. Energetic and economic investigation of Organic Rankine Cycle applications. *Applied Thermal Engineering*, 29:1809–1817, 2009.

[95] D. Manolakos, G. Kosmadakis, S. Kyritsis, G. Papadakis. Identification of behaviour and evaluation of performance of small scale, low-temperature Organic Rankine Cycle system coupled with a RO desalination unit. *Energy*, 34:767–774, 2009.

[96] A. M. Delgado-Torres. Solar thermal heat engines for water pumping: An update. *Renewable and Sustainable Energy Review*, 13:462–472,2009.

[97] Y. Wong, K. Sumathy. Solar thermal water pumping systems: a review. *Renewable and Sustainable Energy Review*, 3:185–217, 1999.

[98] U. Drescher, D. Brüggemann. Fluid selection for the Organic Rankine Cycle (ORC) in biomass power and heat plants. *Applied Thermal Engineering*, 27:223–22, 2007.

[99] H. G. Zhang, E. H. Wang, B. Y. Fan. A performance analysis of a novel system of a dual loop bottoming organic Rankine cycle (ORC) with a light-duty diesel engine. *Applied Energy*, 102:1504–1513, 2013.

[100] G. Shu, G. Yu, H. Tian, H. Wei, X. Liang. A Multi-Approach Evaluation System (MA-ES) of Organic Rankine Cycles (ORC) used in waste heat utilization. *Applied Energy*, 132:325–338, 2014.

[101] I. Vaja, A. Gambarotta. Internal Combustion Engine (ICE) bottoming with Organic Rankine Cycles (ORCs) *Energy*, 35:1084–1093, 2010.

[102] J. Bonafin, P. Pinamontf, M. Rein, P. Tremuli. Performance improving of an internal combustion engine for ship propulsion with a bottom ORC. *Proceedings of ECOS 2010*, 5:73–83, 2010.

[103] Y. Durmusoglu, T. Satir, C. Deniz, A. Kilic. A Novel Energy Saving and Power Production System Performance Analysis in Marine Power Plant Using Waste Heat. *Proceedings in 2009 International Conference on Machine Learning and Applications*, 751–754, 2009.

[104] R. Aumann, A. Grill, A. Schuster, H. Spliethoff. Evaluation of fuel saving and economics for an organic rankine cycle as bottoming cycle in utility vehicles. *Proceedings of ECOS 2010*, 3:59–66, 2010.

[105] S. Quoilin and V. Lemort. Technological Survey of Organic Rankine Cycle systems. *5th European Conference on Economics and Management of Energy in Industry*, 2009.

[106] S. Lion, C.N. Michos, I. Vlaskos, and R. Taccani. A thermodynamic feasibility study of an Organic Rankine Cycle (ORC) for Heavy Duty

Diesel Engine (HDDE) waste heat recovery in off-highway applications. *Article in press for Proceedings of ECOS 2016*.

[107] A. Algieri and P. Morrone. Techno-economic Analysis of Biomass-fired ORC Systems for Single-family Combined Heat and Power (CHP) Applications. *Energy Procedia*, 45:1285–1294, 2014.

[108] A. Algieri and P. Morrone. Energetic analysis of biomass-fired ORC systems for micro-scale combined heat and power (CHP) generation. A possible application to the Italian residential sector. *Applied Thermal Engineering*,71:751–759, 2014.

[109] B. F. Tchanche, S. Quoilin, S. Declaye, G. Papadakis, and V. Lemort. Economic optimization of small scale organic rankine cycles. *Proceedings ECOS 2010*, 3:379–388, 2010.

[110] M. Badami, M. Mura, P. Campanile, and F. Anzioso. Design and performance evaluation of an innovative small scale combined cycle cogeneration system. *Energy*, 33:1264–1276, 2008.

[111] E. Bocci, M. Villarini, L. Bove, S. Esposto, and V. Gasperini. Modeling small scale solar powered ORC unit for standalone application. *Mathematical Problems Engineering*, 124280, 2012.

[112] T. Chambers, J. Raush, and B. Russo. Installation and Operation of Parabolic Trough Organic Rankine Cycle Solar Thermal Power Plant in South Louisiana. *Energy Procedia*, 49:1107–1116, 2014.

[113] S. Declaye, S. Quoilin, L. Guillaume, and V. Lemort. Experimental study on an open-drive scroll expander integrated into an ORC (Organic Rankine Cycle) system with R245fa as working fluid. *Energy*, 55:173–183, 2013.

[114] H. A. Ingley, R. Reed, and D. Y. Goswami. Optimization of a Scroll Expander Applied to an Ammonia/Water Combined Cycle System for Hydrogen Production. *Proceedings Solar World Congress*, 3:2089-2100, 2005.

[115] G. Xiaojun, L. Liansheng, Z. Yuanyang, S. Pengcheng, and S. Jiang. Research on a scroll expander used for recovering work in a fuel cell. *International Journal of Thermodynamics*, 7:1–8, 2004.

[116] T. Herron, R. B. Peterson and H. Wang. Performance of a small scale regenerative power cycle employing a scroll expander. *Journal of Power Engineering*,222: 271-282, 2008.

[117] H. J. Kim, J. M. Ahn, I. Park, and P. C. Rha. Scroll expander for power generation from a low-grade steam source. *Journal of Power Energy*, 221:705–711, 2007.

[118] T. Saitoh, N. Yamada, S. Wakashima. Solar Rankine Cycle System Using Scroll Expander. *Journal of Environmental Engineering*, 2:708–719, 2007.

[119] J. A. Mathias, J. R. Johnston, J. Cao, D. K. Priedeman, and R. N. Christensen. Experimental Testing of Gerotor and Scroll Expanders Used in, and Energetic and Exergetic Modeling of, an Organic Rankine Cycle. *Journal of Energy Resource Technologies*, 131:0122011-0122019, 2009.

[120] V. Lemort, S. Declaye, and S. Quoilin. Experimental characterization of a hermetic scroll expander for use in a micro-scale Rankine cycle. *Journal of Power Energy*, 226:126–136, 2011.

[121] H. Wang, R. B. Peterson, and T. Herron. Experimental performance of a compliant scroll expander for an organic Rankine cycle. *Journal of Power Energy*, 223:863–872, 2009.

[122] K. J. Harada. Development of a small scale scroll expander. *Oregon State University*, 2010

[123] G. Qiu, Y. Shao, J. Li, H. Liu, and S.B. Riffat. Experimental investigation of a biomass-fired ORC-based micro-CHP for domestic applications. *Fuel*, 96:374–382, 2012.

[124] R. Taccani, J. B. Obi, M. De Lucia, D. Micheli, G. Toniato. Development and Experimental Characterization of a Small Scale Solar Powered Organic Rankine Cycle (ORC). *Energy Procedia*, 101:504-511, 2016.

[125] Engineering Equation Solver manual, Commercial and professional version

[126] NIST National Institute of Standards and Technology, Reference Fluid Thermodynamic and Transport Properties Database (REFPROP Ver. 9.1). Sito web.

[127] S. Poles, M. Venturin. Numerical simulation of an Organic Rankine Cycle. Open Source Engineering

[128] J. Freeman, K. Hellgardt, C. N. Markides. An assessment of solar-powered organic Rankine cycle systems for combined heating and

power in UK domestic applications. *Applied Energy*, 138:605–620, 2015.

[129] Transient Simulation Mathematical Refernce volume 4

[130] Quality assurance in solar heating and cooling technology

[131] Solar Collector Factsheet Thermics 20 DTH-CPC

[132] J.A. Duffie and W.A. Beckman. Solar Engineering of Thermal processes. *John Wiley and Sons, Inc* 4th edition, 1958.

[133] D. Micheli, M. Reini, R. Taccani. Multiple expansion ORC for small scale – low temperature heat recovery. *Proceedings of ECOS 2016*, 2016

[134] J. B. Obi, R. Taccani, D. Micheli, M. Reini. Parametric analysis of a solar thermal power plant with an Organic Rankine Cycle (ORC) generator. *Article in press for Proceedings of ECOS 2016.*

[135] Wanner Engineering Inc. Heavy duty industrial pumps. *Technical specifications.*

[136] Air–liquid cooler and condensers for commercial use. *AlfaBlue Junior DG, AG, AGH: Instruction manual.*

[137] Italohm toroidal and linear slider rheostats. *RC Model Technical specifications.*

[138] Reotemp Instrument Corporation. *Thermocouple accuracies.*

[139] JUMO. *Technical specifications JUMO DELOS SI 405052.*

[140] TME General Purpose Coriolis Mass Flowmeter. *Technical specifications.*

[141] JUMO. *Technical specifications JUMO dtrans 403022.*

[142] SUNTEC Industries, France, Web site

[143] Solitem Group Aachen, online site

[144] online site march 2016.

[145] E. Lena. Analisi delle prestazioni di gruppi ORC per la microgenerazione distribuita. *M.Sc Thesis*, Università degli Studi di Trieste, 2014.

[146] L.M. Ayompe, A. Duffy, S.J. McCormack, M. Conlon. Validated TRNSYS model for forced circulation solar water heating systems with flat plate and heat pipe evacuated tube collectors, *Applied Thermal Engineering*,31:1536-1542, 2011.

[147] R. Dickes, D. Ziviani. M. D. Paepe, M. V. D. Broek, S. Quoilin and V. Lemort. ORCmKit: an open-source library for organic Rankine cycle modelling and analysis. *Article in press for Proceedings of ECOS 2016*.

[148] S. Lemmens. Cost Engineering Techniques and Their Applicability for Cost Estimation of Organic Rankine Cycle Systems. *Energies*,9:485–503, 2016.

[149] R.C. Dorf. The Engineering Handbook: Engineering economics and mnanagement. CRC press LLC, 2625-2739, 2000.

[150] E. Boccia, M. Villarini, L. Vecchione, D. Sbordonec, A. Di Carlod, A. Dell'Eraa. Energy and economic analysis of a residential Solar Organic Rankine plant. *Energy Procedia*,81:558–568, 2015.

[151] Gestore Servizio Energetico.*Gazzetta ufficiale website*, 2014.

[152] Impianti solari termodinamici ibridi: tecnologie disponibili e potenziale applicativo in Italia. *Technical report*, 2013.

[153] Memoria per l'audizione presso la 10^a Commissione Industria, Commercio e Turismo del Senato della Repubblica. *Indagine conoscitiva sui prezzi finali dell'energia elettrica e del gas naturale*, 2014.

[154] A. Cressi. Development of a simulation model for a small scale solar thermal power plant. *M.Sc Thesis*, Università degli Studi di Trieste, 2015.